AGU PUBLICATIONS

Reviews of Geophysics

REVIEW ARTICLE
10.1002/2016RG000532

Key Points:
- The glaciers of the Amundsen Sea Embayment have experienced remarkable retreat and thinning over recent decades
- Intrusions of Circumpolar Deep Water have contributed to the glacier thinning
- The complex atmosphere-ocean-ice interactions cannot be simulated in the current generation of models

Correspondence to:
J. Turner,
jtu@bas.ac.uk

Citation:
Turner, J., A. Orr, G. H. Gudmundsson, A. Jenkins, R. G. Bingham, C.-D. Hillenbrand, and T. J. Bracegirdle (2017), Atmosphere-ocean-ice interactions in the Amundsen Sea Embayment, West Antarctica, *Rev. Geophys.*, *55*, 235-276, doi:10.1002/2016RG000532.

Received 11 AUG 2016
Accepted 2 FEB 2017
Accepted article online 27 FEB 2017
Published online 20 MAR 2017

Atmosphere-ocean-ice interactions in the Amundsen Sea Embayment, West Antarctica

John Turner[1], Andrew Orr[1], G. Hilmar Gudmundsson[1], Adrian Jenkins[1], Robert G. Bingham[2], Claus-Dieter Hillenbrand[1], and Thomas J. Bracegirdle[1]

[1]British Antarctic Survey, Cambridge, UK, [2]School of GeoSciences, University of Edinburgh, Edinburgh, UK

Abstract Over recent decades outlet glaciers of the Amundsen Sea Embayment (ASE), West Antarctica, have accelerated, thinned, and retreated, and are now contributing approximately 10% to global sea level rise. All the ASE glaciers flow into ice shelves, and it is the thinning of these since the 1970s, and their ungrounding from "pinning points" that is widely held to be responsible for triggering the glaciers' decline. These changes have been linked to the inflow of warm Circumpolar Deep Water (CPDW) onto the ASE's continental shelf. CPDW delivery is highly variable and is closely related to the regional atmospheric circulation. The ASE is south of the Amundsen Sea Low (ASL), which has a large variability and which has deepened in recent decades. The ASL is influenced by the phase of the Southern Annular Mode, along with tropical climate variability. It is not currently possible to simulate such complex atmosphere-ocean-ice interactions in models, hampering prediction of future change. The current retreat could mark the beginning of an unstable phase of the ASE glaciers that, if continued, will result in collapse of the West Antarctic Ice Sheet, but numerical ice sheet models currently lack the predictive power to answer this question. It is equally possible that the recent retreat will be short-lived and that the ASE will find a new stable state. Progress is hindered by incomplete knowledge of bed topography in the vicinity of the grounding line. Furthermore, a number of key processes are still missing or poorly represented in models of ice-flow.

1. Introduction

The West Antarctic Ice Sheet (WAIS) is the part of the Antarctic Ice Sheet that covers West Antarctica and is separated from the East Antarctic Ice Sheet by the Transantarctic Mountains. The WAIS currently covers an area of 2.25×10^6 km^2 [*Rignot*, 2008] and contains over 3.6×10^6 km^3 of ice (with ice shelves) [*Lythe et al.*, 2001], which is enough to raise global sea level by approximately 4.3 m if melted completely [*Fretwell et al.*, 2013]. The dynamics of the WAIS are characterized by relatively fast-flowing ice streams that carry ice from the interior regions toward the coast. The WAIS is termed a "marine-based ice sheet" because much of its ice is grounded on bedrock that is below sea level and slopes downward from the coast toward the interior. When the ice streams reach the coast they float on the ocean and form ice shelves, which lose ice either by basal melting or calving of icebergs. The ice in the interior is replenished by the accumulation of snow, which is eventually compacted into glacial ice. About 90% of the ice drainage from the WAIS is through a relatively small number of ice streams (≈10) which drain into three major basins—the Ross Sea Embayment, the Weddell Sea Embayment, and the Amundsen Sea Embayment (ASE).

Around 20% of the total volume of the WAIS drains into the ASE via a number of outlet glaciers. Among the largest and fastest flowing of ASE glaciers are Pine Island Glacier (hereafter PIG), Thwaites Glacier (hereafter TG), and Haynes, Smith, Pope, and Kohler Glaciers (see Figure 1). Together, these glaciers and their catchment basins cover an area of 320×10^3 km^2 and contain enough ice to raise global sea level by approximately 1.2 m. As estimated by *Mouginot et al.* [2014] the combined ice flux of all these glaciers into ASE was 226 ± 17 Gt/yr in 1994 (the first year for which estimates of ice flux for all of those glaciers are available) but had increased to 334 ± 15 Gt/yr in 2013. Since 1973 the ASE has experienced a 77% increase in ice discharge due to glacier acceleration, so that this region is now responsible for about 10% of the current global sea level rise [*Mouginot et al.*, 2014]. Concurrently, the glaciers have also experienced thinning and retreat of their grounding-line positions (the location separating the ice grounded on bedrock from the floating ice shelf) raising the specter that an unstable retreat of the grounding line is underway [*Schoof*, 2007] which, if unchecked, would eventually result in West Antarctic-scale rapid diminishing of the grounded ice sheet.

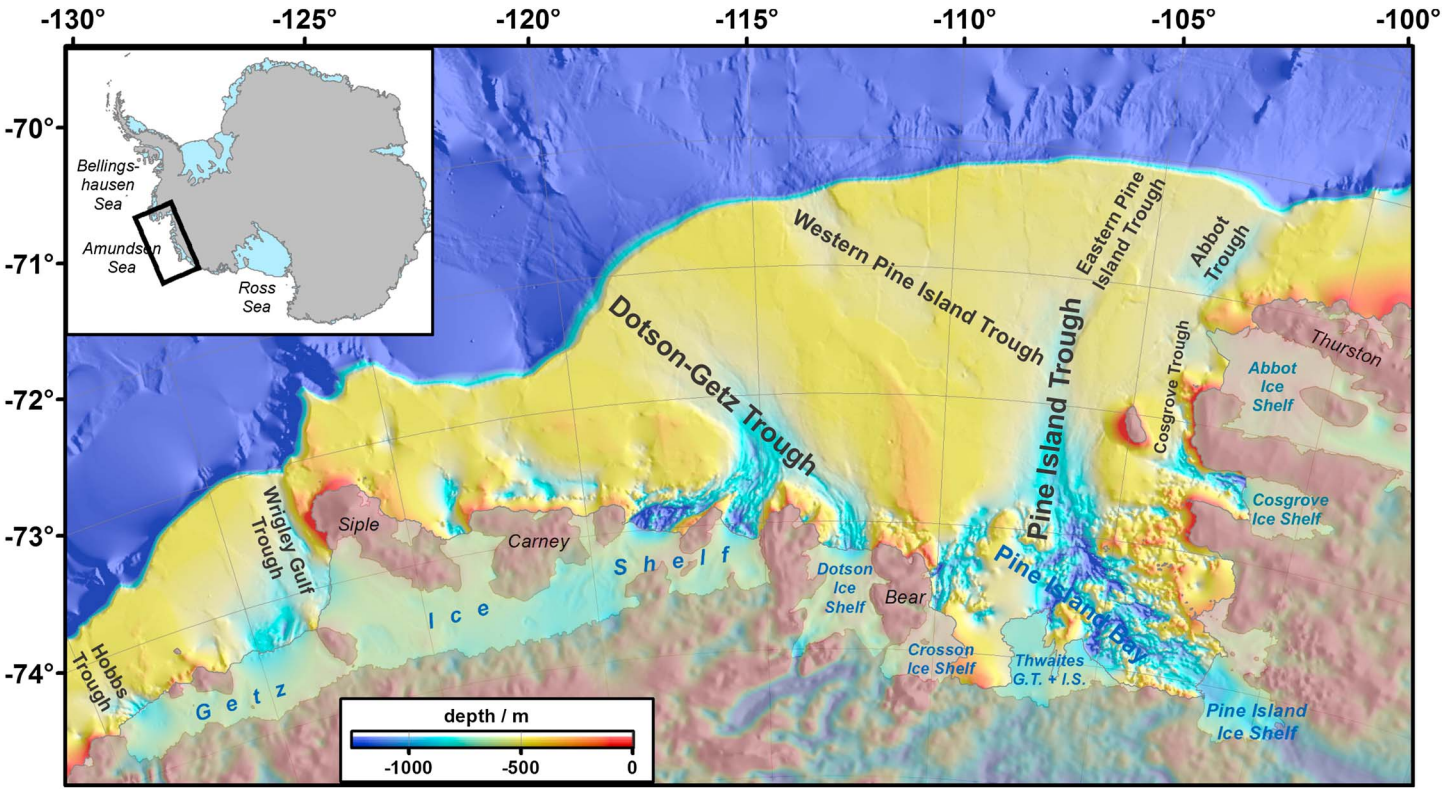

Figure 1. A regional map of the ASE and coastal Marie Byrd Land showing the locations of the glaciers and ice shelves discussed in the text. The inset map shows the location of the ASE in relation to the whole Antarctic continent. The bathymetry of the Amundsen Sea continental shelf (figure courtesy of F. Nitsche, LDEO; modified from *Jacobs et al.* [2012]) is also shown. Locations of bathymetric cross-shelf troughs eroded by paleo-ice streams during past glacial periods are also indicated. Shading under the land and ice shelves shows the bed elevation from the BEDMAP2 data set. The bed elevation is shown by using the same color scheme as that used for the ocean and shown on the key.

Averaged over all of those glaciers, the increase in ice flux into the ASE has been roughly linear with time, although this has not been the case for individual glaciers. PIG alone is responsible for 20% of the total ice discharge from the WAIS [*Rignot*, 2008; *Wingham et al.*, 2009], is grounded up to 1500 m below sea level, and ice flux has increased from ~78 Gt/yr in 1973 to ~133 Gt/yr from 2010 to 2013 [see *Mouginot et al.*, 2014] (Table 1). It flows rapidly into the Amundsen Sea through an ice shelf approximately 55 km long by 30 km wide, and its flow speed at the grounding line has accelerated from 2.3 km/yr in 1973 to 4.0 km/yr in 2013 [*Mouginot et al.*, 2014].

The ice front is subject to periodic, large calving events that remove icebergs of up to 19×32 km in size [*Jenkins et al.*, 1997; *Howat et al.*, 2012]. Between 1992 and 2010 the spatially averaged rate of grounding-line retreat over the central section of PIG was 0.95 ± 0.09 km/yr. Retreat rates along individual flow lines have, however, varied more with time than this spatially averaged value might suggest. For example, along its central flow line, the grounding line of PIG retreated by about 3 km between 1992 and 2000, followed by a retreat of about 20 km between 2000 and 2009 [e.g., *Park et al.*, 2013, Figure 1]. PIG is fed by nine tributary glaciers that converge approximately 175 km inland to form the central trunk.

TG is located to the west of PIG (Figure 1) and is a fast flowing and unusually broad glacier that flows into Pine Island Bay. The speed of the TG is ~4 km/yr near the grounding line of its main trunk, whereas flow speed of its eastern shelf is just 0.8 km/yr [*Mouginot et al.*, 2014]. TG discharged only ~72 Gt/yr in 1973 to 1974 but is currently draining ~126 Gt/yr into the ASE [*Mouginot et al.*, 2014]. Both the PIG and TG are susceptible to accelerated retreat [e.g., *Joughin et al.*, 2014; *Rignot et al.*, 2014] as the bedrock inland lies well below sea level and deepens inland [*Holt et al.*, 2006; *Vaughan et al.*, 2006].

Marine sediment cores and sediments recovered from below the ice sheet indicate that the WAIS has, at least partially, collapsed in the past, possibly as recently as ~400 kyr ago [*Scherer et al.*, 1998; *Naish et al.*, 2009;

Table 1. A Summary of Important Changes in PIG, TG, and the ASE Glaciers as a Whole

Area	Change In	Estimates
All glaciers flowing into ASE	Combined ice flux	226 ± 17 Gt/yr in 1994 334 ± 14 Gt/yr in 2013
	Mass loss (contribution to sea level)	7 ± 26 Gt/yr (0.02 ± 0.08 mm/yr) in 1974 105 ± 27 Gt/yr (0.31 ± 0.08 mm/yr) in 2007
PIG	Ice flux	78 Gt/yr in 1973 133 Gt/yr over 2010–2013
	Flow speed at the grounding line	2.3 km/yr in 1973 4.0 km/yr in 2013
	Spatially averaged grounding-line retreat of the central section	0.95 ± 0.09 km/yr over 1992–2010
	Ice edge	No migration discernibly over the 50 years up to about 2000
	Velocity	Increase of ~75% since 1973
	Thinning	~2 m/yr over 1992–2000 but 10 m/yr at the grounding line in 2006
	Hinge-line retreat	~1.5 km/yr for 1992–2011 1.8 ± 0.9 km/yr over 2009–2011
	Area that became ungrounded	14.2 ± 1.3 km/yr over 1992–2011
	Retreat of the grounding line	1.5 km/yr over 1996–2009
	Mass loss (contribution to sea level)	3.9 ± 0.9 Gt/yr (0.01 mm/yr) over 1992–1999 2.6 ± 0.3 Gt/yr in 1995 (0.007 mm/yr) 46.0 ± 5.0 Gt/yr in 2007 (0.13 mm/yr)
	Basal melt rate	12 ± 3 m/yr over 1973–1994 24 ± 4 m/yr over 1992–1996 16.2 ± 1 m/yr over 2003–2008
TG	Ice flux	72 Gt/yr over 1973–1974 126 Gt/yr in 2014
	Ice edge	The terminus of floating ice between the Thwaites Glacier Tongue and the Thwaites Eastern Ice Shelf retreated by 26 km from 1973 to 2009. Thwaites Glacier Tongue calved within 16 km of the grounding line in 2010.
	Velocity	Thwaites Ice Tongue accelerated over 1973–1996 (33%) and 2006–2013 (33%). Thwaites Eastern Ice Shelf accelerated over 1996–2006 (50%).
	Thinning	0.55 m/yr over 1991–2001
	Retreat of the grounding line	0.7 km/yr over 1992–2011
	Mass loss (contribution to sea level)	54 ± 5 Gt/yr (0.16 mm/yr) over 2002–2010
	Basal melt rate	17.7 ± 1 m/yr over 2003–2008

Teitler et al., 2015]. How the ice of the ASE will change in the future is one of the most important questions in Antarctic science because of the possible destabilization of the WAIS [*Mercer*, 1978; *Hughes*, 1981] and the associated dramatic increase in mass loss over decadal to centennial scales, along with the consequences for global sea level rise. A number of factors can possibly influence the stability of the WAIS, including volcanoes below the ice sheet [*Blankenship et al*., 1993] and geothermal heating [*Maule et al*., 2005], as well as ice loss at the coast.

The influx of relatively warm Circumpolar Deep Water (CPDW) onto the Amundsen Sea continental shelf and into sub-ice-shelf ocean cavities [*Jenkins et al*., 2010; *Hellmer et al*., 2012] is thought to be responsible for the recent substantial grounding-line retreat and mass loss of ASE glaciers [*Payne et al*., 2004; *Rignot et al*., 2014]. This suggests that changes in the ocean circulation have increased melting at the base of the floating ice shelves marking the glaciers' termini, resulting in loss of ice-shelf buttressing and consequent drawdown and loss of the grounded ice. It has been suggested that the delivery of CPDW to the continental shelf is closely linked to the pattern of winds at the continental shelf edge [*Thoma et al*., 2008] and involves complex atmosphere-ocean-interactions on a range of time scales, with both regional and hemisphere-wide climatic changes playing a part. It is essential to understand these linkages if we are to predict how the WAIS will evolve over the coming decades and determine the possible impact on sea level. However, understanding

the processes involved in the observed changes and simulating these in numerical models that can help predict the future evolution of this part of the WAIS presents many challenges.

In this paper we review our current understanding of the changes that have taken place in recent decades in the atmosphere, ocean, and ice of the ASE, and the mechanisms responsible for these changes. We first consider how the observed changes in the glaciers of the ASE have been monitored by satellite and aircraft-borne sensors, and in situ measurement campaigns over recent decades. We then examine the oceanographic changes that have taken place in the vicinity of the ASE, along with the wind forcing from the atmospheric circulation. Efforts to model various components of the system and their interactions are then examined. We consider our current understanding of the reasons for the marked changes observed in the ASE area before examining predictions of change for the next century. We finish by suggesting future research needs.

2. Glaciological Changes in the ASE

2.1. Marine and Terrestrial Geological Records

The WAIS and the glaciers of the ASE have undergone considerable changes in the past. Multibeam-swath bathymetry data revealed that several bathymetric troughs extend from the modern ASE coast across the continental shelf to near the shelf break [e.g., *Nitsche et al*., 2007; *Jacobs et al*., 2012; *Livingstone et al*., 2012; *Larter et al*., 2014] (see Figure 1). A variety of subglacial bedforms mapped within these troughs give evidence that the troughs mark the pathways of fast-flowing paleo-ice streams, which had advanced across the ASE shelf during past glacial periods [*Lowe and Anderson*, 2002; *Evans et al*., 2006; *Graham et al*., 2009, 2010; *Larter et al*., 2009; *Jakobsson et al*., 2011, 2012; *Nitsche et al*., 2013; *Klages et al*., 2014, 2015]. In contrast, a distinct bed form assemblage observed on an intervening shallow ridge suggests that paleo-ice flow there was slower than in the neighboring troughs [*Klages et al*., 2013]. Seismic profiles collected from the ASE continental shelf and slope indicate that ice sheet advance and retreat had occurred repeatedly over hundreds of thousands to millions of years, and possibly even since the mid-Miocene [*Lowe and Anderson*, 2003; *Dowdeswell et al*., 2006; *Graham et al*., 2009; *Gohl et al*., 2013; *Hochmuth and Gohl*, 2013].

Today, two main paleo-ice stream trough systems dominate the seafloor on the ASE shelf: the Pine Island Trough in the east and the Dotson-Getz Trough in the west (Figure 1). The PIG and TG coalesced on the inner shelf, i.e., south of 73°S, and merged with the Pope and Smith glaciers at the inner to middle shelf transition, where they formed a major paleo-ice stream draining northward through Pine Island Trough across the midshelf [*Lowe and Anderson*, 2002, 2003; *Graham et al*., 2010; *Jakobsson et al*., 2012; *Nitsche et al*., 2013]. On the middle shelf at ~72.5°S Pine Island Trough bifurcates into an eastern and a western branch, which both extend seaward across the outer shelf and reach the shelf break at water depths of ~550 m near 105°W and ~600 m at 113.5°W, thereby enclosing a sill with a water depth locally shallower than 500 m [*Lowe and Anderson*, 2002; *Evans et al*., 2006; *Graham et al*., 2010]. Grounded ice emanating from the Dotson Ice Shelf and the easternmost parts of the Getz Ice Shelf also converged on the inner shelf, from where it flowed within a single major ice stream in a NW-direction toward the outer shelf at ~118°W [*Graham et al*., 2009; *Larter et al*., 2009]. To the east of Pine Island Trough, smaller ice streams fed by the Cosgrove and Abbot ice shelves coalesced on the midshelf at ~72.5°S to a paleo-ice stream and eroded Cosgrove-Abbot Trough into the continental shelf [*Jakobsson et al*., 2012; *Klages et al*., 2013, 2015; *Hochmuth and Gohl*, 2013]. The floor of its northern part, called Abbot Trough (Figure 1), reaches its greatest water depth of ~760 m north of 72°S and shoals northeastward to a water depth of ~625 m when reaching the shelf edge at 102.5°W [*Klages et al*., 2015].

At the Last Glacial Maximum (LGM) the WAIS certainly extended northward onto the outer continental shelf elsewhere in the ASE [e.g., *Lowe and Anderson*, 2002; *Graham et al*., 2010; *Smith et al*., 2011, 2014; *Kirshner et al*., 2012; *Livingstone et al*., 2012; *Larter et al*., 2014]. It is under debate, however, whether grounded ice reached the shelf break everywhere in the ASE, because intense scouring by icebergs subsequent to the LGM obliterated the majority of preexisting subglacial bedforms not only on the relatively shallow banks between the paleo-ice stream troughs but also on the floor of the most seaward parts of the troughs, thereby also disturbing the stratigraphy of the seabed sediments recovered in cores [*Lowe and Anderson*, 2002; *Larter et al*., 2014]. Moreover, the timing of paleo-ice stream drainage on the outer shelf into the eastern and western branches of Pine Island Trough is under debate [*Evans et al*., 2006; *Jakobsson et al*., 2012] because

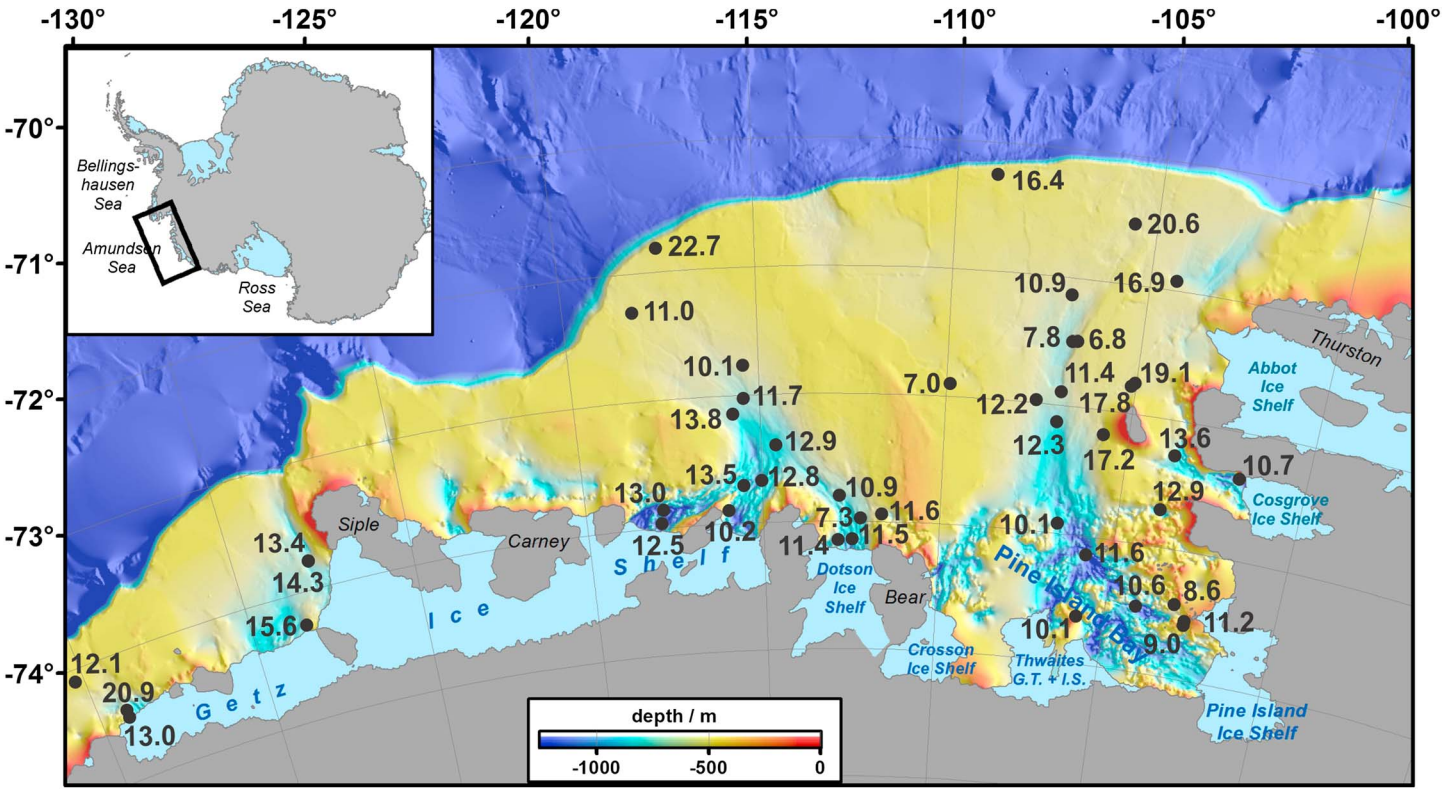

Figure 2. Bathymetric map of the ASE with locations of marine sediment cores (black dots) providing minimum ages, predominantly based on radiocarbon dates of marine microfossils and marine organic matter, for post-LGM ice sheet retreat from the shelf (black numbers; in calibrated kiloyears before present). Maximum ice sheet advance at the LGM is assumed to have reached the outermost shelf and shelf break, respectively. Exceptionally, old deglaciation ages may result from problems with radiocarbon dating of Antarctic shelf sediments (for details, see *Larter et al.* [2014]), while exceptionally, young ages may constrain the onset of open-marine conditions at a core site (e.g., the onset of marine productivity after retreat of an ice-shelf front) rather than the time of grounding-line retreat. Core sites with ages compiled from *Larter et al.* [2014], *Smith et al.* [2014], and *Klages et al.* [2014].

currently no deglaciation ages are available for the outer shelf part of the western branch [*Larter et al.*, 2014]. Subglacial features eroded into bedrock on the inner shelf of the ASE suggest that the WAIS was thick enough at the LGM to ground in deep basins there which are up to 1200–1600 m deep [*Lowe and Anderson*, 2003; *Graham et al.*, 2009]. It has also been suggested that some of these basins hosted, at least temporarily, subglacial lakes during the last glacial period [*Nitsche et al.*, 2013; *Witus et al.*, 2014]. Surface exposure ages of glacially transported rocks have shown that the LGM surface of the WAIS lay at least ~140 m and 190 m higher than today to the north and to the east of the modern PIG grounding-line position, respectively [*Johnson et al.*, 2008, 2014], while in the hinterland of the Crosson and Dotson ice shelves the LGM ice sheet was ~300 to 330 m thicker than today [*Johnson et al.*, 2008; *Lindow et al.*, 2014].

Grounded ice had started to retreat from its maximum LGM extent on the ASE shelf by ~22.5 ka B.P. in both the eastern Pine Island Trough and the Dotson-Getz Trough [*Smith et al.*, 2011, 2014], while onset of retreat outside of the troughs may have occurred slightly later [*Kirshner et al.*, 2012; *Larter et al.*, 2014]. In the eastern ASE, grounded ice had retreated from the outer shelf by ~16 ka B.P. and from the middle shelf by ~13.5 ka B.P. [*Kirshner et al.*, 2012; *Klages et al.*, 2013; *Larter et al.*, 2014; *Smith et al.*, 2014] (Figure 2). Similarly, the Dotson-Getz paleo-ice stream had retreated to the inner shelf by ~13.8 ka B.P. [*Smith et al.*, 2011; *Larter et al.*, 2014]. Wedge-shaped sediment accumulations consisting of subglacial till (so-called "grounding-zone wedges") are found in the outer and middle shelf sections of both Pine Island Trough [*Graham et al.*, 2010; *Jakobsson et al.*, 2011, 2012] and Cosgrove-Abbot Trough [*Smith et al.*, 2014; *Klages et al.*, 2015]. These wedges give evidence that post-LGM ice sheet retreat in the eastern ASE was episodic and interrupted by phases of grounding-line stillstands lasting approximately several hundreds to thousands of years [*Jakobsson et al.*, 2012; *Kirshner et al.*, 2012; *Larter et al.*, 2014; *Smith et al.*, 2014]. Similar features were also observed in the middle and inner shelf sections of the Dotson-Getz Trough [*Graham et al.*, 2009; *Larter et al.*, 2009]. Radiocarbon ages and

chronological constraints from relative palaeomagnetic intensity dating on marine sediment cores from the inner shelf suggest that the grounding line of the WAIS had retreated to within 110 km of its present location before 11.2 ka B.P. in both the eastern and the western ASE [*Hillenbrand et al*., 2010, 2013; *Larter et al*., 2014]. The driving mechanisms for the ice retreat from the ASE shelf following the LGM are only poorly constrained. The topography of the seafloor seems to have played a significant role in accelerating the deglaciation of the deep inner shelf, while the timing of retreat also suggests that post-LGM global sea level rise during the last deglaciation may have also driven grounding-line retreat. In addition, melting induced by upwelling warm water has been invoked in driving post-LGM WAIS retreat from the ASE shelf but firm data evidence is currently lacking [*Lowe and Anderson*, 2002; *Smith et al*., 2011, 2014; *Jakobsson et al*., 2011; *Kirshner et al*., 2012; *Larter et al*., 2014].

Estimates of the time that surface rocks around the ASE have been exposed (see *Dunai* [2010] for details of the types of technique used) indicate that significant post-LGM ice sheet thinning occurred in the hinterland of the Dotson Ice Shelf between 12.6 and 8.6 ka [*Lindow et al*., 2014] and in the hinterland of the Crosson Ice Shelf between 14.5 and 11.7 ka [*Johnson et al*., 2008], which is consistent with the reconstructions from the marine sediment cores. However, the data also revealed rapid WAIS thinning in the Pine Island Bay region at ~8 ka, i.e., >3000 years later than the deglaciation of the inner shelf [*Johnson et al*., 2014]. Notably, detailed geomorphological and sediment core data from the outer and middle shelf parts of Pine Island Trough were interpreted to indicate that there the buttressing effect of ice shelves formed during the last deglaciation temporarily halted and deferred post-LGM grounding-line retreat and that only the subsequent breakup of these ice shelves triggered further major and rapid landward retreat [*Jakobsson et al*., 2011, 2012; *Kirshner et al*., 2012]. *Larter et al*. [2014] pointed out that such an ice shelf, extending for more than 200 km from the inner to the middle shelf in Pine Island Trough, is required to reconcile the marine deglaciation ages published from the midshelf [*Kirshner et al*., 2012] with those from inner Pine Island Bay [*Hillenbrand et al*., 2013]. If an ice shelf also existed in inner Pine Island Bay from 11.2 ka B.P. until its collapse around 8 ka, its buttressing effect might explain the delay between grounding-line retreat from the shelf and ice sheet thinning in the Pine Island Bay hinterland [*Johnson et al*., 2014]. Until now, however, no unequivocal evidence for the existence of any extended ice shelf in the eastern ASE during the early Holocene has been presented [cf. *Jakobsson et al*., 2011; *Graham et al*., 2013], and various explanations can be given for reconciling all the available marine and terrestrial deglaciation ages from the area [*Larter et al*., 2014; *Smith et al*., 2014; *Witus et al*., 2014]. For example, it has to be kept in mind that all marine radiocarbon dates give only minimum ages for grounded ice sheet retreat and that microfossils, from which many of the radiocarbon dates were obtained, might have been reworked.

Only limited geological information is available about glaciological changes in the ASE during the last few millennia. *Kirshner et al*. [2012] reported silt-rich sedimentary units in cores from the eastern ASE shelf, which they interpreted as meltwater plume deposits. From further analyses of these units, the authors concluded that at least three meltwater plume events affected sediment deposition in Pine Island Bay since 7–8 ka B.P., with the latest event occurring in modern times [*Witus et al*., 2014]. *Kellogg and Kellogg* [1987] reported that the first sediment cores collected from inner Pine Island Bay were almost barren of planktic microfossils and attributed this to deposition beneath a former extension of the floating terminus of PIG, probably within the last 100 years [cf. *Steig et al*., 2012]. However, *Kellogg and Kellogg* [1987] also observed a general lack of planktic microfossils in outer shelf sediments of the eastern ASE and alluded to the possibility that winnowing by ocean currents may have prevented the deposition of the planktic microfossils.

Interestingly, the terrestrial surface exposure ages in the vicinity of PIG show no further ice sheet thinning after ~6 ka and 7.5 ka, respectively [*Johnson et al*., 2014]. Thus, the data suggest either a stoppage of post-LGM thinning of the WAIS in this area from 6 ka until recently or a local ice sheet thickening during the last few millennia or centuries. Surface exposure ages on an erratic boulder and bedrock collected from islands in inner Pine Island Bay range from 13.8 ka to 2.2 ka, but currently, it is unclear whether these dates indicate the timing of local ice margin retreat or the emergence of the islands above regional sea level caused by glacioisostatic rebound [*Johnson et al*., 2008; *Larter et al*., 2014; *Lindow et al*., 2014].

2.2. Observational Records

Direct observational records began with the discovery of Pine Island Bay in 1947 during a visit to the area by the U.S. Navy vessel USS *Pine Island* during Operation High Jump [*Byrd*, 1947]. During the operation, aerial

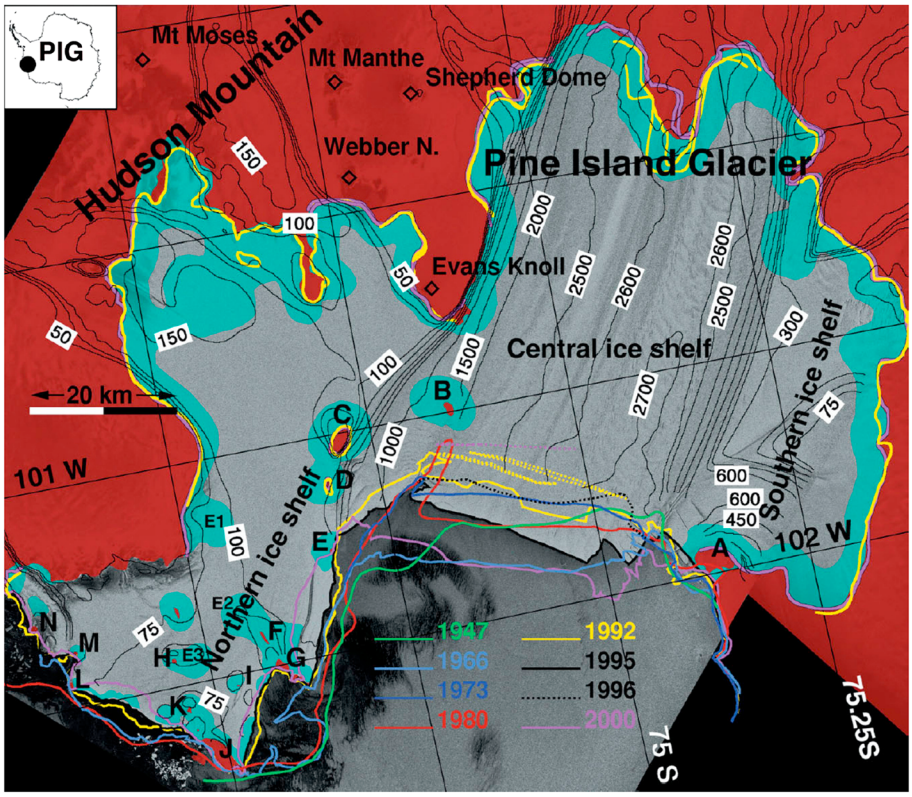

Figure 3. ERS-1 image of Pine Island Bay acquired on 12 November 1995 overlain on the ice-front position in 1947 (green), 1966 (light blue), 1973 (dark blue), 1980 (red), 1992 (yellow), 1995 (black), and 2000 (purple). The dotted lines indicate the location of cracks which appeared prior to a large calving event, with a color coding corresponding to the year of observation (e.g., dotted yellow for 1992 crack). The grounding-line positions in 1992 and 2000 are shown in yellow and purple, respectively. In places where two 1992 or 2000 curves are present, the mapping was done twice with independent pairs. The 1996 grounding-line position (not shown in black) is equivalent to the transition between grounded and floating ice. Tidal flexure zones are colored light blue, with an intensity modulated by radar brightness. Landmarks used for geometric control are indicated with black diamonds and annotated. Ice rises A-N are discussed in *Rignot* [2002]. Latitude is plotted every 0.25°, longitude every degree. Ice velocity is shown in black contours, in m a^{-1}. From *Rignot* [2002].

photographs were taken of the area that allowed the production of the first cartographic map of the region, although there was considerable uncertainty in the absolute georeferencing of the locations on the map. A more complete set of aerial photographs of the area was taken in 1966 allowing the preparation of a new map of the region [see *Rignot*, 2002]. The aerial photographs were supplemented with satellite imagery of the ASE, which became available from the 1970s, although there were large intervals between the successful collection of cloud-free scenes. However, Landsat imagery was collected in January 1973, with routine coverage of the area becoming available from the late 1970s via the lower (1 km) resolution advanced very high resolution radiometer imagery. A major advance in the monitoring of the ASE came with the introduction of the polar-orbiting satellites carrying radar imagers that could provide data regardless of cloud cover, with the first high-resolution radar images of the ASE being obtained by the European Remote-Sensing (ERS) satellites in the early 1990s. As well as providing imagery, the ERS synthetic aperture radar (SAR) data also allowed the application of interferometric techniques to detect the grounding line and to obtain glacier velocity through feature tracking.

2.2.1. Ice-Front Changes

A number of studies have examined changes to the location of PIG's ice front by using the data records that start in the 1940s [*Jenkins et al.*, 1997; *Rignot*, 1998, 2002]. The changes observed in the ice fronts and a number of other parameters relating to PIG, TG, and the ASE as a whole are summarized in Table 1. A comprehensive study of changes was carried out by *Rignot* [2002] using a combination of the early aerial photographs (1947 and 1966), satellite optical imagery (1973 and 1980), and SAR data (1992, 1996, and 2000) to examine a number of aspects of the ice shelves in Pine Island Bay. Figure 3 summarizes the changes to PIG Ice Shelf's

front over the 50 year period covered by the various forms of data. It can be seen that there have been substantial changes in the ice front over the period, but no discernible trend in the overall mean position. The greater data availability in the 1990s revealed year-to-year fluctuations in the ice-front position as a result of major calving events when tabular icebergs up to several kilometers long and 10–20 km wide broke away from the ice shelf. *Rignot* [2002] examined the presence of tabular icebergs at the front of the glacier in all the data since the 1940s and found a reduction in the residence time of the icebergs between the periods 1947–1980 and the 1990s. He suggested that this could be a result of changes in the winds or surface currents, or a decrease in sea ice cover. In more detail, three distinct sections of PIG Ice Shelf (Figure 3) have changed differently over the period examined. The ice front of the southern ice shelf did not migrate between 1947 and 2000. However, the front of the northern ice shelf retreated rapidly, especially in the later part of the period considered.

High-resolution swath bathymetry mapping of a ridge located under the present ice shelf of PIG carried out with an autonomous underwater vehicle (AUV) revealed the presence of particular small-scale bedforms ("corrugations") on the back slope of the ridge at water depths between ~700 and 720 m [*Graham et al*., 2013]. One interpretation of these corrugations is their formation by tidal movements of icebergs [e.g., *Jakobsson et al*., 2011], which would imply that the calving front of the PIG ice shelf was located at least 32 km upstream of its present position at some time during the last 11 kyr [*Graham et al*., 2013]. However, other genetic processes, such as strong bottom currents, may have been responsible for the formation of the corrugations observed under the PIG Ice Shelf, so the scenario of a Holocene ice-front location significantly landward of the modern calving line still needs to be verified [*Graham et al*., 2013].

Two distinct floating parts can be distinguished offshore from the grounding line of TG: the Thwaites Glacier Tongue, which is located downstream of the central trunk of fastest flow, and the Thwaites Eastern Ice Shelf, which became completely separated from the glacier tongue to the west in 2010. The terminus of floating ice between the Thwaites Glacier Tongue and the Thwaites Eastern Ice Shelf has retreated by 26 km from 1973 to 2009 [*MacGregor et al*., 2012] (Figure 4). Thwaites Glacier Tongue calved within 16 km of the grounding line in 2010, but an ice melange still connects the 2,240 km^2 large iceberg and the smaller remaining ice tongue [*MacGregor et al*., 2012]. The floating part of Haynes Glacier had loosely connected the Crosson Ice Shelf, which is fed by the Pope Glacier in the east and the Smith Glacier in the west, to the Thwaites Glacier Tongue back in 1973, but since 1984 it progressively disintegrated, and since 2004 its front has remained close to the grounding line of Haynes Glacier [*MacGregor et al*., 2012]. The terminus of Crosson Ice Shelf has retreated since 1984 as a consequence of its progressive rifting and separation from Bear Peninsula. Its northwestern front retreated by 24 km from 1990 to 2011 [*MacGregor et al*., 2012].

Relatively little work has been carried out to examine the changes in the ice front locations of other glaciers around the ASE. However, *Ferrigno et al*. [1998] used Landsat imagery from the early 1970s and middle to late 1980s/early 1990s to examine ice-front changes over this period. They found that there had been advance of the floating ice front in some areas of the ASE and recession in others, with an overall small advance over the entire study area, but no major trend. Specifically, they found that there had been advance of the TG and Cosgrove Ice Shelf, but with retreat of Smith Glacier and Dotson Ice Shelf.

For the more recent period of 2003–2008 *Pritchard et al*. [2012] found that there had been no changes in the frontal positions of the ice shelves in the region. They also confirmed the earlier finding that the frontal position of the central ice shelf of PIG had not migrated discernibly over the 50 years up to about 2000.

2.2.2. Velocity Estimates and Acceleration of the Glaciers

Estimation of the surface velocity of the ASE glaciers has been possible from the 1970s onward, initially using Landsat satellite imagery, then being refined as improved satellite platforms became available for the purpose [*Mouginot et al*., 2014]. Ground-based instrumentation installed from 2006 onward [e.g., *Scott et al*., 2009] has also provided additional measurements. The consistent spatial pattern over all epochs is that velocities and acceleration are greatest from the grounding line to the floating-portion (ice-shelf) front, while with distance inland from the grounding line, velocities, and acceleration decrease. This provides a first-order indicator of the relative importance of marine influences to the overall changes being observed in the ASE.

Mouginot et al. [2014] presented a comprehensive record of velocity changes along flow lines of all the major glaciers of the ASE for the period 1973 to 2013 (Figures 5 and 6), representing an update and integration of

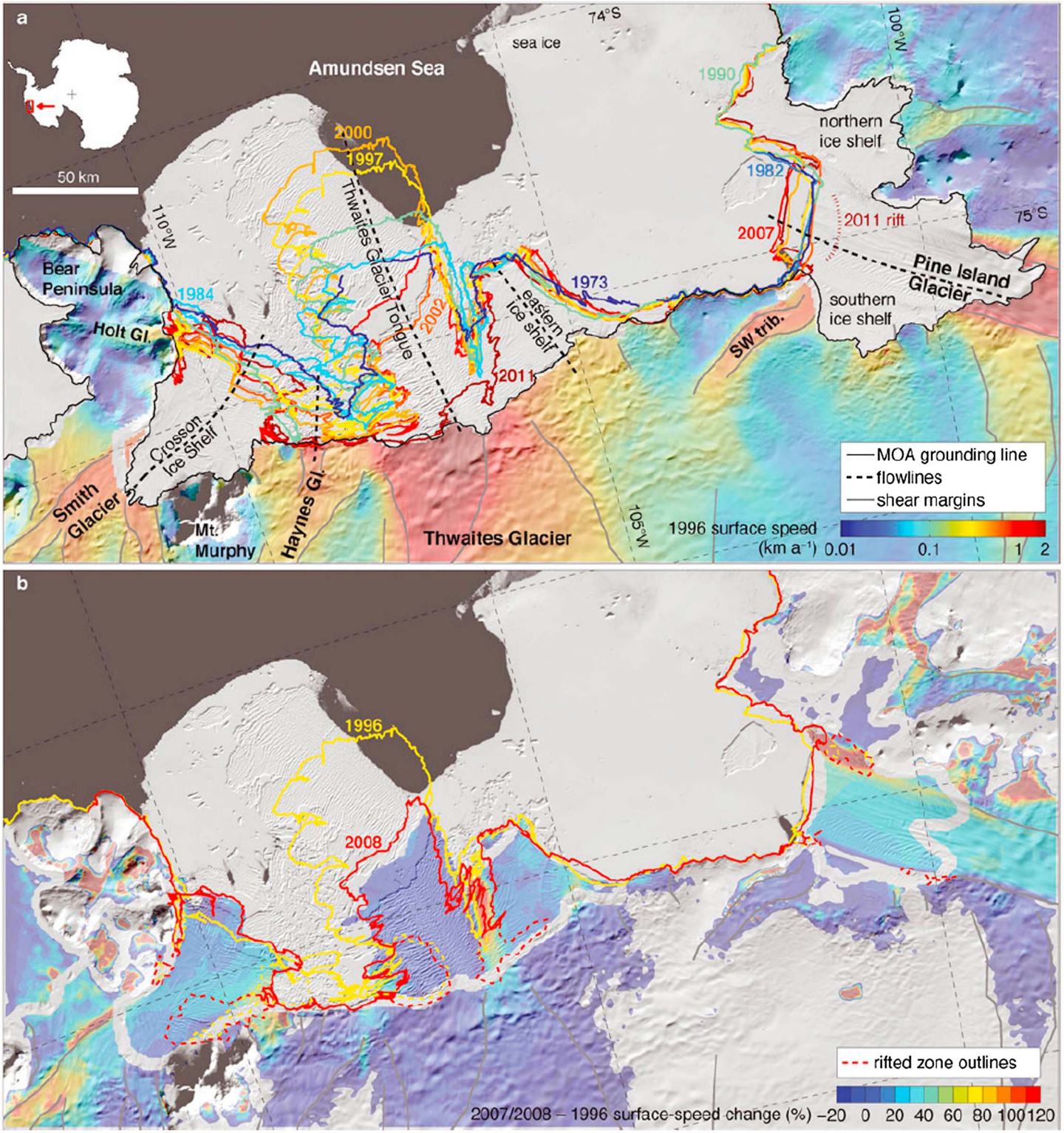

Figure 4. (a) Evolution of the eastern ASE coastline between 1972 and 2011. The gray scale background is 2003–2004 Mosaic of Antarctica (MOA). Superimposed coastlines are traced Landsat 1 through Landsat 7 imagery. The 1996 surface velocities [*Joughin et al.*, 2009] are shown only for ice upstream of the 2003–2004 MOA grounding line [*Scambos et al.*, 2007]. Key central flow lines are shown for the five major ice shelves and tongues in the eastern ASE. Inset map shows the location of the study area in Antarctica. (b) Percent change in surface speed between 1996 [*Joughin et al.*, 2009] and 2007–2008 [*Rignot et al.*, 2011]. The two coastlines bounding this period (1996 and 2008) are also shown, along with outlines of rifted zones at those times. The missing data across the grounding zone are due to missing 1996 surface speeds there. Note that the color scales are saturated to better illustrate the spatial variation of speed change and that portions of some slower-flowing regions ($<50\ m\ a^{-1}$; e.g., Bear Peninsula) show large relative speed changes that are likely spurious. From *MacGregor et al.* [2012].

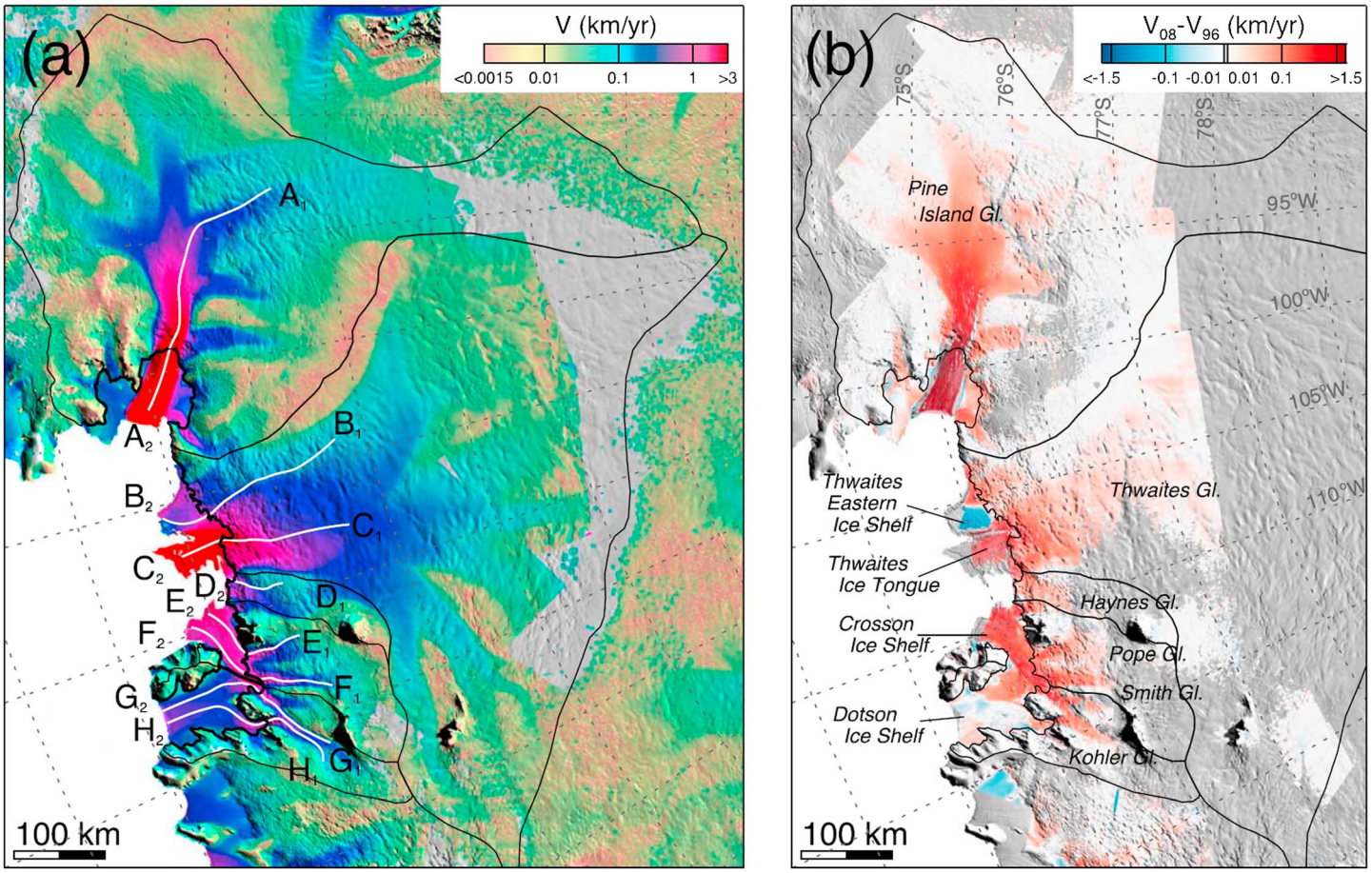

Figure 5. (a) Flow speed of the Amundsen Sea Embayment (ASE) sector of West Antarctica, color coded on a logarithmic scale and obtained combining satellite observations spanning from year 1996 to year 2013 with fluxgates at the location of the grounding lines in 2011 (thick black lines) [*Rignot et al*., 2011] and topographic divides (thin black lines). (b) Change in flow speed between 2008 and 1996, color coded on a logarithmic scale and overlaid on a MODIS mosaic. From *Mouginot et al*. [2014].

earlier studies [*Rignot*, 2002; *Joughin et al*., 2003]. This demonstrates that the ASE glaciers have collectively accelerated over the last four decades, although the acceleration has been nonuniform and variably timed with respect to location.

The satellite observations indicate that PIG accelerated by 11% at its grounding line between 1974 and 1987, maintained largely steady flow from 1987 to 1994, then accelerated by 53% at the grounding line to 2008, before again steadying [*Mouginot et al*., 2014]. Hence, the overall speedup of PIG's floating ice of ~75% since 1973 was, in fact, largely accounted for by two distinct shorter (but still multiple-year) periods of acceleration. Despite the steadying of ice speed at the grounding line from 2008, however, upstream PIG continued to accelerate between 2010 and 2013 [*Mouginot et al*., 2014].

TG has exhibited a more spatially complex response, apparently related to the varying nature of its ice shelf (or shelves) from west to east along the margin. The faster-flowing western TG terminates in the 50 km wide Thwaites Ice Tongue, an ice shelf that has progressively shortened with ice calving since observations began, while the slower-flowing eastern TG flows into Thwaites Eastern Ice Shelf that is buttressed by ice rumples. From 1973 to 1996 Thwaites Ice Tongue accelerated by 33% with the upstream ice in western TG experiencing complementary drawdown [*Rignot et al*., 2002]. From 1996 to 2006, however, Thwaites Ice Tongue and western TG maintained uniform speed, while the Thwaites Eastern Ice Shelf accelerated by 50% [*Rignot*, 2008; *Mouginot et al*., 2014]. From 2006 to 2013, Thwaites Ice Tongue (western TG) again accelerated by a further 33%, but eastern TG initially decelerated by 80% to 2008, but then accelerated once again by 25% [*Mouginot et al*., 2014]. Throughout the whole period of observations the "fast-flow" trunk of TG has also steadily widened.

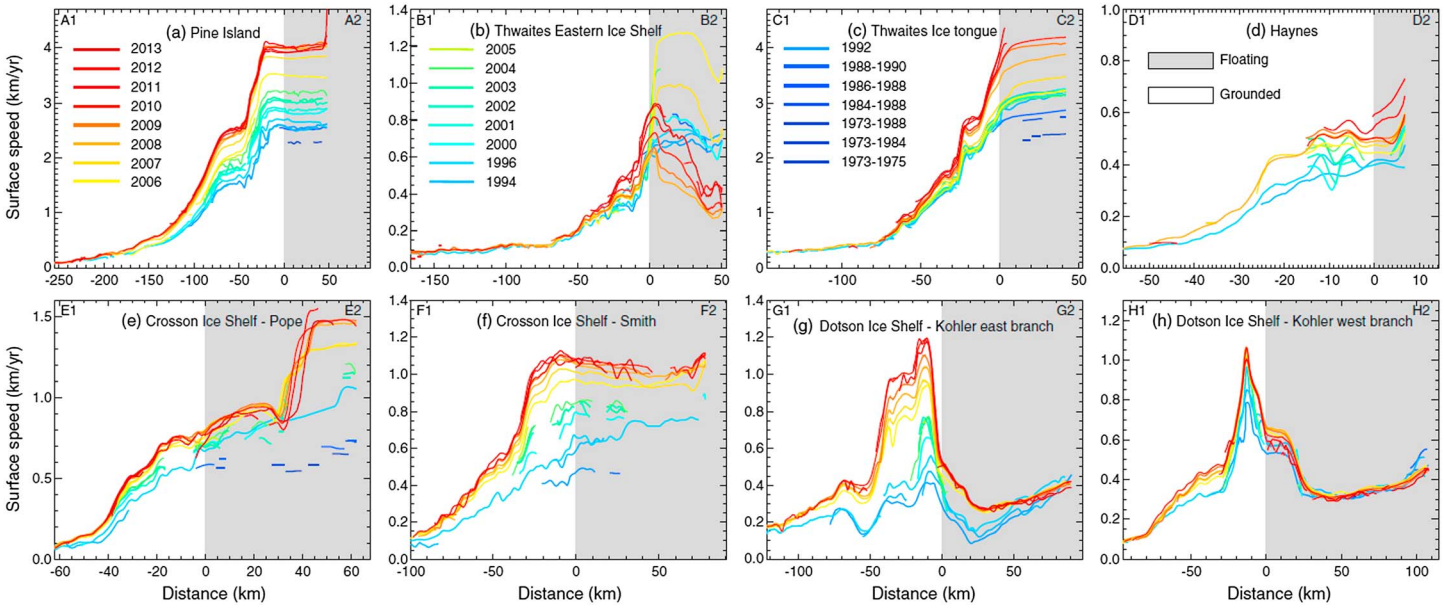

Figure 6. (a–h) Flow speed along the flow lines, A1/A2 to H1/H2, respectively, shown in Figure 5 spanning from year 1973 (blue) to year 2013 (red). Gray shading is used for the floating part of the glaciers in 1996. From *Mouginot et al.* [2014].

Moving west from TG, Haynes, Pope, Smith, and Kohler Glaciers represent the ASE's remaining major fast-flow features, and all these, too, have increased in speed relative to the 1990s, yet exhibiting different specific behaviors over the last 25 years.

Ground-based GPS monitoring of ice velocity on PIG at sites 55, 111, and 171 km upstream of the grounding line between December 2006 and February 2008 [*Scott et al.*, 2009] yielded velocity and acceleration values compatible with *Mouginot et al.*'s [2014] satellite-derived values for the same period. Where the GPS measurements supplement understanding of the processes obtained from satellite remote sensing is that they also permitted an assessment of potential interseasonal ice-velocity variation. They did not, however, reveal a difference in ice velocity in austral summer versus austral winter. The same GPS stations were also monitored at 10 s intervals between December and February during each of the two austral field seasons 2006/2007 and 2007/2008, with the aim of potentially capturing tidal influences on ice flow as seen elsewhere in West Antarctica [cf. *Gudmundsson*, 2007]; however, no discernible variations in ice-velocity were observed over these shorter time scales either. Thus, despite ice-velocity observations being undertaken over tens to annual time scales, the only trend which has been captured from >50 km upstream of PIG's grounding line has been a gradual acceleration of ice flow over decades, with negligible short-term variability.

Of the other ASE glaciers, only TG has also been monitored with GPS instrumentation: stations monitored there between 60 and 335 km upstream of the grounding line showed 1–2% velocity increases between 2007/2008 and 2008/2009 (K. Christianson, personal communication, 2016).

2.2.3. Thinning

While PIG has been retreating and accelerating in recent decades, the glacier, along with the Thwaites, Smith, and Kohler glaciers, has also been thinning due to ice dynamics [*Rignot*, 1998; *Shepherd et al.*, 2001; *Mouginot et al.*, 2014]. Various satellite data have been used to investigate the thinning of PIG. ERS SAR data were used by *Rignot* [1998] to estimate that the PIG had been thinning at a rate of 3.5 ± 0.9 m/yr over 1992–1996. Altimeter measurements from the ERS satellite were also used to determine the changes in ice thickness of the entire PIG drainage basin between 1992 and 1999. Altimeter range measurements were differenced at individual crossing points of the satellites' ground tracks to determine the elevation changes within the basin [*Shepherd et al.*, 2001]. They used range measurements from ERS-1 and ERS-2 35 day orbit repeat cycles to create a time series of elevation change at each individual crossing point (Figure 7). They found that between 1992 and 1999 the interior of the drainage basin thinned at a rate of approximately 0.1 m/yr. They also found that this thinning extended into the neighboring TG drainage basin. However, the data showed a more rapid thinning of the PIG in areas where the ice motion was faster. Thinning of 1.6 ± 0.2 m/

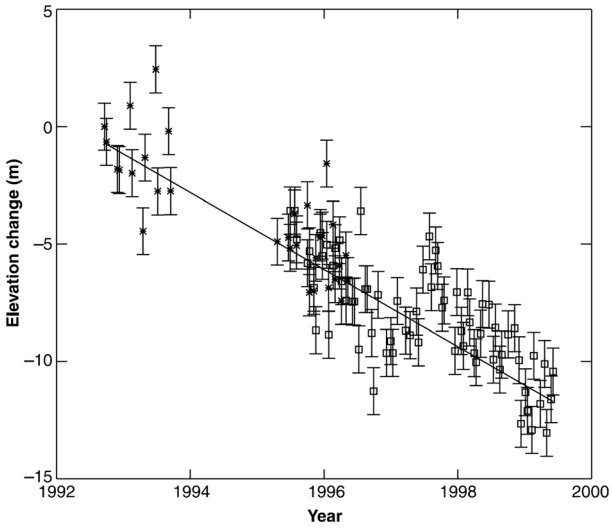

Figure 7. The change in surface elevation 13 km upstream of the grounding line of PIG between 1992 and 1999, observed by the ERS-1 (stars) and ERS-2 (squares) satellite altimeter. From *Shepherd et al*. [2001].

yr occurred near the grounding line. Although the thinning was less inland, it could be detected 150 km upstream from the grounding line. *Park et al*. [2013] found that the ice thinning of the PIG started about 200–250 km inland and increased sharply toward the PIG hinge line, which is the limit of tidal flexing.

Rignot [2002] estimated that the PIG was thinning at a rate of 1.9 m/yr for 1992–2000 and 2.1 m/yr for 1992–1996. These values are consistent with the estimate of 1.6 m/yr over 1992–1999 produced by *Shepherd et al*. [2001]. No trend was found in the rate of ice thinning over the 8 years considered.

The study of *Thomas et al*. [2004] used laser altimeter measurements made from aircraft flights over the glaciers of the ASE in 2002, which were compared with surface elevation values derived from satellite laser altimeter data acquired by the ICESat satellite in late 2003 and early 2004 to estimate changes in elevation. They made four flights across the glaciers of the ASE, with the mean thinning rate being 1.0 m/yr. All flights revealed thinning, with average values ranging from 0.4 m/yr (for the flight primarily over PIG tributaries) to 1.8 m/yr (for the flight crossing the seaward ends of TG, Haynes Glacier, Pope Glacier, Smith Glacier, and Kohler Glacier). The thinning rate for TG was broadly consistent with the value of 0.55 ± 0.09 m/yr found by *Shepherd et al*. [2002], although their figure of 3.21 ± 0.24 m/yr for the thinning of the Smith Glacier was larger. Overall, *Thomas et al*. [2004] found that the rate of thinning over 2002–2004 was double that of 1992–1999.

As more satellite data became available it was possible to gain greater insight into the temporal and spatial evolution of the thinning, which revealed that the area of the PIG experiencing thinning has been expanding. In 1995, thinning was only detected in the central trunk, with rates in excess of 1 m/yr confined to the ice plain. *Wingham et al*. [2009] used ERS-2 and Envisat radar altimeter data to determine the changes in the thinning of the PIG over 1995 to 2006. They found that the thinning had accelerated and spread inland over this period, and by 2006 encompassed all the glacier's tributaries with rates exceeding 1 m/yr extending to 100 km upstream of the grounding line. At the grounding line the thinning rates increased from 3 m/yr in 1995 to 10 m/yr in 2006. *Wingham et al*. [2009] estimated that the cumulative effect of thinning at the PIG grounding line amounted to a change of approximately 80 m over 1995 to 2008. *Wingham et al*. [2009] also found that the terminus was not the region of greatest accelerated thinning but found this to have been about 50 km inland.

Scott et al. [2009] estimated the thinning of the PIG from their GPS data using their observations of the speed in the direction of flow, the vertical speed, the surface gradient in the direction of flow, and the rate of accumulation. They found a decrease in surface elevation during both the 2006/2007 and 2007/2008 seasons at all the GPS sites. This can be compared with elevation change derived for the same sites using satellite laser altimetry, calculated from ICESat data, for the period of 2003–2007. The comparison showed that the thinning is increasing and that it is strongest close to the grounding line. The *Scott et al*. [2009] analysis of ICESat data was consistent with the earlier ICESat results presented by *Thomas et al*. [2004], which showed that during

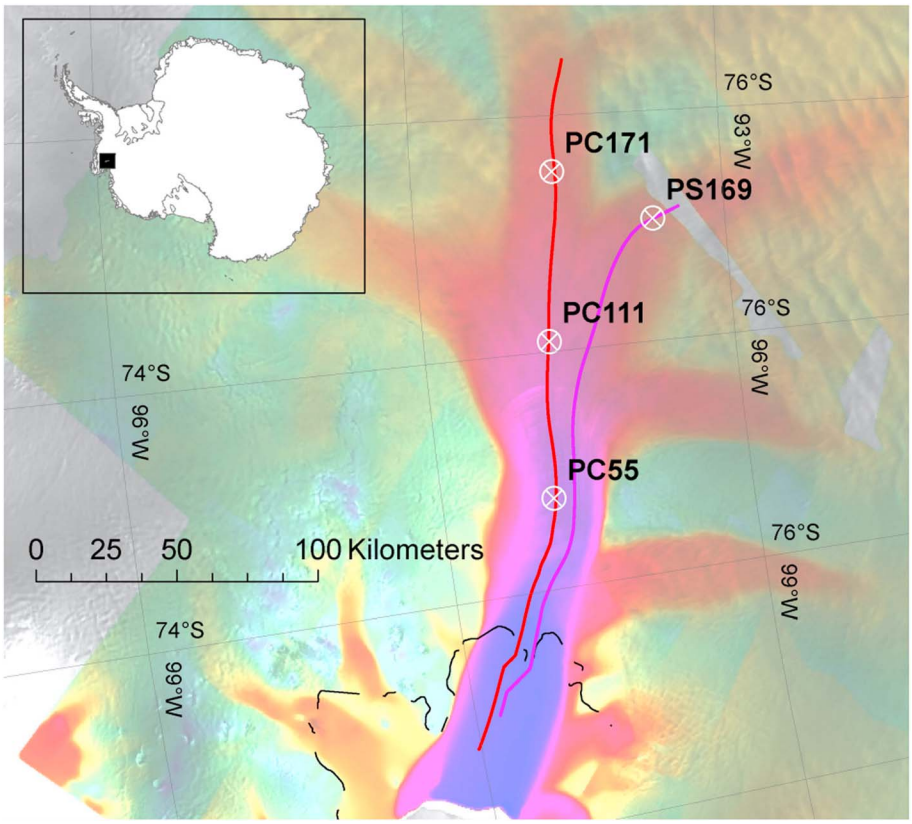

Figure 8. PC55, PC111, and PC171 are locations of GPS receives on PIG used in the study of *Scott et al.* [2009]. Flow lines in red and purple; grounding line (2000) in black. Background is velocity magnitude from ERS-1/ERS-2 data overlaid on a RADARSAT-1 mosaic. From *Rignot* [2006].

2004 thinning was approximately double that of the 1990s. The rates of thinning from late 2006 to early 2008 from GPS are even higher at around 3 times greater than in the 1990s. The rate of slope increase over the central region of PIG between locations PC55 and PC171 (see Figure 8) was found to be approximately constant at $2.06 \times 10^{-5}\,\mathrm{yr}^{-1}$ during the 2006/2007 season and $2.28 \times 10^{-5}\,\mathrm{yr}^{-1}$ for 2007/2008. The thinning rates from the Scott et al. study showed that the PIG was steepening at an increasing rate.

While a great deal of research has been focused on the thinning of PIG, there has been less study of other glaciers in the ASE. However, *Rignot et al.* [2013] identified an area-average thinning rate of 2.9 ± 0.3 m/yr over the Dotson Ice Shelf over 2003 to 2008.

An Antarctic-wide study was carried out by *Pritchard et al.* [2012] using satellite laser altimeter data to examine thickness changes for all the major ice shelves and neighboring grounded ice for the period of 2003–2008. This was carried out with repeat track elevation measurements from the NASA ICESat satellite [*Pritchard et al.*, 2009]. The study showed that the most rapid ice shelf thinning of up to 6.8 m/yr was occurring along the coast of the Amundsen and Bellingshausen Seas. The observations of *Pritchard et al.* [2012] [cf. *Rignot et al.*, 2013] support the suggestion that the most rapid thinning affects glaciers with thick ice shelves floating on seawater with relatively high temperatures, with the water able to access the base of the ice shelves and the grounding zone by advection through deep bathymetric troughs spanning the continental shelf [e.g., *Jacobs et al.*, 1996, 2011, 2013; *Walker et al.*, 2007; *Wåhlin et al.*, 2010; *Nakayama et al.*, 2013; *Dutrieux et al.*, 2014].

2.2.4. Changes in the Locations of the Hinge Lines

The hinge and grounding lines of the ice streams, which tend to be a few kilometers apart, can be located via satellite radar interferometry observations and used to estimate the retreat with time. Various estimates have been made of the changes in these positions with the time series of locations gradually being extended with time. One of the first estimates was produced by *Rignot* [1998], who used SAR data from the ERS-1 and ERS-2

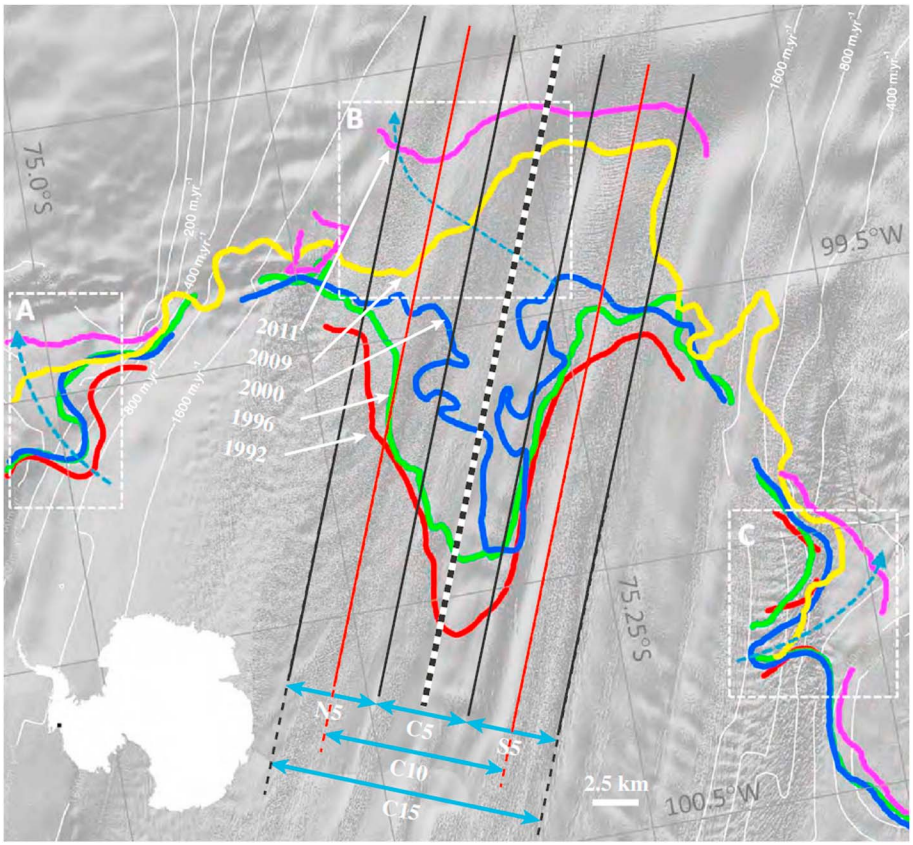

Figure 9. Hinge-line positions of PIG (colored lines) superimposed on a Landsat image (gray scale). Successive hinge-line positions are marked with colored lines (red = 1992, green = 1994, blue = 2000, yellow = 2009, magenta = 2011). The thin white contours show ice velocity (m yr^{-1}). Average rates of hinge-line retreat [see *Park et al*., 2013, Table 1 and Figure 2] were calculated within the northern, central, and southern 5 km sections (N5, C5, and S5, respectively), and within the central 10 and 15 km sections (C10 and C15, respectively). The dotted line marks the satellite radar altimeter track. Boxes A, B, and C highlight other regions of notable hinge-line retreat (blue dotted arrows). Rapid hinge-line retreat has occurred beyond the margins of the glacier in the vicinity of boxes A and C in recent years, despite little apparent change in the glacier surface geometry, suggesting that increased ocean melting has occurred in these regions. Rapid hinge-line retreat in the vicinity of box B has occurred, despite the apparent position of stability in 2009, due to a combination of factors; a narrow channel of lightly grounded ice has favored retreat in a northwest direction in tandem with an evolution of the ice surface slope, which has also promoted retreat. From *Park et al*. [2013].

satellites collected in 1992, 1994, and 1996. He showed that the hinge line of the PIG had retreated at a mean rate of 1.2 ± 0.3 km/yr over this period, which he attributed to thinning of the ice. Further ERS-1 SAR imagery became available in 2000 and was used by *Rignot* [2002] to examine the retreat over the period of 1992 to 2000 and update his earlier results (Figure 3).

Recent studies of changes in the PIG hinge line have been carried out by *Park et al*. [2013] (see Figure 9) and *Rignot et al*. [2014], both based on satellite data for 1992 to 2011. *Park et al*. [2013] found that the greatest retreat had occurred near the central section of the glacier, where the ice had retreated by as much as 28.4 km over the 19 years (1.5 km/yr), although the rate decreased rapidly toward the glacier margins and some places had retreated by as little as 9.5 km. This result is close to the retreat of 31 km identified by *Rignot et al*. [2014].

Park et al. [2013] found that between 1992 and 2010 the average rate of retreat within the central 15 km sector of PIG was broadly constant at 0.95 ± 0.09 km/yr. The near-constant rate of retreat has occurred despite a steepening of the glacier surface and shoaling of the bedrock slopes, which should have impeded the retreat. However, there were considerable temporal variations in the hinge-line retreat, with periods of rapid and asymmetric migration. For example, over the periods of 1992–2000, 2000–2009, and 2009–2011 the hinge-line retreat was concentrated in the central, southern, and northern sections of the PIG, respectively.

The largest measured rate of hinge-line retreat found by *Park et al*. [2013] (2.8 ± 0.7 km/yr) occurred in the northernmost 5 km wide section of the PIG over 2009–2011. Changes in the rate of retreat are a result of differences in the glacier geometry. For a constant rate of ice thinning, the rate of hinge-line retreat is dependent on the surface and bedrock slopes. The PIG bedrock and surface slopes shoal and steepen inland of the 1992 hinge-line position, respectively, and this geometry tends to impede retreat [*Park et al*., 2013]. Therefore, the near-constant rate of hinge-line retreat during the study period of *Park et al*. [2013] reflects an accelerated rate of ice thinning. For the central 10 km of PIG the rate of ice thinning associated with hinge-line retreat has increased from 2.1 ± 0.7 m/yr for 1992–1996 to 11.6 ± 1.1 m/yr for 2009–2011. The average rate of ice thinning at the PIG hinge line has accelerated by 0.53 ± 0.15 m yr^{-1} over the 19 year study period.

The rates of hinge-line retreat of PIG agree well between studies carried out with different forms of data during overlap periods. For example, average retreat rates of 0.64 and 0.55 km/yr estimated across a 14 km wide center profile were computed by *Rignot* [1998] for the periods of 1992–1996 and 1996–2000, respectively. These compare with the estimated retreat rates of 0.63 ± 0.23 and 0.92 ± 0.23 km/yr across a partially overlapping 15 km wide profile in the study of *Park et al*. [2013]. Before 2009 the steep surface slopes to the north of the PIG hinge line presented an obstacle to retreat. Since then the hinge line has retreated across a submarine ridge (Figure 9) and the trajectory of retreat has been northward and inland, eroding a grounded promontory that was present in 2009. The PIG hinge line has now migrated into the trough within which the main trunk of the glacier is seated, where basal slopes shoal and impede retreat, and it is now retreating at a faster mean rate (1.8 ± 0.9 km/yr) than at any time since it was first located [*Park et al*., 2013]. The retreat has resulted in an area of 14.2 ± 1.3 km^2 becoming ungrounded each year [*Park et al*., 2013].

2.2.5. Changes in the Locations of the Grounding Lines

Considering the whole ASE, *Rignot* [2002] found that grounding-line retreat had been greatest for the PIG, continuing the retreat observed up to 1996. However, there was little retreat observed along the southern and northern ice shelves (see Figure 3). This is in agreement with other studies, such as *Shepherd et al*. [2001], who found a retreat of the grounding line along several of the tributaries of the PIG, but the amplitude of the retreat was much less than along the PIG itself. *Rignot* [2002] noted that the grounding-line position of PIG in 2000 was more sinuous than seen in the previous years, which could be attributed to the presence of a low-slope region immediately upstream of the 1996 grounding line. Further satellite data from the Terra-SAR-X satellite collected in 2009 showed that the grounding-line position had retreated by 20 km between 1996 and 2009 [*Joughin et al*., 2010], significantly more than the 5 km retreat over 1992 to 1996 noted by *Rignot* [1998]..

At present the grounding line of PIG is crossing a retrograde bedrock slope that lies well below sea level, raising the possibility that the glacier is susceptible to the marine ice sheet instability mechanism [*Schoof*, 2007; *Durand et al*., 2009; *Joughin et al*., 2010]. However, the stability of a marine ice sheet is not only a function of local slope at the grounding line [*Gudmundsson*, 2013]. Although it appears from the Bedmap2 compilation [*Fretwell et al*., 2013] that the grounding line of PIG is already partly located on a reverse bed slope, the grounding line is therefore not necessarily unstable. Recent estimates of velocity change show almost no change in velocity of PIG around the grounding line between 2012 and 2014, and the flow speeds over the ice shelf have not increased since 2010 [*Mouginot et al*., 2014]. It therefore appears that the strong acceleration phase between 1973 and 2010, when ice shelf flow speeds increased by 75% [*Mouginot et al*., 2014], has ended, and we have now entered a new period of little or no change. Although further up-stream of the grounding line of PIG, velocities continue to increase, this is possibly simply a delayed response to past changes around and downstream of the grounding line, rather than the beginning of an unstable retreat phase.

The *Rignot et al*. [2014] study also examined grounding-line retreat of other glaciers in the ASE over 1992 to 2011. They found that the greatest retreat of 35 km had been experienced by the Smith/Kohler glaciers, with 14 km of retreat in the fast-flowing core of TG and 10 km on the flanks of the Haynes Glacier.

2.2.6. Estimated Net Loss of Ice

The change in the mass of ice in an area can be considered as the difference between the input of snow and the loss of ice from the edge of the ice shelf and melting from below. These are rather difficult quantities to estimate, and over the last few decades a number of different attempts have been made to determine the

different components that affect the balance and to estimate the overall mass loss of PIG and other glaciers of the ASE and how this has changed with time.

In the ASE region, snow accumulation is the dominant component of the surface mass balance, with ablation processes such as meltwater runoff, sublimation, and blowing snow processes small by comparison [*Lenaerts et al*., 2012a], although some studies [e.g., *Kellogg et al*., 1985] suggest that these quantities might be significant on the floating tongue of PIG, although probably only on very limited horizontal scales. However, the ASE is a sparsely observed region, and there is limited availability of field measurements, which makes determining snow accumulation highly challenging. For example, *Medley et al*. [2013] reported that although a few ice core records of accumulation exist at elevations above 1200 m above sea level, no such ice cores exist at low-level coastal sites. Moreover, *Favier et al*. [2013] identified the ASE region (and more broadly West Antarctica) as one of the areas of Antarctica, where there are no reliable field measurements of snow accumulation, and recommended that addressing this be made a scientific priority. The considerable uncertainties in mass balance and future contribution to sea level rise from glaciers in the ASE region are therefore in part because of significant uncertainties in estimating snow accumulation.

Recently, a number of airborne-radar surveys have taken place over the Pine Island-Thwaites drainage system, which are able to provide annual accumulation measurements for the region [*Medley et al*., 2013, 2014] The results report accumulation rates of up to 0.7 m water equivalent (we) yr^{-1} in the lower elevation coastal zone, compared to rates of around 0.3 m we yr^{-1} over the high-elevation interior. These values are broadly in agreement with the estimates using satellite microwave observations [*Arthern et al*., 2006].

The spatial distribution of snow accumulation over the ASE region is largely determined by cyclonic activity in the Ross and western Amundsen Seas (predominately found in winter-spring), which steers the circumpolar belt of westerlies toward the ASE coastline [*Nicolas and Bromwich*, 2011]. The low coastal orography of the ASE region allows these winds to penetrate inland, resulting in enhanced intrusions of moisture-laden air. The ensuing orographic lifting of the air over the coastal slopes causes some of the highest snow accumulation rates in Antarctica. Accumulation rates derived from atmospheric modeling suggest values in excess of 1 m we yr^{-1} along the coastal margins of the ASE [*Monaghan et al*., 2006a; *Lenaerts et al*., 2012b].

Turning to the mass balance, estimates have been made for the Antarctic as a whole and the main ice sheets. *Shepherd et al*. [2012] used a variety of satellite data to compute the mass balance of sectors of the Antarctic for the period of 1992–2011, with their estimates being East Antarctica ($+14 \pm 43$ Gt yr^{-1}), West Antarctica (-65 ± 26 Gt yr^{-1}), and the Antarctic Peninsula (-20 ± 14 Gt yr^{-1}).

The mass balance of the glaciers of the ASE, except for TG, were approximately in balance in the 1970s, but after that time experienced a mass loss that increased, first slowly, then increasingly rapidly in the latter decades of the 20th century and early part of the present century [*Rignot*, 2008].

One of the first detailed studies to examine the mass changes of the PIG was carried out by *Rignot* [1998] who estimated the ice discharge of the glacier to be 76 ± 2 km^3/yr at the hinge line over 1992–1996. With the input of ice from the interior estimated as 71 ± 7 km^3 of ice per year, he suggested that the mass deficit was 5 ± 7 km^3/yr upstream of the hinge line. The subsequent study by *Shepherd et al*. [2001] estimated that the mass of the PIG was decreasing at a rate of 3.9 ± 0.9 Gt/yr or 5% of the mass across the grounding line, which is equivalent to 0.01 mm/yr of eustatic sea level rise. Based on a combined analysis of airborne laser altimetry and radio echo sounding data and interferometric SAR and ERS-1/ERS-2 satellite altimetry data, *Rignot et al*. [2004] concluded that the mass balance of PIG in 2002 was -9 ± 8 km^3/yr in 2002, contributing to a mass loss totaling 81 ± 17 km^3/yr for all glaciers draining into the ASE. Figures for mass loss of PIG obtained by *Wingham et al*. [2009] indicated that the ice loss at the trunk of the PIG quadrupled from 2.6 ± 0.3 km^3/yr in 1995 to 10.1 ± 0.3 km^3/yr in 2006, which is comparable to the rates estimated by using ground-based observations [*Scott et al*., 2009].

The later work of *Rignot* [2008] involved a comparison of the ice fluxes with snow accumulation. He estimated that the total ice flux from this entire sector increased from 184 ± 8 Gt/yr in 1974 to 215 ± 7 Gt/yr in 1996, 237 ± 7 Gt/yr in 2000, and 280 ± 9 Gt/yr in late 2007. More recently, *Mouginot et al*. [2014] estimated that the ice fluxes of the ASE drainage sector were 189 ± 17 Gt/yr in 1974 and increased to 235 ± 9 Gt/yr in 1996, 247 ± 12 Gt/yr in 2001, 306 ± 10 Gt/yr in 2007, 328 ± 13 Gt/yr in 2010, and 334 ± 14 Gt/yr in 2013. This gives overall increases in ice losses from the ASE region from 7 ± 26 Gt/yr in 1974 to 39 ± 27 Gt/yr in 1996,

and 105 ± 27 Gt/yr in 2007 [*Rignot*, 2008]. In addition, between 1996 and 2006 net loss from the combined PIG and TG drainage basins rose from 41 to 90 Gt/yr [*Rignot et al*., 2008]. The PIG basin alone, which only comprises 10% of the WAIS, had an estimated rate of net mass loss of 46 Gt/yr in 2007 giving it the greatest imbalance of any ice stream in the world [*Rignot*, 2008]. Satellite-gravimetry estimates by *King et al*. [2012] indicate that between 2002 and 2010 mass losses were on average 24 ± 7 Gt/yr in the PIG drainage basin and 54 ± 5 Gt/yr in the TG drainage basin.

2.2.7. Basal Melting

The regional thinning of the glaciers in the ASE sector cannot be explained by negative surface mass balance, firn compaction, retreating ice shelf fronts, or by reduced glacier influx [*Pritchard et al*., 2012; *Rignot et al*., 2013]. The consensus view [e.g., *Wingham et al*., 2009] is that the evidence pointed to the thinning being caused by greater ocean-driven basal melt (for a full discussion of subaqueous melt of glaciers see *Truffer and Motyka* [2016]), with the greatest thinning taking place where warm water is accessing the thick ice shelves via bathymetric troughs extending from the coast to the shelf break. However, determining the magnitude of the melt under a glacier is difficult to determine, although various estimates have been made over recent decades.

A hydrographic survey in 1994 found that PIG was experiencing basal melt rates 1 order of magnitude larger than those recorded under large Antarctic ice shelves [*Jacobs et al*., 1996; *Hellmer et al*., 1998]. *Jenkins et al*. [1997] determined that the position of the ice-shelf front of PIG showed no persistent trend in the period of 1973–1994 and combined this with an estimate of the flux divergence between grounding line and ice front, and an assumption of steady state to calculate a mean basal melt rate over the ice shelf of $12 \pm 3\ \mathrm{m\ yr^{-1}}$. Using similar techniques, but with new and more extensive measurements of ice velocity and grounding-line position, *Rignot* [1998] estimated an average of basal melt rate of $24 \pm 4\ \mathrm{m\ yr^{-1}}$ between the grounding line and the calving front, but with most of that melting occurring near the grounding line with rates in excess of $50 \pm 10\ \mathrm{m\ yr^{-1}}$ over the first 20 km of the subice cavity. Comparable melt rates were found in subsequent investigations with rates of more than 40 m/yr over the first ~30 km of the ice shelf being driven by the strongest thermal forcing found near the deep grounding line [*Rignot and Jacobs*, 2002]. *Payne et al*. [2007] derived the spatial distribution of melting and found rates well in excess of $100\ \mathrm{m\ yr^{-1}}$ in regions very close to the grounding line, while *Dutrieux et al*. [2013] showed that even greater spatial heterogeneity in melting was associated with a network of basal channels incised into the ice shelf base. Near the grounding-line melting was found to be highest within the channels, suggesting a role for the ocean in enhancing the features, while further downstream the reverse was true. Recent area-averaged estimates indicate sub-ice-shelf melt rates of around 15–18 m/yr for PIG, TG, and for the Crosson Ice Shelf; 1.7 and 2.8 m/yr for the Abbot and Cosgrove Ice Shelves; and 7.8 and 4.3 m/yr for the Dotson and Getz Ice Shelves [*Shepherd et al*., 2004; *Depoorter et al*., 2013; *Rignot et al*., 2013].

Oceanographic observations at the ice front allow estimates of meltwater transport away from the subice cavity. They typically rely on the assumptions of steady state conditions within the cavity and a cross-ice-front circulation that is close to geostrophic balance, but with those caveats provide an estimate of melting with relatively little inherent temporal averaging. The results are, however, spatially integrated over the indeterminate area from which the meltwater that crosses the oceanographic section is gathered. *Jacobs et al*. [2011] applied the techniques described by *Jenkins and Jacobs* [2008] to two sections along the PIG ice front observed in 1994 and 2009. They found the meltwater transport away from the shelf to be 50% higher in 2009 compared with 1994 and argued that a relatively modest change in ocean temperature was only partly responsible. Conditions over the wider continental shelf were cooler in 2000 [*Jacobs et al*., 2012], yet there was apparently no glaciological response to the cooling [*Rignot*, 2008], suggesting that geometrical change in the subice cavity as the ice shelf thinned and the grounding-line retreat may have exerted a stronger control on the basal melt rate than the far-field ocean conditions. *Dutrieux et al*. [2014] used the same techniques and added oceanographic sections from 2007, 2010, and 2012 to the time series. They found that melt rates in 2007 and 2010 were comparable to those in 2009, but that melting dropped by a factor of 2 in 2012 when the waters in Pine Island Bay cooled. The highest melt transport of $110\ \mathrm{km^3\ yr^{-1}}$ was found in 2007 across a section that was far enough out in Pine Island Bay to capture most of the meltwater produced over the entire ice shelf and compares favorably with the $110 \pm 9\ \mathrm{km^3\ yr^{-1}}$ estimated by *Rignot et al*. [2013]. The fall in melting at the end of the time series must have been a response to the far-field ocean conditions, and *Dutrieux et al*. [2014] argued that the geometry of the subice cavity made the melt rates particularly

sensitive to the depth of the broad thermocline separating the warm CPDW at the seabed from near-freezing point waters in the upper water column. They also argued that the change in thermocline depth was at least partly attributable to atmospheric forcing associated with a strong La Niña event, supporting earlier suggestions of a link with the tropical Pacific that were based on a modeling study [*Thoma et al*., 2008; *Steig et al*., 2012].

2.2.8. Observations Under the Glaciers

Obtaining information on conditions under this part of the WAIS is obviously difficult; however, gaining insight into the subglacier environment is essential because of the importance for ice flow. Using remote sensing techniques a number of studies have gained insight into basal conditions and geothermal heat flux. Basal roughness of PIG was investigated by *Rippin et al*. [2011] using radio echo sounding data, and they found a relationship between faster ice flow and lower basal roughness across significant parts of the glacier. They interpreted the presence of a smooth bed as the result of deposition of marine sediments during earlier periods when the WAIS disappeared. Airborne radio sounding data, along with a model, were also used to investigate geothermal heat flux and basal melting under TG [*Schroeder et al*., 2014], which is an area considered of high importance for future research. They showed that large parts of TG are actively melting in response to geothermal heat flux consistent with rift-associated magma and volcanism.

3. Oceanographic Conditions in the Amundsen Sea

Near-surface air temperatures along the coast of the ASE are almost always below freezing, even in summer, with only one or two reports of temperatures slightly above freezing each summer field season. Surface melt is therefore negligible. Ice shelves are insensitive to surface temperature changes until summer temperatures are high enough to produce sufficient meltwater to fill surface crevasses, at which point they are prone to collapse [e.g., *Doake et al*., 1998; *Scambos et al*., 2003; *DeConto and Pollard*, 2016]. So the main climatic forcing on the ice shelves in the ASE comes from changes in the ocean circulation that can bring warmer waters under the ice. Such a role for ocean change in the flow acceleration, grounding-line retreat, and thinning of the WAIS had long been discussed [*Hughes*, 1973], as had the potential vulnerability of the glaciers of the ASE [*Thomas et al*., 1979; *Hughes*, 1981], but the remoteness of the region and its perennial sea ice cover discouraged oceanographic exploration of the ASE.

The first systematic oceanographic observations of the Amundsen Sea were undertaken from the research ship RV/IB *Nathaniel B. Palmer* in early 1994 [*Jacobs et al*., 1996]. This revealed deep flooding of the continental shelf by CPDW that was almost unmodified from its off-shelf source. CPDW originates in the wind-driven Antarctic Circumpolar Current (ACC) [*Meredith et al*., 2011], and its core, which is upwelling onto the continental shelf of the ASE at water depths of $>$300 m, is relatively warm with a temperature of $>$3.5°C above the in situ freezing point, and salinity $>$34.6. A thermocline (halocline) defined by strong vertical temperature (salinity) gradients lies between the CPDW and the colder, fresher surface waters. Water in and above the resulting pyncnocline (density gradient) is cooled and modified by sea surface processes, but wind and buoyancy forcing are insufficient to deepen the surface layer to the seabed and exclude the CPDW from the shelf as happens around much of the coast of Antarctica. *Jacobs et al*. [1996] argued that the warmth of the CPDW and the deep draft of PIG gave rise to mean melt rates that were 5 times higher than those previously published for George VI Ice Shelf [*Bishop and Walton*, 1981], which is also underlain by CPDW but is considerably thinner. *Jenkins* [1999] showed that the outflows of meltwater from PIG generate near-surface warming, since the mix of CPDW and meltwater is warmer and saltier than the waters above the pycnocline.

At the time of the 1994 survey the topography of the Amundsen Sea continental shelf, including the location of the shelf edge, was almost completely unknown, but that and subsequent cruises gradually added detail. *Nitsche et al*. [2007] combined all the bathymetric sounding data then available to produce a fairly comprehensive map (Figure 1) that revealed a series of bathymetric troughs extending from the deep inner shelf offshore from the main outlet glaciers across the continental shelf to the shelf edge. These bathymetric troughs appear to be the main conduits that guide the flow of the warmest CPDW from the shelf edge to the sub-ice-shelf cavities. Significant on-shelf flows of 0.2–0.4 sverdrup of CPDW have been inferred from oceanographic measurements made in the western branch of Pine Island Trough at 113°W [*Walker et al*., 2007] and in the neighboring Dotson-Getz Trough [*Wåhlin et al*., 2010]. Moorings in the latter trough revealed a bottom intensified southward flow of CPDW on the eastern flank of Dotson-Getz Trough [*Arneborg et al*.,

2012; *Wåhlin et al*., 2013]. The vertical structure was relatively steady in time, but the currents throughout the water column responded to variations in the wind. *Wåhlin et al*. [2013] showed that the flow was part of a cyclonic gyre within the trough transporting warm, salty water toward the ice shelves in the east and cooler and fresher water away in the west. Although a great deal has been learned regarding the flow off the ice shelf, there are few oceanographic moorings from the eastern embayment.

The link between basal melting of the glaciers of the ASE and CPDW intrusions onto the continental shelf is now well established, especially in inner Pine Island Bay [e.g., *Schodlok et al*., 2012; *Dutrieux et al*., 2013; *De Rydt et al*., 2014], where significant progress has been made over recent years in constraining the roles of (i) the geometry and bathymetry of sub-ice-shelf cavities [*Jenkins et al*., 2010; *Tinto and Bell*, 2011; *Muto et al*., 2013, 2016], (ii) features present at the bases of the ice shelves (such as subglacial channels) [*Bindschadler et al*., 2011; *Mankoff et al*., 2012; *Vaughan et al*., 2012; *Stanton et al*., 2013], and (iii) variability of oceanic circulation [*Dutrieux et al*., 2014; *Thurnherr et al*., 2014], in influencing sub-ice-shelf melt processes. However, the amount of CPDW that reaches the sub-ice-shelf cavity is rather variable on interannual time scales. For example, repeat ocean stations on the inner shelf close to 105°W, 74°S showed slightly cooler and fresher waters in 2000 compared to 1994 [*Jacobs*, 2006]. In addition, it is difficult to determine long-term oceanographic changes in the area of the ASE, although *Rignot* [2008] suggested that the inferred near-balance of the ice in the 1970s implied that the ocean changes responsible for the evolution originated for the most part around that time.

Jacobs et al. [2012] described the broader water column structure over the Amundsen Sea continental shelf east of 135°W. CPDW is present in all the cross-shelf troughs but the overlying thermocline deepens and the core temperature declines from east to west. Oceanographic sections from the coast to the shelf break indicate that the thermocline deepens sharply at the shelf break to form a weak version of the Antarctic Slope Front (ASF) that in most other places around Antarctica excludes the CPDW completely from the continental shelf [*Jacobs et al*., 2012]. The cooling of the CPDW as the thermocline deepens to the west is likely to be the result of increased dilution of the thinner layer of CPDW that intrudes beneath the deeper ASF. Similarly, temporal variability of the on-shelf waters seems to be associated with shelf-wide changes in thermocline depth. A deeper thermocline in 2000 led to a thinner layer of cooler CPDW in the troughs compared with a shallower thermocline in 2007 [*Jacobs et al*., 2012]. Since the thermocline is shallowest in the east, the thickest and warmest inflow of CPDW is found in Abbot Trough near 103°W. *Nakayama et al*. [2013] showed that the CPDW in Pine Island Bay was a mixture of that derived from Abbot Trough and the western branch of Pine Island Trough, with the latter contributing about 60% of the total at the time of the observations.

Walker et al. [2013] analyzed a series of high-resolution oceanographic sections that crossed the shelf break in and around the mouth of the western branch of Pine Island Trough at 113°W. They inferred geostrophic currents from the density structure and referenced those to detided shipboard current measurements. The landward dip of the pycnocline (thermocline) gave rise to vertical current shear such that a westward flow at the surface transitioned to an eastward undercurrent at the seabed. Eastward flow at the seabed is significant since the associated Ekman transport in the bottom boundary layer carries CPDW up the continental slope and onto the shelf [*Wåhlin et al*., 2013]. Furthermore, *Walker et al*. [2013] found that the undercurrent was strongest on the western, upstream flank of western Pine Island Trough, all but disappeared over its central part, then reappeared, weaker, on its downstream eastern flank, consistent with the current turning landward within the trough to supply the southward flow that had been identified earlier [*Walker et al*., 2007]. *Walker et al*. [2013] argued that a poorly resolved version of the undercurrent had been responsible for the on-shelf transport of CPDW in an earlier modeling study [*Thoma et al*., 2008]. In that study the strength of the inflow had been found to correlate with the zonal wind at the shelf edge. The zonal wind component is approximately parallel to the shelf edge at 113°W, so if strong easterly winds add a depth-independent current to the west, the undercurrent is weakened, while weak easterly or westerly winds permit a stronger undercurrent. The picture of a bottom intensified, density-driven flow that is enhanced or suppressed by a time-varying, depth-independent, wind-forced current is consistent with the mooring records of *Arneborg et al*. [2012] and *Wåhlin et al*. [2013] from the neighboring Dotson-Getz Trough.

During a 2009 RV/IB *Nathaniel B. Palmer* cruise to Pine Island Bay the Autosub3 AUV was deployed under PIG and collected 510 km of along-track data during a total of 94 h beneath the ice [*Jenkins et al*., 2010].

Bathymetric data collected beneath the ice revealed the existence of a 300 m high submarine ridge on which the glacier had formerly been grounded [*Jenkins et al*., 2010; *Graham et al*., 2013]. The earliest available satellite imagery from the mid-1970s showed a subtle surface feature that *Jenkins et al*. [2010] argued was consistent with the ice shelf being still lightly grounded at that time on the highest point of the ridge. If the retreat of the grounding line down the landward side of the ridge has been a continuous process, the most recent part of which has been captured in the satellite record, and the rates that have been recently observed are typical, it was thought that the start of the process could have been as recent as a few decades prior to the 1970s imagery. The discovery of the ridge was significant for a number of reasons, particularly, that the recent changes may be part of a multidecadal-scale process. A clearer picture of the role of the seafloor ridge came with analysis of data from sediment cores collected from beneath the PIG ice shelf in 2012/2013 [*Smith et al*., 2016]. The core data suggested that the grounding line started to retreat from the deeper parts of the ridge just before 1945, possibly as a result of marked El Niño conditions between 1939 and 1942. This allowed warm CPDW to access the cavity below a large part of the ice shelf, although some parts of the shelf remained grounded until the 1970s. While the ridge crest would have provided a stable grounding-line position, once initiated, the downslope retreat would have been susceptible to the marine ice sheet instability [*Schoof*, 2007]. The ridge now blocks the deepest CPDW from access to the deepening grounding line and explains the high sensitivity of the melt rates to the depth of the thermocline found by *Dutrieux et al*. [2014], since the lower part of the thermocline is typically found around the depth of the ridge crest. It also offers an explanation of why melting in the 1990s may have been more sensitive to changes in geometry than thermocline depth [*Jacobs et al*., 2011]. At the time of the earliest oceanographic observations in 1994, the ice shelf was some 70–80 m thicker than it was in 2009 [*Wingham et al*., 2009], so the gap between ice base and seabed over the crest of the ridge may have been less than 100 m in places, restricting exchange between inner and outer cavity and promoting mixing between inflow and outflow [*Jenkins et al*., 2010].

4. Atmospheric Forcing on the Amundsen Sea Embayment and Recent Changes

4.1. Atmospheric Conditions Across the South Pacific

Changes in the atmospheric circulation over the South Pacific play an extremely important part in modulating the environment of the ASE through forcing of the oceanographic conditions and also changing the precipitation and surface melting across the area, with these factors influencing the glaciology. However, investigating atmospheric circulation changes on decadal time scales is difficult because the meteorological records are relatively short in terms of the glaciological changes. Meteorological observations have been made in Antarctica since the earliest days of exploration, although initially the data were only collected for short periods and for a few well-separated locations. A major advance was the International Geophysical Year (IGY) 1957/1958 when many of the Antarctic research stations that we have today were established and which began the period of collection of long-term meteorological data allowing the investigation of climate change. During the IGY, meteorological analyses were prepared on a routine basis, although there were few observations over the Southern Ocean, so the analyses here are of questionable accuracy. Recently, all the global meteorological data collected since the IGY have been reanalyzed by using current, state-of-the-art data assimilation schemes to produce what are referred to as the reanalysis data sets [*Onogi et al*., 2007; *Saha et al*., 2010; *Dee et al*., 2011; *Rienecker et al*., 2011]. In relatively data-rich areas, such as the U.S., Europe, and the Atlantic Ocean, these reanalyses can provide valuable data on atmospheric circulation variability since the late 1950s. However, over the Southern Ocean the lack of in situ data means that the reanalyses cannot be used until 1979 when satellite sounder data became available [*Hines et al*., 2000; *Marshall and Harangozo*, 2000; *Bromwich and Fogt*, 2004]. This means that we have no detailed information on atmospheric circulation in the vicinity of the ASE until the late 1970s. However, for the post-1979 period the European Centre for Medium-range Weather Forecasts (ECMWF) Interim reanalysis (ERA-Interim) fields are considered to be the best reanalysis data available for depicting recent Antarctic climate [*Bromwich et al*., 2011; *Bracegirdle and Marshall*, 2012].

The atmospheric circulation over the Amundsen Sea is more variable than any other region on Earth [*Connolley*, 1997], which is primarily a result of the large variability in the depth and location of the Amundsen Sea Low (ASL) [*Fogt et al*., 2012; *Turner et al*., 2012a; *Hosking et al*., 2013]. Variability in the ASL, and particularly its longitudinal location, has a strong influence on the atmospheric circulation between the Antarctic Peninsula and the Ross Sea, influencing precipitation, temperature, and the wind field

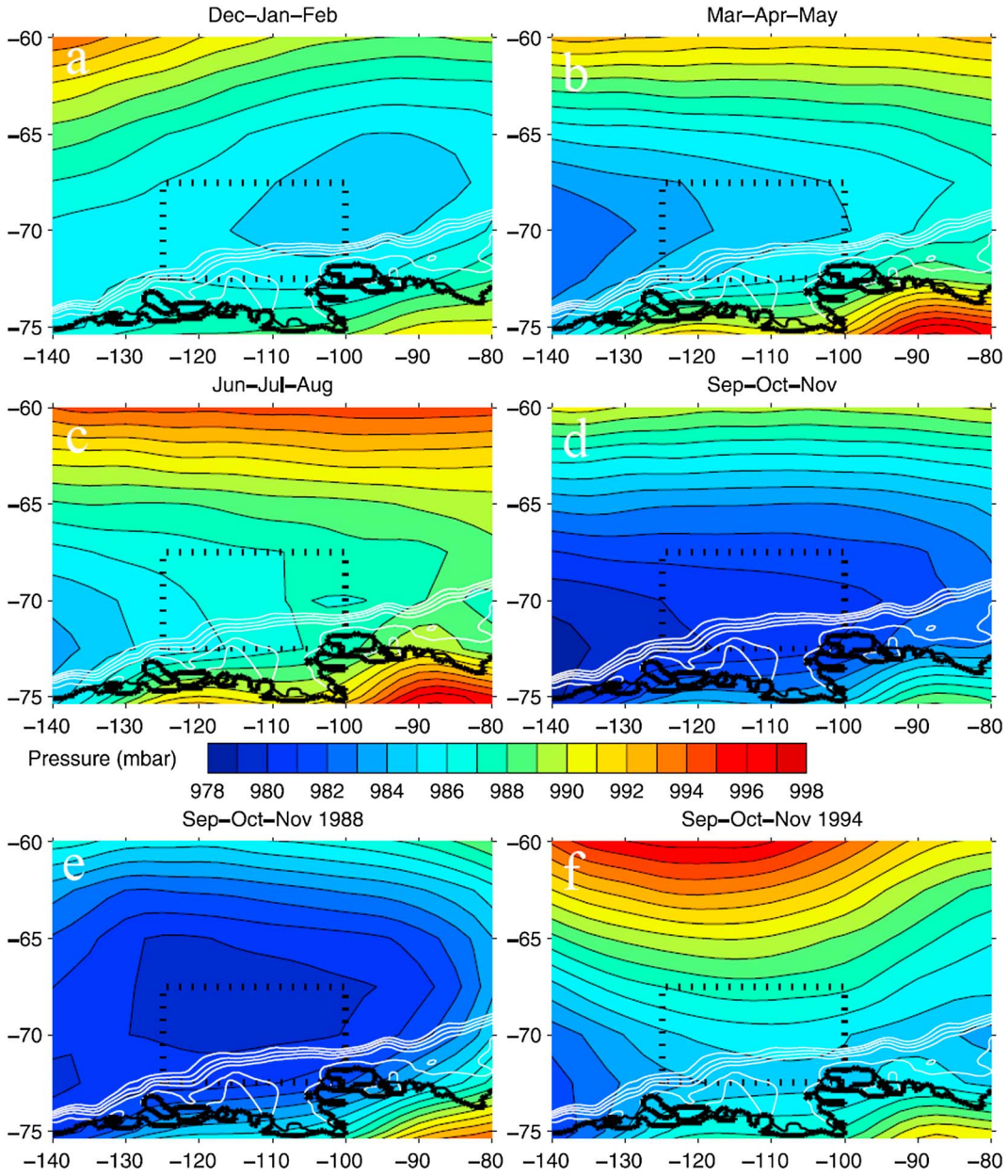

Figure 10. (a–d) Mean seasonal MSLP fields over the model domain for the 1980 to 2004 period and (e–f) springtime means for 1988 and 1994. The box outlined by the heavy dotted line is used to define the north-south pressure index discussed in the text. The heavy black lines indicate the grounding line, while the light black lines show the ice fronts. The white lines are contours of seabed depth (at 500 m intervals from 500 to 2500 m). From *Thoma et al.* [2008].

[*Hosking et al.*, 2013]. The mean longitudinal location of the ASL follows an annual cycle, migrating westward from a mean location of around 110°W to 150°W between austral summer and winter (Figure 10). There is also substantial interannual variability in the location of the ASL, with the standard deviation of the longitude ranging from a minimum of around 20° in summer to a maximum of 35° in winter. The mean latitudinal position of the ASL also exhibits an annual cycle, migrating a few degrees southward between summer and winter.

The atmospheric variability in the Amundsen Sea region is large because of the off-pole nature of the Antarctic orography [*Lachlan-Cope et al.*, 2001] and the location of the region at the southern end of the Pacific South American (PSA) association teleconnection with the tropics. The PSA is a chain of statistically significant atmospheric geopotential height/pressure anomalies extending from the tropical Pacific Ocean

into both hemispheres during El Niño events. The ASL is therefore strongly influenced by tropical climate variability associated with the El Niño–Southern Oscillation (ENSO) and sea surface temperature changes in non-ENSO areas [*Hoskins and Karoly*, 1981; *Ding et al*., 2011; *Li et al*., 2014; *Clem and Renwick*, 2015; *Li et al*., 2015]. In addition, the depth of the ASL is affected by the Southern Annular Mode (SAM), which is the primary mode of climate variability of high southern latitudes [*Thompson and Wallace*, 2000]. The SAM is an oscillation of air mass between midlatitude and high latitude that influences the strength of the westerly winds over the Southern Ocean. During the positive (negative) phase of the SAM, surface atmospheric pressure is lower (higher) over the Antarctic and higher (lower) in midlatitudes, and the westerlies are stronger (weaker). Although we do not have reliable atmospheric analyses prior to 1979, it has been possible to estimate the phase of the SAM back to 1957 using the in situ observations from the Antarctic research stations on the edge of the continent and data from island stations around the Southern Ocean [*Marshall*, 2003; *Fogt et al*., 2009]. Experiments with climate models show that the phase of the SAM has a large natural variability, but that increasing concentrations of greenhouse gases and the depletion of stratospheric ozone can both put the SAM into its positive phase and increase the strength of the Southern Ocean westerlies [*Arblaster and Meehl*, 2006].

The depth of the ASL is influenced by both the phase of the SAM and the teleconnection (wave train of long, planetary or Rossby waves) from the tropics present during El Niño events, and there are complex interactions between these two modes of climate variability [*Fogt et al*., 2011]. When the SAM is in its positive phase mean sea level pressure (MSLP) is lower throughout the whole of the circumpolar trough, including in the region of the ASL. When ENSO is in the El Niño (La Niña) phase, overall, the ASL is weaker (deeper) as a result of the Rossby wave train from the tropics [*Turner*, 2004]. A weaker ASL will result in weaker westerlies in this sector of the Southern Ocean. *Fogt and Bromwich* [2006] described decadal variability of the atmospheric circulation of the South Pacific, linked to different phases of the SAM and ENSO in the 1980s and 1990s.

4.2. Atmospheric Forcing of CPDW Delivery

Thoma et al. [2008] suggested that regional atmospheric variability plays a fundamental role in the variability of the delivery of warm CPDW intrusions onto the continental shelf around Pine Island Bay, and thus ultimately the amount of CPDW flowing beneath PIG. Using a regional model of ocean circulation run for the area shown in Figure 10 and forced with daily MSLP and surface air temperature data from the National Centers for Environmental Prediction/National Center for Atmospheric Research (NCEP/NCAR) reanalysis for the period of 1980–2004, they found that fluctuations in the amount of ocean heat offshore of PIG were determined by the variability imposed by wind forcing on the shelf edge currents and their interaction with the bathymetry. They argued that periods with westerly winds over the shelf edge region strengthened an eastward-flowing current of CPDW that turned on-shelf near 113°W, then flowed to the east and south to reach the inner shelf. They noted that changes in wind forcing associated with the mean annual cycle in the location of the ASL resulted in seasonal fluctuations of on-shelf flow, with maximum on-shelf flow during winter and weaker on-shelf flow during summer, while changes in wind forcing associated with interannual variability of the ASL resulted in fluctuations of on-shelf flow on longer time scales. Figure 11 shows the modeled inflow of the warmest waters onto the shelf in contrasting spring (1988 and 1994) and fall (1989 and 1995) seasons. Sensitivity studies showing that little on-shelf flow occurred if the model was forced with climatological mean winds, supported their findings.

To quantify the variability of the atmospheric forcing, *Thoma et al*. [2008] defined a zonal geostrophic wind index as the mean north to south MSLP difference over the box shown on Figure 10. This reflected marked easterly winds in the spring of 1988 (Figure 10e) when temperatures were supposedly low under PIG. In contrast, during spring 1994 there was extensive warm CPDW under PIG that was associated with strong westerly atmospheric flow over the outer shelf and is consistent with oceanographic observations during that year [*Hellmer et al*., 1998]. This arose because of a marked ridge of high pressure extending south close to 120°W, with the ASL being located further west and south in 1994. These impacts of atmospheric circulation changes were found despite the ocean being largely sea ice covered during the spring season.

The model used by *Thoma et al*. [2008] simulated a substantial increase in the delivery of on-shelf CPDW flow after the early 1990s, which coincided approximately with a period of thinning and acceleration of PIG [*Joughin et al*., 2003]. *Steig et al*. [2012] argued that this resulted from a pronounced increase in westerly

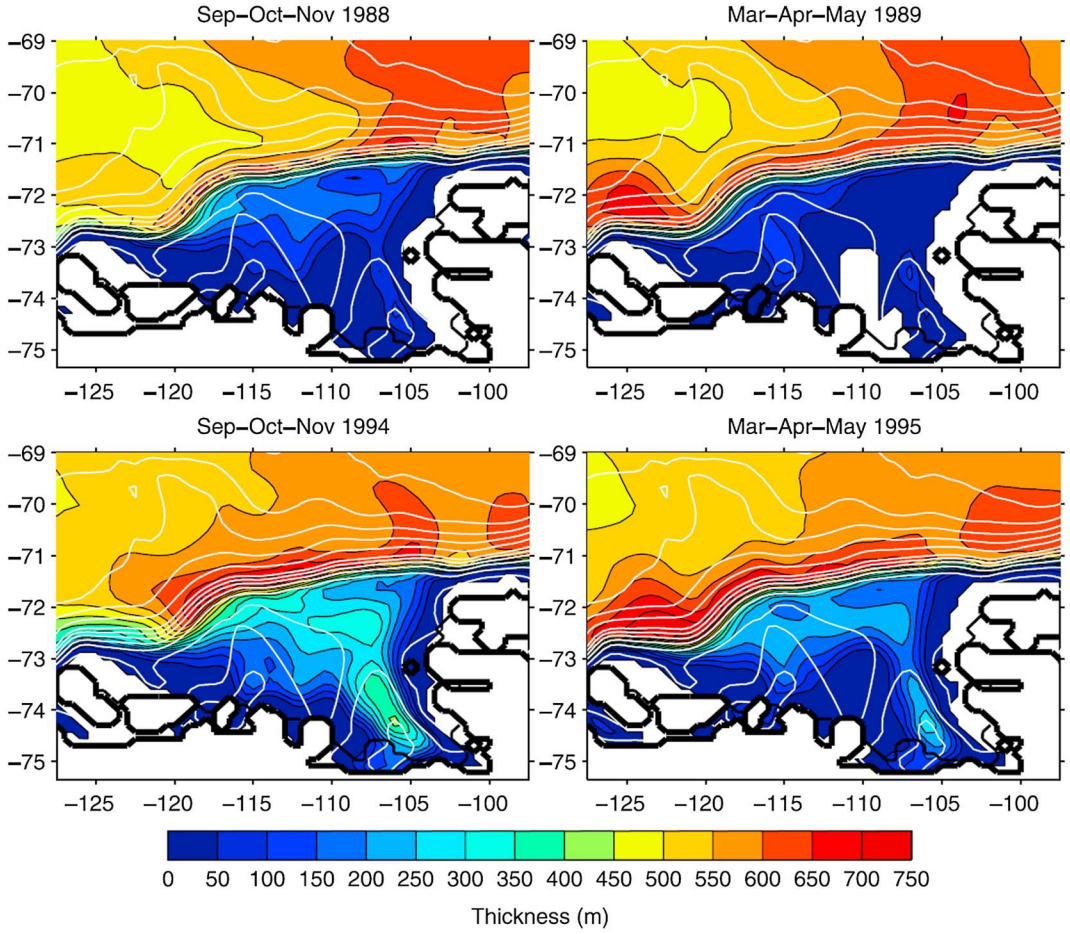

Figure 11. Thickness of the CPDW layer averaged through the spring and fall of two contrasting years over the ASE and adjacent Southern Ocean. The heavy black lines indicate the grounding line, while the light black lines show the ice fronts. The white lines are contours of seabed depth (at 200 m intervals from 100 to 1500 m, and 500 m intervals thereafter). From *Thoma et al.* [2008].

wind stress over the ASE shelf edge in fall and early winter, resulting from more blocking in the region of the ASL in response to the Rossby wave train associated with warming trends in the central tropical Pacific region.

The SAM is the primary mode of climate variability at high southern latitudes and influences the winds in the Antarctic coastal region. An examination of the wind differences between the years of positive and negative SAM index obviously shows stronger westerlies when the SAM is positive, but during these years the easterly winds over the shelf north of the ASE were weaker, which could promote greater CPDW delivery to the ASE.

The study of *Thoma et al.* [2008] has a number of caveats. First, the model used poorly constrained seabed geometry. Second, the paucity of oceanographic observations meant that validation of the model output was very limited. Third, the coarse-resolution reanalysis data used to drive the model did not capture important localized atmospheric forcing, which influences the exchange of water across the shelf edge [*Klinck and Dinniman*, 2010]. Nevertheless, the observations of *Dutrieux et al.* [2014] lend some support to the main conclusions. They suggested that the relatively thin layer of CPDW that was observed in January 2012 was partly due to a deeper than normal ASL, with strong easterly anomalies over the Amundsen Sea in the months leading up to that date.

As discussed above, the role of the atmospheric flow in modulating CPDW to the ASE is complex, with multiple local and remote factors playing a part, including the SAM, ENSO, and the ASL. In Table 2 we have

Table 2. A Summary of Factors Affecting CPDW Delivery to the ASE

Driver	Effect on Atmospheric Flow	Impact on CPDW Inflow	Uncertainty
ASL	The mean annual cycle in the location of the ASL results in seasonal fluctuations in the westerly winds in the shelf. Interannual variability of the ASL resulted in fluctuations on longer time scales	Gives maximum on-shelf flow during winter and weaker on-shelf flow during summer	Do the reanalysis data sets have a good resolution of the regional winds? What is the long-term variability of the ASL?
SAM	A positive SAM is associated with weaker coastal easterlies north of the ASE.	Has the potential to lead to more CPDW inflow	Interaction of the SAM with other modes of variability
ENSO	El Niño events can give more blocking in the Amundsen Sea and stronger westerly flow on the shelf.	Greater inflow of CPDW	Relative roles of the Rossby wave train from the tropics with internal variability

summarized their possible influence on CPDW delivery and some of the outstanding questions that future research should address.

4.3. Changes in the Atmospheric Circulation Since the Late 1970s and the Impact on the ASE

There have been a number of changes in the atmospheric circulation off West Antarctica in recent decades. One of the largest changes to the Antarctic climate system has been the loss of stratospheric ozone during the spring of each year (the "ozone hole"), beginning around 1980. This has contributed to the SAM being in its positive state more frequently and increased the strength of the westerly winds over the Southern Ocean. One consequence of this has been a poleward shift in the ACC [*Gille*, 2008] and increased eddy heat flux [*Hogg et al*., 2008].

The annual mean central MSLP of the ASL has also decreased since 1979, resulting in a more cyclonic atmosphere circulation between the Antarctic Peninsula and the Ross Sea. This has given stronger northerly (southerly) flow over the Bellingshausen (Ross) Sea contributing to less (more) sea ice in these areas [*Turner et al*., 2015]. However, there have been large variations in the trend in the depth of the ASL over the year. Importantly, considering the possible impact on CPDW delivery to the ASE, the ASL has weakened slightly since the late 1970s in winter but has deepened markedly in May and September.

With a deeper ASL the easterly winds immediately north of the ASE have increased very slightly over the year as a whole, with the ECMWF reanalysis data set giving a trend in the 10 m zonal component of the wind of −0.1 m/sec-dec for the area used by Thoma et al. and shown in Figure 10. The reasons for the deepening of the ASL over the year as a whole since 1979 are not fully understood but are probably a result of several factors, including changes in tropical forcing and intrinsic variability. As discussed earlier, higher sea surface temperatures (SSTs) in the tropics and greater convection result in a Rossby wave train to the ocean area off West Antarctica. For the year as a whole, SSTs across the central and western parts of the tropical Pacific have fallen slightly, which is consistent with a slightly deeper ASL. However, *Steig et al*. [2012] point out that SSTs in the central tropical Pacific have increased in fall and early winter, leading to a weaker ASL and anomalously higher MSLP to the north of the ASE at that time of year. This in turn has led to stronger westerly flow off the ASE and consequent impact of changes of CPDW delivery to the ASE.

A number of studies have considered the change in precipitation across the ASE and West Antarctica as a whole over recent decades, including *Monaghan et al*. [2006a], who estimated Antarctic snow accumulation back to the IGY. *Monaghan et al*. [2006b] simulated Antarctic P-E (precipitation-evaporation) with the Polar MM5 model forced by two different reanalyses covering 1985–2001. Both analyses revealed "accumulation" increases in the PIG-TG region. *Rignot* [2008] estimated that the increase in snow accumulation between 1980 and 2004 was less than 5% in the study area.

In their investigation of the thinning of PIG over 1995 to 2006, *Wingham et al*. [2009] took the increase of snowfall across the region to be 6 Gt yr^{-1}. Such an increase in accumulation since the late 1950s [*Thomas et al*., 2015] is consistent with a deepening of the ASL, the warming of the Antarctic Peninsula during the second half of the 20th century [*Turner et al*., 2005, 2016] and a general warming of West Antarctica estimated from the reconstructed Byrd temperature record [*Bromwich et al*., 2013a], and the temperature record from an ice core from the coast of the southern Bellingshausen Sea [*Thomas et al*., 2013]. However, it should be noted that *Medley et al*. [2013] found no trend in snow accumulation over the Thwaites catchment for 1980–2009 using airborne measurements and ice core data.

Surface accumulation estimates from models have been used in a number of modeling studies. For example, *Favier et al*. [2014] used estimates from the Regional Atmospheric Climate Model (RACMO) [*van de Berg et al*., 2006] in their modeling study of the future of PIG. RACMO was developed at the University of Utrecht [*van Meijgaard et al*., 2008] and has been used to examine surface mass balance at a resolution of 27 km [*Lenaerts et al*., 2012b], as well as the near-surface wind field [*van Lipzig et al*., 2004].

We have atmospheric reanalysis fields, including precipitation, for the Antarctic since 1979 when large amounts of satellite sounder data became available. However, these data need to be used with care as the orography is smoother than in reality in order to keep the models numerically stable. Nevertheless, the data are useful for investigating precipitation change in the ASE. Considering a latitude/longitude box covering the ASE (73–77°S, 100–120°W), the precipitation increased in all seasons except winter for the period of 1979–1998, with the largest increase of approximately 5%/decade being in the summer. However, since 1998 the reanalysis data suggest that the precipitation has been decreasing throughout the year by a small amount.

5. Modeling the Atmosphere-Ocean-Ice Interactions

The changes observed in the ASE represent a complex interaction between the near-surface atmospheric flow, the ocean conditions under the ice, and the dynamics of the ice streams. Our current understanding of the ASE changes has been obtained through a combination of observational investigations and modeling studies, with the modeling experiments being essential since the ASE is remote and presents many challenges in routinely monitoring the ocean and atmosphere. In this section we consider the models that have been developed to represent conditions in the ASE.

5.1. The Ice Streams

A number of modeling studies have been carried out to investigate how the glaciers of the ASE are influenced by various forcing factors and how the glaciers may change in the future. One of the earliest studies was carried out by *Schmeltz et al*. [2002]. At that time observational data on the ice thickness, bed topography, and ice temperature were rather limited. They used a time-independent finite element model of coupled ice-stream-ice-shelf flow [*MacAyeal*, 1989; *MacAyeal et al*., 1995] to study the sensitivity of PIG to changes in ice shelf and basal conditions. The focus of the study was on the instantaneous response of PIG to various perturbations, and the grounding-line migration was prescribed directly. As most models applied to the area still continue to do, the ice-flow model of *Schmeltz et al.* used the shallow-ice-shelf assumption (SSA). SSA ice flow models are vertically integrated models that include full stress balance in the horizontal and somewhat simplified stress balance in the vertical direction. The key assumption of the SSA is that vertical shear of ice is small enough for most of the forward motion of the ice to be due to basal sliding so that, in comparison, the ice deformational velocity can be ignored. Schmeltz et al. solved the SSA equations in both horizontal dimensions (2HD), which is an essential requirement for any calculations of ice-shelf buttressing. As also subsequently became a common practice, Schmeltz et al. matched the ice stream velocity in the model to that observed by interferometric SAR by tuning the mechanical softening coefficient of the ice along the glacier margins, and the basal friction coefficient controlling the distribution of basal shear stress underneath the ice stream. Once they had set up (i.e., initialized) the model in this manner, they calculated the instantaneous response to a number of perturbations, such as reduction in grounded area, and ice-shelf calving. They found that a 5.5–13% reduction in initial ice-shelf area increased the glacier velocity by 3.5–10% at the grounding line. The removal of the entire ice shelf increased the grounding-line velocity by $>$70%, with the changes in velocity associated with ice-shelf removal being felt several tens of kilometers inland. It was also found that a 5% reduction in basal shear stress increased the glacier velocity by 13% at the grounding line. The importance of this factor was highlighted as softening of the glacier side margins has to be increased a lot more to produce a comparable change in the ice velocity.

Another early ice-flow study was that of *Payne et al*. [2004], who used a time-dependent numerical flow-line model to simulate the effects of perturbations at the grounding line to investigate the impacts of ocean change. They used the SSA approximation in one horizontal dimension (i.e., SSA-1HD) and could therefore not account directly for the effects of ice-shelf buttressing on the flow of grounded ice. Instead, they parameterized side drag as a function of width. Although the flow model was time-dependent, the position of the grounding line was fixed. They found that changes in PIG's ice shelf and/or ice plain could be transmitted

rapidly upstream on decadal time scales. They suggested that the speed at which perturbations propagated upstream implied a tight coupling between the ice sheet and the surrounding ocean, with an ocean trigger capable of affecting the deep interior of the ice stream. Their experiments added weight to the argument that recent changes in the oceanography of the Amundsen Sea giving basal melting and thinning of PIG's ice plain could lead to widespread thinning in the interior of the glacier. However, as later pointed out by *Joughin et al*. [2010], it quickly became apparent that the predicted thinning rates in this study were too small.

Joughin et al. [2010] conducted a basin-wide flow modeling study of PIG. The flow model was a transient SSA model including both horizontal dimensions. In their paper they state that they initialized the basal stress distribution from observed flow velocities, but as they used viscous sliding law it appears that their approach was much more general and that they in fact inverted for the spatial distribution of a parameter in their basal sliding law. The (tangential) basal traction [*Cuffey and Paterson*, 2010] was hence not constant during model runs. Basal melt rate over the ice shelf was adjusted to produce a steady state for the 1996 grounding-line position. They then gradually reduced the friction over the area known from observations to have become ungrounded between 1996 and 2009. In doing so they in effect forced the model to simulate the observed grounding-line retreat over that period. For this model experiment, calculated thinning rates were found to be close to observations. In a further modeling experiment, they used a depth-dependent melt rate, where the ocean-induced melt rate over the ice shelf was parameterized as a function of ice-shelf draft. A steady state configuration with the (freely evolving) grounding line close to the observed 2009 position was generated, and subsequently subjected to perturbations in ice-shelf melt and ice-shelf geometry. They concluded that sensitivity of the grounding line to external perturbations in applied ice-shelf melt was to a large degree a function of bed geometry around the grounding line and that the period of rapid grounding-line retreat observed between 1992 and 2010 was likely to come to an end. Furthermore, they concluded that the observed grounding-line position of PIG in 2010, i.e., in the year their study was published, was close to a point of a multidecadal stability. Recent observations by *Mouginot et al*. [2014], showing no increase in ice-shelf flow velocities after 2010, now seem to be in good agreement with the findings of *Joughin et al*. [2010].

The study by *Gladstone et al*. [2012] was the first to include a coupling between the ice and the ocean. A time-dependent ice flow-line model (i.e., SSA-1HD) was coupled to a physically based ocean box model. As a flow-line model cannot directly represent the effects of reduction in side drag or ice-shelf buttressing on ice flow, the side drag was, similar to *Payne et al*. [2004], parameterized as a function of width. The flow-line setup allowed for the impact of a large number of different model parameter values to be tested. Rather than inverting for basal slipperiness [*Cuffey and Paterson*, 2010] using measurements of surface velocities, as done in some other studies, they used a parameterised basal slipperiness distribution motivated by the basal slipperiness profile obtained in a previous study by *Vieli and Payne* [2003]. Model parameters related to surface mass balance (the surface mass balance term included lateral contributions from tributaries and the effect of transverse convergence on ice thickness), and basal slipperiness, as well as ocean-induced melt, were all varied in a systematic fashion. The model was then calibrated against observations of grounding-line positions at different times. They predicted a monotonic retreat of the grounding line of PIG over the next 200 years, albeit with large uncertainties attached.

Favier et al. [2014] was the first study focusing specifically on PIG to involve several different tried-and-tested numerical ice sheet models run by three different modeling groups (Laboratoire de Glaciologie et Géophysique de l'Environnement, Grenoble; University of Bristol, Bristol; and British Antarctic Survey, Cambridge). The models were all used to perform similar, although not strictly identical, numerical experiments. The three numerical models used were Elmar/Ice [*Favier et al*., 2012], BISICLES (Berkeley Ice Sheet Initiative for Climate Extremes) [*Cornford et al*., 2013], and Úa [*Gudmundsson et al*., 2012]. All these models had previously been used in a number of international model-intercomparison experiments, and the performance of each model in those experiments is well documented [e.g., *Pattyn et al*., 2013]. The Elmer/Ice is a 3-D full-Stokes model, BISICLES is a hybrid shallow-shelf approximation (SSA) + shallow ice approximation (SIA) model [*Cuffey and Paterson*, 2010] (although the SIA contribution of ice deformation to forward velocity is not included), and Úa was run in its SSA mode. All models were initialized independently of each other using observed surface velocities and driven by various melt-rate parameterizations of ocean-induced melt. Similar to the approach taken by *Joughin et al*. [2010], these melt-rate parameterizations prescribed ice-shelf melt as a function of ice-shelf draft. Depending on the particular melt-rate parameterization used, various different

types of response were observed, reflecting the large sensitivity of the modeled grounding-line migration to changes in ocean conditions and ice-shelf buttressing. In more moderate types of applied ice-shelf melt, the grounding line of PIG was found not to deviate significantly with time from a prominent bedrock high in the area where the grounding line was located at the time of the study, i.e., in 2013. However, all models found that it was possible to push the grounding line back from the local bedrock high provided that the melt rate was raised sufficiently. Most importantly, they found that once such a retreat started it was irreversible; i.e., it continued even if the melt rate was reduced again. This result must be viewed as a statement about the potential of PIG to become unstable at a future point in time, rather than a direct prediction of the future of PIG. Those experiments do suggest that if the grounding line of PIG were to retreat back from the local high on which it is currently located, an irreversible retreat will start. Such a retreat would be self-sustained and could not be stopped even if ocean conditions were to change.

Seroussi et al. [2014] conducted a model study of PIG and estimated ice-flow response to perturbations in surface mass balance, calving front position, and ice-shelf melting. The flow model used was based on the *Blatter* [1995] flow approximation and included the contribution of vertical shearing of the ice that is ignored in the SSA approximation. Similar to SSA, the Blatter approximation is a "shallow ice approximation"; i.e., it is assumed that the ratio between ice thickness and width is small. The model was initialized by using observations of surface velocities using a linear sliding law. In line with previous findings, *Seroussi et al*. [2014] found ice flow over grounded areas to be highly sensitive to changes in ice-shelf geometry and ocean-induced ice-shelf melt. For example, a doubling of ice-shelf melt increased ice-shelf speeds by 800 m/yr, and the impact was felt hundreds of kilometers inland in 1 to 5 years. However, for all perturbation scenarios, variations in grounding-line position from the observed 2007 position (used as a starting point in the model runs) were limited. For example, even multiplying the reference ice-shelf melt rate distribution by a factor of 10 resulted in a grounding-line retreat of less than 10 km over the 50 year time period modeled. *Seroussie et al*. [2014] did not observe in any of their experiments the kind of unstable retreat found in the most extreme melt-rate scenario used by *Favier et al*. [2014]. Possibly, this difference is due to the fact that *Seroussi et al*. [2014] did not update their melt-rate distribution with time; i.e., the melt-rate distribution was not a function of ice-shelf draft as done by *Joughin et al*. [2010] and *Favier et al*. [2014], and in most runs no ice melt was applied to areas that became ungrounded during the model run. In agreement with previous findings, *Seroussi et al*. [2014] concluded that PIG is highly sensitive to ocean-induced ice-shelf melting, pointing to the need for better representation of this process in ice-flow models. They further concluded that the grounding line of PIG is currently not undergoing an unstable retreat. To the contrary, according to *Seroussi et al*. [2014], the grounding line of 2007 is not only stable but also rather insensitive to changes in external forcing. This supports the conclusions of *Joughin et al*. [2010] and appears in good agreement with recent observations suggesting that the velocities and the grounding-line position of PIG have remained almost unchanged since about 2010.

5.2. The Ocean Circulation

The output from general circulation models (GCMs) is commonly used to investigate past and possible future broadscale climatic change. However, both the atmospheric and oceanographic components struggle to simulate the complex atmosphere-ocean-ice interactions in the ASE, at least in part because the horizontal and vertical resolutions employed limit the representation of key topographic and bathymetric features. In addition, ocean models that include the circulation beneath the ice shelves are only now being incorporated into GCMs. Therefore, modeling investigations of the ocean circulation in the ASE sector of the Southern Ocean have tended to use regional domains forced at the boundaries by atmospheric reanalyses and larger-scale ocean models.

As discussed earlier, *Thoma et al*. [2008] investigated CPDW delivery to the inner continental shelf around Pine Island Bay by using a version of the Miami Isopycnic Coordinate Ocean Model [*Bleck et al*., 1992] adapted to include sub-ice-shelf cavities [*Holland and Jenkins*, 2001] and coupled to a simple sea ice model [*Holland*, 2001]. The domain was discretized by using an isotropic grid with a horizontal resolution ranging from 28 km in the north to 13.5 km in the south. The model was spun up for 10 years by using NCEP/NCAR reanalysis data for 1979 in a repeating cycle, and then run for 1980 to 2004. Although the sub-ice-shelf cavities were included within the domain, the poor-resolution and unknown subice bathymetry yielded unrealistic melt rates, so the analysis focused on the delivery of warm CPDW to Pine Island Bay.

Their key findings have been discussed earlier and included showing that CPDW was channelled through a bathymetric cross-shelf trough, accessed via bathymetric irregularities along the shelf break. The densest waters moved onto the shelf through the western branch of Pine Island Trough at 113°W, in agreement with the observational study of *Walker et al*. [2007], then flowed to the east and south to reach the inner shelf. There was a strengthening of the inflow during the winter and spring, and marked interannual variability in the CPDW layer thickness on the inner shelf, dependent on the strength of the winter/spring input. *Walker et al*. [2013] pointed out that the vertical shear in the modeled shelf edge currents was much weaker than in the observations, probably because of the coarse resolution of the model. They argued that a better resolved undercurrent would have given a more persistent inflow of CPDW with reduced seasonality, much like the observations of *Arneborg et al*. [2012] and *Wåhlin et al*. [2013]. Similar undercurrents are a robust feature of higher-resolution models [*Assman et al*., 2013; *Nakayama et al*., 2014], in which they represent the main sources of CPDW on the shelf. *Nakayama et al*. [2014] found that a horizontal resolution of 5 km was required to simulate the undercurrents and their interaction with the bathymetry.

Schodlok et al. [2012] ran a 1 km resolution model of the ASE by using the MITgcm [*Marshall et al*., 1997] as modified by *Losch* [2008] to include the pressure loading and thermodynamic forcing of a steady ice shelf. They found the circulation on the continental shelf to be dominated by cyclonic gyres circulating within the bathymetric troughs. The strength of the gyres varied, being stronger when the CPDW on the shelf was warmer, and they argued that the strength of the on-shelf circulation was a key factor in determining CPDW delivery to the subice cavities. *Kalén et al*. [2016] observed such a gyre in the Dotson-Getz Trough, and their model results also showed that it was stronger and subject to greater variability when the CPDW on the shelf was warmer. While these results highlight a key role for the local ocean circulation in transporting CPDW to the ice shelves and meltwater away, the input of CPDW to the gyres must ultimately come from the continental shelf edge.

Hellmer et al. [1998] used the two-dimensional model of *Hellmer and Olbers* [1989] to investigate the overturning circulation within the cavity beneath PIG and the resulting melt rates. They found a single overturning cell generating outflows that matched reasonably well with observation, but the simulated melt rate was sensitive to the unknown subice bathymetry. *Schodlok et al*. [2012] used two different bathymetries in their model runs and also found the resulting melt rates to be dependent on the ease of access of CPDW to the deep grounding line. A high-resolution (900 m horizontal, 20 m vertical) version of the adjoint MITgcm was used by *Heimbach and Losch* [2012] to investigate the sensitivity of the melt rate. They found melting to be linked to conditions outside the cavity on timescales of 30 to 60 days via advective pathways that were determined by the subice bathymetry. An even higher-resolution (400 m horizontal, 10 m vertical) version of the forward model was used by *de Rydt et al*. [2014] to systematically investigate the impact of different sub-ice-shelf geometries on the ocean circulation beneath PIG. They used a synthetic geometry that comprised laterally invariant ice draft and seabed topographies that approximated the form of the cavity beneath PIG, and they varied the height of the seabed ridge, the thickness of the ice, and the depth of the thermocline. They found that the ridge heightened the sensitivity of the melt rates to thermocline depth by acting as a physical barrier to the warmest waters and that melting was also sensitive to the width of the gap over the ridge when that was less than a threshold value, found to be 150 m. The latter result supports the implications of the observations of *Jacobs et al*. [2011] and *Dutrieux et al*. [2014]. During the early stages of PIG's retreat from the ridge, melt rates would have been more sensitive to cavity geometry than to thermocline depth, and this could have been the case as late as the 1990s, but recent thinning would have widened the gap over the ridge beyond the threshold at which geometry ceases to be so important and thermocline depth takes over as the main control on melt rates.

5.3. Atmospheric Modeling

As discussed earlier, the horizontal resolution of the atmospheric component of current GCMs is too coarse to represent the steep orographic gradient in the coastal region of West Antarctica, which rises rapidly from sea level to 1 km within around 200 km. This limits the simulation of many important processes in the area of the ASE, such as the downslope katabatic wind, which is so important in the correct simulation of atmosphere-ocean-ice interactions. High horizontal resolution reanalysis data sets and the output of limited area atmosphere-only models have therefore been used to investigate important processes in the ASE, such as the role of atmospheric forcing on CPDW delivery to the sub-ice-shelf cavities.

The reanalysis data sets, such as those produced by ECMWF [*Dee et al*., 2011] and NCEP [*Kanamitsu et al*., 2002], have a generally realistic representation of the broadscale atmospheric flow back to 1979 when satellite sounder data became available. These data sets have a horizontal resolution on the order of 70 km and can provide broadscale forcing for driving ocean models (see earlier). The operational numerical weather prediction models now have a much higher horizontal resolution, with the current ECMWF operational model having a 9 km resolution. However, the time series of operational fields are not ideal for driving ocean models because of the frequent changes of resolution and model formulation. The reanalysis data sets have been used to investigate the role of tropical climate variability on the atmospheric circulation over the portion of the Southern Ocean north of the ASE and its part in melt under the ice shelves.

In recent years a number of high-resolution ($<$15 km in the horizontal), limited area atmosphere-only models, such as the RACMO model described earlier, have been used to simulate the airflow over the ASE and the whole of West Antarctica. In particular, the polar version of the Weather Research and Forecasting model [*Skamarock et al*., 2008; *Bromwich et al*., 2013b] has proven very valuable and has been shown to perform well over West Antarctica [*Deb et al*., 2016]. Such models are able to give improved simulation of the flow around the complex orography and can better represent the interaction between depressions over the Southern Ocean and the katabatic winds [*Orr et al*., 2013]. However, they are expensive to run for long periods but should be used more over the ASE as computer power increases.

6. Attribution of Recent Changes in the ASE

The remarkable changes observed over recent decades in the glaciers feeding into the ASE have prompted a great deal of discussion about the possible mechanisms responsible and the degree to which anthropogenic influences could be playing a part. It is well known that the changes in an ice stream occur as a result of changes in its force balance [*Payne et al*., 2004], which is between gravitational driving stress and the sum of resistances from lateral drag, basal drag, and longitudinal stress gradients within the ice stream [*Vanderveen and Whillans*, 1989]. Changes in the thermodynamics and hydrology of ice streambeds have been linked to stagnation and migration of ice streams on the scale of decades to centuries in other parts of Antarctica. However, the fact that major change is taking place in PIG, TG, and Smith Glaciers tends to suggest that this mechanism is not the key factor driving change. Similarly, the lack of change observed in the lateral extent of the PIG suggests that there has been little alteration in the lateral drag. So changes in the driving stress or longitudinal stress gradients within the ice streams could be responsible for the changes. The observed changes could be a result of long-term retreat of the ice sheet from its maximum extent near the continental shelf break approximately 20,000 years B.P. However, this is unlikely because of the speed of recent change [*Hillenbrand et al*., 2013; *Larter et al*., 2014]. Alternative hypotheses that could explain the retreat of the PIG are that it is responding to changes in drag in either its ice plain or ice shelf. Such changes could be associated with iceberg calving or ice shelf/plain thinning in response to enhanced oceanic melting, which then generate an initial perturbation near the grounding line that is then transmitted around 200 km upstream.

Changes in precipitation across a region can affect the ice flow, and this region has a large variability in snowfall, but the change in elevation of the PIG is almost an order of magnitude greater than expected because of variations in snowfall [*Shepherd et al*., 2001]. *Shepherd et al*. [2001] also considered the role that changes in the katabatic wind regime may play in modulating the snow accumulation on the PIG and altering the thickness of the glacier and estimated that the thinning was 13 times larger than the variability from this factor. Rapid changes in the mass supply from the interior of the WAIS are also unlikely to account for the observed changes, and there is no evidence of thinning in the interior of the WAIS or the tributaries feeding PIG. Rapid change as a result of surge-type variability is also unlikely since the rapid glacier thinning has been observed across the PIG, TG, and Smith Glaciers. The magnitude of the acceleration is sufficient to explain the observed thinning on the basis of flux balance calculations [*Joughin et al*., 2003], which implies a change in the flow dynamics of the ice stream. The section of PIG 55 to 171 km inland is steepening at a rate which provides an increase in driving stress of sufficient magnitude to produce the observed acceleration. Acceleration is highly correlated to slope increase and no sustained increase in longitudinal stress gradient, or decrease in basal drag, is needed to explain the force balance. Transmission of the acceleration inland has been exceptionally fast at around 200 km/decade, or possibly even quicker [*Scott et al*., 2009]. The results are

consistent with the hypothesis that changes in PIG result from changes at the downstream end, including the grounding area and floating ice shelf. It appears that PIG is not only out of balance but continues to move further out of balance.

All these factors lead to the conclusion that the thinning and ice loss from the glaciers feeding into the Amundsen Sea are a result of greater basal melting as a result of ocean interaction. So the origin of the current imbalance in PIG lies almost certainly within the ocean [*Payne et al*., 2004; *Shepherd et al*., 2004] and associated with a long-term warming [*Gille*, 2002] or decadal variability in ocean circulation [*Thoma et al*., 2008], possibly as a result of changes in atmospheric circulation on those time scales. Evidence for this also comes from the observation that the only ice shelves found not to be thinning by *Pritchard et al*. [2012] (the Abbott, Nickerson, and Sulzberger Ice Shelves) were those not exposed to warm water at depth because they have shallow draft, lack deep bathymetric troughs, or are remote from CPDW.

Because the ASE shelf and its hinterland are underlain by relatively thin crust [e.g., *Gohl et al*., 2007; *Jordan et al*., 2010; *Kalberg et al*., 2015] and recent volcanic activity has been recorded in the region [*Wilch et al*., 1999; *Corr and Vaughan*, 2008], the role of enhanced geothermal heat flow for mass loss of the glaciers draining into the ASE has also been considered [e.g., *Joughin et al*., 2009; *Schroeder et al*., 2014]. However, its effect on basal sliding conditions is not well understood since we have little knowledge of the composition and hydrological processes at the ice-to-bed of most ice streams. Direct measurements of geothermal heat flow would therefore be of great value. Regarding the impact on modeling, *Larour et al*. [2012] pointed out that for fast-flowing ice streams errors in ice thickness contribute more to model uncertainty than errors in geothermal heat flux.

A feature that has played a major part in recent changes in the PIG is the submarine ridge beneath the PIG ice shelf that rises up to 300 m above the surrounding bathymetry. The glacier sat on the ridge up until the mid-1940s and then started to break free allowing a phase of rapid grounding-line retreat to start, which accelerated in subsequent decades. When PIG was free from the ridge a large ocean cavity formed increasing the inflow of warm CPDW. It is unlikely that the recent mass loss in the ASE drainage sector is a continuation of the long-term retreat and thinning of the WAIS since the LGM [*Hillenbrand et al*., 2013; *Johnson et al*., 2014; *Larter et al*., 2014] and the initial detachment of PIG from the ridge in the 1940s has been linked to El Niño conditions in the tropical Pacific [*Smith et al*., 2016], with subsequent atmosphere/ocean changes since that time contributing to the ice loss [e.g., *Ding et al*., 2011; *Steig et al*., 2012].

A similar feature had previously been identified slowing the TG's seaward motion, and using graviemetric data collected during flights over TG in 2009 under NASA's Ice Bridge campaign, *Tinto and Bell* [2011] were able to connect it to a larger ridge. The newly discovered ridge is 700 m tall, with two peaks—one that currently anchors the eastern part of the glacier tongue and another farther west that held the western part of the glacier tongue in place between 55 and 150 years ago [*Tinto and Bell*, 2011].

Determining the atmospheric circulation off West Antarctic over the last century is clearly important in understanding the retreat of the glaciers of the ASE. Unfortunately, we do not have reliable atmospheric analyses before 1979 that can be used to determine climate change. However, some indication of broadscale pre-1979 change can be estimated by using other means. The near-surface air temperatures from Faraday/Vernadsky station on the western side of the Antarctic Peninsula are closely linked to the amount of sea ice over the eastern Bellingshausen Sea and consequently the depth of the ASL, especially in winter [*Turner et al*., 2012b]. During the 1950s and 1960s Faraday/Vernadsky experienced much lower winter temperatures implying that the ASL was weaker during this period with weaker northerly winds to the west of the Antarctic Peninsula. A weaker ASL with more atmospheric blocking episodes would imply weaker easterly winds along the continental shelf of the ASE and more westerly atmospheric flow, possibly giving greater CPDW delivery to Pine Island Bay.

Although parts of the Antarctic Peninsula have experienced marked warming over the second half of the 20th century [*Turner et al*., 2016], this does not seem to be unique on longer time scales. An ice core collected on the coast of West Antarctica has provided a proxy temperature record for the Antarctic Peninsula region extending back 300 years B.P. [*Thomas et al*., 2013]. This shows the marked warming that has been observed at stations such as Faraday/Vernadsky over the second half of the 20th century, which has taken place as the ASL has deepened and as the sea ice extent has decreased over the Bellingshausen Sea. However,

importantly, the ice core record shows that the recent warming was not the largest in the last 300 years and that there were even greater periods of rapid warming. In contrast, ice cores from coastal West Antarctica [*Thomas et al*., 2015] suggest that the snowfall in recent decades was exceptional in terms of century-scale climate variability, indicating the complexity of long-term change. Such data show the highly variable nature of the atmospheric circulation in the region of the ASL and the possibility of decadal variability in the delivery of CPDW to the ASE.

7. Possible Future Changes in the ASE

How the glaciers of the ASE will change in the future is extremely important because of the potential impact on sea level. However, the future changes will be dependent on alterations in the atmospheric flow and the ocean circulation and will also be dependent on changes that are already underway. Determining how these quantities will change over the coming decades presents many problems, but in this section we will examine the current estimates of future change.

7.1. Atmosphere

The Intergovernmental Panel on Climate Change (IPCC) initiative was tasked with investigating how the climate of the Earth had changed in the past, what might happen in the future, and how society can act to counter possible global warming. At the heart of the IPCC are the coupled atmosphere-ocean-sea ice GCMs that have been run to simulate past conditions and to produce projections for the next century and beyond with a range of greenhouse gas emission scenarios. The modeling effort was carried out as part of the Coupled Model Intercomparison Project 5 (CMIP5) initiative, which is part of the World Climate Research Programme. CMIP5, which involves around 50 state-of-the-art GCMs, provides predictions of atmospheric and oceanographic conditions in the ASE over the next century. The models were run with a range of Representative Concentration Pathways (RCPs) that describe the integrated effects of radiative forcing on the climate system. The CMIP5 RCPs cover various scenarios of increases in greenhouse gas concentrations and also the recovery of the Antarctic "ozone hole."

The phase of the SAM has a large influence on the strength of the westerlies, and in recent decades there has been a shift toward the positive phase with strong westerlies, which has been attributed, at least in part, to the depletion of stratospheric ozone [*Thompson and Solomon*, 2002]. Over the next century it is likely that greenhouse gas concentrations will increase, leading to a positive trend in the SAM, although recovery of the ozone hole would push the SAM in the opposite direction. However, it is anticipated that the combined effect will be to make the SAM more positive and for the strength of the westerly winds to increase further [*Gillett and Fyfe*, 2013]. Nevertheless, over the Amundsen Sea, climate models have a wide intermodel range in projected 21st century atmospheric circulation [*Bracegirdle et al*., 2008].

The possible changes in the westerly winds over the Amundsen Sea over the rest of the 21st century based on CMIP5 data [*Taylor et al*., 2012] was considered by *Bracegirdle et al*. [2014]. They found that by 2090–2099 the westerly winds within the area used by *Thoma et al*. [2008] (Figure 10) were predicted to increase by 0.3 and 0.7 m/s, respectively, with the 4.5 and 8.5 RCPs. However, since the area has a large internal climate variability it will be around 2030 (2065) for the RCP 8.5 response to exceed one (two) standard deviation(s) of decadal internal variability. There was a clear annual cycle in the RCP 8.5 ensemble mean response, with the largest increase in the speed of the westerlies in fall (1.1 m/s) and the smallest in spring (0.3 m/s).

7.2. Ocean

How the broadscale circulation of the Southern Ocean is predicted to evolve over the next century by the CMIP5 models has been considered by *Meijers* [2014]. He found that by the end of this century the midlatitude wind stresses were predicted to increase and shift poleward, which is consistent with the SAM being in its positive phase more frequently. It was found that all water masses were predicted to warm, with a freshening of intermediate waters and an increase in salinity of bottom waters. As noted in earlier studies, the extent of sea ice over the Southern Ocean was predicted to decrease, with the surface mixed layers becoming shallower, warmer, and fresher. Other projected changes were an intensification of the upper overturning circulation and a reduction in bottom water formation. Meijers noted the significant disagreement that exists between models in the response of the ACC strength and the need for more research into this.

Although the CMIP5 models can give projections of how the open ocean may evolve, their low horizontal resolution and lack of representation of flow under the ice shelves mean that they cannot give detailed projections of changes in CPDW delivery to the ASE. We therefore have to use our current understanding of the relationship between CPDW delivery and the winds on the continental shelf, which can be predicted with the CMIP5 models. As noted above, *Bracegirdle et al*. [2014] showed that the CMIP5 models indicate that the frequency of westerly winds off the ASE will increase over the coming century. Based on the work of Thoma et al. this would suggest an increase in the frequency of the conditions that lead to greater CPDW delivery into the ASE.

7.3. Ice

Predicting how the glaciers of the ASE will evolve in the future is challenging. A key problem is to understand the nature of ongoing retreat. If current rates of ice retreat are an expression of ongoing marine ice sheet instability [*Schoof*, 2007], then retreat can be expected to continue until a new stable grounding-line position has been found. It is important to understand that in this case the retreat is primarily a manifestation of internal ice dynamics and as such expected to be almost entirely independent of external forcing. Alternatively, the retreat of the grounding line and upstream thinning may be a response to a reduction in ice-shelf buttressing due to ocean-induced thinning of ice shelves [*Mengel et al*., 2015]. Distinguishing between these internal and external causes is best done by using a processed based approach, and considerable efforts have been aimed toward developing, testing, and running numerical models capable of describing the processes involved.

Estimates of glacier change have been made with models for some time. *Payne et al.* [2004] carried out numerical experiments that applied a single, instantaneous change to the ice plain of PIG but did not find that this led to a catastrophic retreat of the glacier. Rather, a new equilibrium state was attained after approximately 150 years with a total thinning of about 8 m over the majority of PIG and 16 m in the ice plain. However, applying a single, instantaneous change in the ice plain is not an ideal forcing. In reality, ice-plain thinning (and loss of basal drag) may well continue into the future (especially if they are indeed brought about by sustained ocean forcing), in which case the eventual response of PIG would be far greater.

Today, the grounding line of the PIG lies over bedrock that has a steep retrograde slope [*Vaughan et al*., 2006], so PIG may already be engaged in an irrevocable retreat. Assuming that ice flow is dominated by basal sliding, grounding lines located on retrograde slopes are in the absence of lateral drag always unstable [*Schoof*, 2007]. However, buttressing provided by confined ice shelves can potentially reverse the stability regime of grounding lines, rendering grounding lines on landward deepening basins stable rather than unstable, as they must be in the absence of ice-shelf buttressing [*Gudmundsson et al*., 2012; *Gudmundsson*, 2013].

A substantial bedrock peak occurs about 25 km inland of the present hinge-line position of PIG, but this feature does not straddle the entire glacier width [*Vaughan et al*., 2006] and relief to the south side of the glacier in particular slopes gently. Although the hinge line has retreated since 2009, analysis of glacier velocities reveals that the glacier speed has yet to increase [*Park et al*., 2013; *Mouginot et al*., 2014], suggesting that further dynamical imbalance has yet to occur.

The shoaling of the PIG in the vicinity of the 2011 hinge line does not favor retreat, and further retreat is at odds with simulations of the glacier evolution under conditions of increased ocean melting [*Joughin et al*., 2010]. However, the PIG geometry has impeded retreat at other times in the past, and yet the retreat has progressed over time. Recent simulations of the PIG evolution have suggested that the grounding line may be able to retreat much further inland should ocean melting persists [*Gladstone et al*., 2012].

Wingham et al. [2009] estimated that if the volume rate of the PIG central trunk continued to accelerate at a rate of $-0.65 \pm 0.02\,\mathrm{km^2\,yr^{-1}}$ then based on the current geometry, the main trunk of the PIG would be entirely afloat within about 100 years—6 times sooner than was anticipated by *Shepherd et al*. [2001] based on the thinning rate in the mid-1990s. They noted that because the thinning of PIG was no longer restricted to the central trunk, projections of change over the 21st century must take into account mass loss from the wider drainage basin. The rate at which the imbalance has propagated inland has been considerably faster than predicted by numerical simulation of the glacier response to a short-lived external forcing [*Payne et al*., 2004].

In a recent study *Favier et al*. [2014] used three state of the art ice flow models to investigate the possible future change in the PIG. They found that PIG's grounding line was probably engaged in an unstable 40 km retreat. The associated mass loss increased substantially over the course of their simulations from the average value of 20 Gt/yr observed for the 1992–2011 period [*Shepherd et al*., 2012] up to and above 100 Gt/yr over the following 20 years. Beyond this time the mass loss remained elevated and ranging from 60 to 120 Gt/yr. All three models in the study, despite having different physics, numeric, and parameters, support the notion of marine ice sheet instability in PIG, and two of the three cast doubt on any possible recovery.

After the initial retreat of PIG over 20 years, the models diverge in their estimates of change dependent on further retreat of the grounding line across a region of gentler slopes and stronger basal traction behind the instability zone. Once the grounding line has crossed the steep retrograde slope, imbalance decreases but remains between 3 and 6 times higher than the mean estimates obtained for the past 20 years (20 Gt/yr).

The future evolution of TG is dependent on the underwater ridge that is currently holding it back [*Tinto and Bell*, 2011]. Presently, the Thwaites Ice Shelf is pinned on the eastern peak and ungrounding from the eastern peak in the coming decades may cause an acceleration across a wide (45 km) segment of grounding line. The retreat of the TG is expected to speed up within 20 years, once the glacier detaches from the underwater ridge that is currently holding it back. In a more recent modeling study, *Joughin et al*. [2014] concluded that unstable retreat for TG has already started. These authors concluded that mass loss will be moderate during the 21st century but increase significantly in 200–900 years. Similarly, *Rignot et al*. [2014] concluded that widespread and rapid retreat of the grounding lines of the ice streams flowing into the ASE will continue well into the future and lead to the draw down of their drainage basins because no major bed obstacles are observed upstream of their 2011 grounding lines.

The near-future evolution of Thwaites Glacier Basin was also the subject of the numerical ice-flow study of *Joughin et al*. [2014]. The methodology applied in the study was similar to several other studies of PIG. A time-dependent plan view shallow-shelf model (SSA-2HD) was initialized by using known surface velocities, and then perturbed by using a number of melt-rate parameterizations with ocean-induced ice-shelf melt prescribed as a function of ice-shelf draft. Similarly, as with the *Favier et al*. [2014] study of PIG, *Joughin et al*. [2014] found that if TG is subjected to high enough melt rate for long enough, it will eventually start to retreat rapidly. For example, if the reference melt-rate distribution is multiplied by a factor of 4, a rapid period of retreat starts after about 100 years. It is not clear from the paper if this retreat is irreversible, i.e., if reducing the melt rate once the fast phase of retreat as started, will cause the retreat to halt.

Cornford et al. [2015] conducted century-scale simulations of WAIS by using various future climate scenarios. Within the ASE, modeled mass loss was dominated by that of PIG and TG. The single biggest source of variability in modeled results was found to be the timing of the retreat of TG, which depended strongly on its initial state. Besides the initial state, the main factor affecting the modeled evolution was the perturbation in ocean-induced melt over the underside of the ice shelves, which was assumed to be a linear function of changes in far-field ocean temperatures.

7.4. Sea Level Rise

The possible rise in sea level over the next century from the glaciers of the ASE is obviously closely linked to the thinning and retreat of the ice and is equally difficult to predict. However, the predictions have been refined as greater observational data have become available and models have been improved.

The modeling study of *Favier et al*. [2012] estimated that over the next 20 years the PIG could contribute 3.5–10 mm of eustatic sea level rise. *Rignot et al*. [2008] found that the flow rate of grounded ice of PIG increased by 34% from 1996 to 2006, contributing a sea level rise of 1.2 mm/decade, indicating the current contribution to sea level rise. For the future *Park et al*. [2013] noted that there were a wide range of projections of 2–14 cm of the contribution that PIG may make to sea level rise by 2100. The estimates are bounded at the lower end by the results of a coupled ice-ocean interaction model of the glacier response to modest ocean forcing [*Joughin et al*., 2010]. A hypothetical scaling of glacier discharge rates suggests a potential sea level contribution over the 21st century of 4 to 15 cm [*Pfeffer et al*., 2008]. However, the extrapolation of recent PIG volume trend acceleration gives a much smaller contribution of about 2 cm by 2100 [*Wingham et al*., 2009]. This is close to the estimate of 1.8 cm from a basin-scale model of the glacier response to ocean forcing [*Joughin*

et al., 2010]. *Wingham et al*. [2009] estimated that a volume of ice equivalent to about 30 mm of eustatic sea level rise could be lost from the PIG to the oceans within 130–140 years. But they note that it is unclear to what extent the remainder of the PIG drainage basin will be drawn down. The most recent modeling studies indicate that PIG will probably contribute 3.5–10 mm global sea level rise over the next two decades [*Favier et al*., 2014], while TG is likely to raise sea level by $<$0.25 mm/yr for the rest of the 21st century, but that its contribution will increase to well above 1 mm/yr in ~200–900 years [*Joughin et al*., 2014]. These findings are consistent with the conclusion of *Rignot et al*. [2014] that the ASE drainage sector, which contains enough ice to raise global sea level by 1.2–1.5 m [*Rignot*, 2008; *Vaughan*, 2008], will significantly contribute to sea level rise in decades to centuries to come.

8. Conclusions and Further Research Required

Research has shown that the changes taking place in the ASE are complex and involve atmosphere-ocean-ice interactions on a range of spatial and temporal scales. Our current understanding has been achieved through a combination of observational campaigns and modeling initiatives. Data have been collected by space-based, aircraft and oceanographic instrumentation, from GPS receivers on the ice and from on-ice traverses.

Over recent decades the outlet glaciers of the ASE have accelerated, thinned, retreated, and experienced basal melting, and are now contributing approximately 10% to global sea level rise. All the ASE glaciers flow into ice shelves, and it is the thinning of these since the 1970s, and their ungrounding from "pinning points" that is widely held to be responsible for triggering the glaciers' decline. The influx of relatively warm CPDW onto the Amundsen Sea continental shelf and into sub-ice-shelf ocean cavities is thought to be responsible for the recent substantial grounding-line retreat and mass loss of ASE glaciers. The ungrounding of parts of the PIG glacier from a submarine ridge in the mid-1940s was particularly important in allowing warm CPDW access to the sub-ice-shelf cavity and accelerating the thinning of the shelf.

CPDW delivery to the ASE is highly variable and is closely related to the regional atmospheric circulation and especially the zonal component of the surface wind on the continental shelf north of the ASE. The ASE is south of the ASL, which has a large variability and which has deepened in recent decades. The ASL is influenced by the phase of the SAM, along with tropical climate variability and especially the phase of ENSO, with El Niño events promoting westerly winds along the coast of West Antarctica and greater CPDW delivery to the ice shelves of the ASE. In particular, the El Niño events from 1939 to the early 1940s have been linked to the ungrounding of the PIG Ice Shelf from the submarine ridge. More recently, tropical Pacific SSTs have increased in fall and early winter, contributing to a weaker ASL during these seasons and more westerly atmospheric flow off the ASE continental shelf, leading to more CPDW inflow.

At present it is not possible to simulate the complex, observed atmosphere-ocean-ice interactions in models, especially as circulation beneath the ice shelves is only now being incorporated into the ocean models, and ice stream models are not coupled directly to ocean models. This hampers investigation of past change and prediction of future conditions.

The model output used for the IPCC Fifth Assessment Report initiative suggest that the westerly winds to the north of the ASE will increase over the coming century, possibly leading to greater CPDW delivery to the ice shelves of the region. The models also give projections that ocean temperatures will increase; however, the models have a wide range of possible changes in both the atmospheric and oceanic conditions.

Predicting how the glaciers of the ASE will change over the coming century presents many challenges. The current retreat could mark the beginning of an unstable phase of the glaciers that, if continued, will result in collapse of the WAIS, but numerical ice sheet models currently lack the predictive power to determine if this will be the case. It is equally possible that the recent retreat will be short-lived and that the ASE will find a new stable state. Progress is hindered by incomplete knowledge of bed topography in the vicinity of the grounding line. Furthermore, a number of key processes are still missing or poorly represented in models of -ice-flow.

A number of major initiates are underway or planned to gain greater insight into the oceanography, meteorology, geology, geophysics, and glaciology in the ASE, and several important documents have been published describing visions for future research. The U.S. National Science Foundation recently set out their strategic vision for Antarctic and Southern Ocean research in a substancial document [*Committee on the*

Development of a Strategic Vision for the U.S. Antarctic Program, 2015]. A multinational group of scientists led by the Scientific Committee on Antarctic Research carried out a horizon scan to determine the research priorities for the next few decades [*Kennicutt et al.*, 2014].

Already underway is the Ice Sheet Stability Programme of the UK Natural Environment Research Council, which will give new insights into the changes taking place in the ASE through a research vessel cruise and an on-ice component targeting the PIG, TG, and Union Glacier that involves a tractor traverse. Such multidisciplinary projects are essential to understand the complex changes taking place and determine the link between changes in the wind field and oceanic heat redistribution in coastal Antarctica.

Realistically modeling the atmosphere-ocean-ice interactions within the ASE will be very difficult. High-quality, high-resolution near-surface atmospheric fields are needed to both investigate past changes in the area and to predict future conditions. The reanalysis data sets have been used in a number of studies to drive ocean models, although because of the relative lack of observational data in the area, there are differences in the fields that can have a major impact on the ocean forcing. There are now several high-quality reanalysis data sets, and these have been compared in several studies [*Bromwich et al.*, 2007; *Bracegirdle and Marshall*, 2012]. It is hoped that there will be a convergence in the near-surface flow in future reanalyses and that higher horizontal resolution data will become available.

Although the reanalysis data sets are extremely valuable in examining the past atmospheric circulation in the ASE regions, especially as some of the latest data sets have a relatively high horizontal resolution, such as the ERA Interim reanalysis with its 70 km resolution, this is still not high enough to drive many of the ocean models. With the current generation of operational numerical weather prediction models having horizontal resolutions as high as 9 km in the case of the ECMWF model, it is hoped that future reanalysis initiatives generate data sets that will give better representation of the complex wind field in the ASE area.

In order to improve models simulating ocean melting it is crucial to collect reliable in situ data of ocean melt rates at the grounding zones because these have a major impact on future predictions of ice loss [e.g., *Joughin et al.*, 2010]. Such data could either be collected by AUV missions [e.g., *Jenkins et al.*, 2010] or sub-ice-shelf drilling [e.g., *Stanton et al.*, 2013]. Data/samples are also required from the subglacial bed (e.g., sediments) for better characterization of glacial sliding conditions. In addition, higher-resolution data sets of sub-ice-shelf and subglacial topography [e.g., *Tinto and Bell*, 2011; *Fretwell et al.*, 2013; *Muto et al.*, 2013, 2016] are required to improve estimates of current melting and future ice stream behavior [e.g., *Schodlok et al.*, 2012; *De Rydt et al.*, 2014].

The current generation of coupled atmosphere-ocean-sea ice models used in initiatives such as IPCC has a number of issues that limit investigation of conditions in the ASE. None of the models have ocean circulation below the ice shelves, and the flow in such areas has to be investigated with standalone models. Some of the IPCC CMIP5 models also have large biases in ocean temperature and salinity [*Turner et al.*, 2013], which is a problem when their output is used at the lateral boundaries of regional models. The poor representation of ocean conditions and sea ice extent is a major failing of the current generation of GCMs, and improvements need to be made in order to simulate conditions in the ASE.

With so little in situ historical and paleo-climate data available before the 1970s it is important to collect archives of atmospheric and oceanographic changes, for example, ice cores such as the WAIS Divide ice core [e.g., *WAIS Divide Project Members*, 2013] and marine sediment cores [e.g., *Larter et al.*, 2014], including deep drilling records from past warm periods, and to develop proxies so that decadal time scale variability can be investigated. Data are also needed on geothermal heat flux, glacial isostatic adjustment, and lithospheric/crustal properties.

Ice core data have been used to investigate atmospheric flow patterns such as the ASL, but this is a difficult feature to investigate and there are indications that ice cores have not been collected in the best areas to determine variability of the ASL. Marine sediment core data from the ASE shelf have the potential to provide long-term records of various parameters, such as the variability of sea ice coverage or ocean temperature, although the dating of these cores remains challenging while their temporal resolution is usually relatively low [e.g., *Hillenbrand et al.*, 2010; *Larter et al.*, 2014; *Smith et al.*, 2014; *Witus et al.*, 2014]. Very important for the study of marine sediment cores from the ASE is the development and application of innovative proxies for sea ice coverage and paleo-temperatures because such proxies are usually based on the analysis of

microfossil assemblages and organic compounds in the sediments, which, however, are very rare in the predominantly terrigenous sediments from the ASE shelf. A very high priority should be assigned to the development of a robust proxy for the upwelling of CPDW as currently no reliable CPDW proxy is available. It is planned that the Integrated Ocean Drilling Program Expedition 379 will drill in the ASE in early 2019, with the goal of collecting marine sediments that will shed light on CPDW processes and environmental conditions in previous warm times. Reliable proxies for ice-shelf presence (or absence) are also required for evaluating the role of ice-shelf buttressing for delaying or even halting ice sheet retreat and thinning. In addition, more rock samples for reconstructing the thinning history of the ASE drainage basin by surface exposure age dating are required because currently only a few locations in the hinterland of the ASE have been studied [*Johnson et al*., 2008, 2014; *Larter et al*., 2014; *Lindow et al*., 2014]. In addition, the recovery and analysis of further marine sediment cores from below the modern ASE ice shelves [e.g., *Smith et al*., 2013, 2016] will help to reconstruct the (sub) recent ice-ocean and ice-bed topography interactions.

Acknowledgments
This study is part of the British Antarctic Survey Polar Science for Planet Earth Programme. It was funded by the UK Natural Environment Research Council and is part of the synthesis element of the NERC grant NE/H02333X/1. No unpublished data were used in the preparation of this paper.

References

Arblaster, J., and G. A. Meehl (2006), Contributions of external forcings to Southern Annular Mode trends, *J. Clim.*, *19*, 2896–2905.

Arneborg, L., A. K. Wåhlin, G. Bjork, B. Liljebladh, and A. H. Orsi (2012), Persistent inflow of warm water onto the central Amundsen shelf, *Nat. Geosci.*, *5*(12), 876–880.

Arthern, R. J., D. P. Winebrenner, and D. G. Vaughan (2006), Antarctic snow accumulation mapped using polarization of 4.3-cm wavelength microwave emission, *J. Geophys. Res.*, *111*, D06107, doi:10.1029/2004JD005667.

Assman, K. M., A. Jenkins, D. R. Shoosmith, D. P. Walker, S. S. Jacobs, and K. W. Nicholls (2013), Variability of circumpolar deep water transport onto the Amundsen Sea continental shelf through a shelf break trough, *J. Geophys. Res. Oceans*, *118*, 6603–6620, doi:10.1002/2013JC008871.

Bindschadler, R. A., D. G. Vaughan, and P. Vornberger (2011), Variability of basal melt beneath the Pine Island Glacier ice shelf, West Antarctica, *J. Glaciol.*, *57*(204), 581–595, doi:10.3189/002214311797409802.

Bishop, J. F., and J. L. W. Walton (1981), Bottom melting under George VI Ice Shelf, Antarctica, *J. Glaciol.*, *27*, 429–447.

Blankenship, D. D., R. E. Bell, S. M. Hodge, J. M. Brozena, J. C. Behrendt, and C. A. Finn (1993), Active volcanism beneath the West Antarctic ice sheet and implications for ice-sheet stability, *Nature*, *361*, 526–529.

Blatter, H. (1995), Velocity and stress-fields in grounded glaciers: A simple algorithm for including deviatoric stress gradients, *J. Glaciol.*, *41*, 333–344.

Bleck, R., C. Rooth, D. M. Hu, and L. T. Smith (1992), Salinity-driven thermocline transients in a wind-forced and thermohaline-forced isopycnic coordinate model of the North-Atlantic, *J. Phys. Oceanogr.*, *22*(12), 1486–1505.

Bracegirdle, T. J., and G. J. Marshall (2012), The reliability of Antarctic tropospheric pressure and temperature in the latest global reanalyses, *J. Clim.*, *25*, 7138–7146.

Bracegirdle, T. J., W. M. Connolley, and J. Turner (2008), Antarctic climate change over the twenty first century, *J. Geophys. Res.*, *113*, D03103, doi:10.1029/2007JD008933.

Bracegirdle, T. J., J. Turner, J. S. Hosking, and T. Phillips (2014), Sources of uncertaintly in projections of twenty-first century westerly wind changes over the Amundsen Sea, Antarctica, in CMIP5 climate models, *Clim. Dyn.*, doi:10.1007/s00382-013-2032-1.

Bromwich, D. H., and R. L. Fogt (2004), Strong trends in the skill of the ERA-40 and NCEP-NCAR reanalyses in the high and middle latitudes of the Southern Hemisphere, 1958–2001, *J. Clim.*, *17*, 4603–4619.

Bromwich, D. H., R. L. Fogt, K. I. Hodges, and J. E. Walsh (2007), A tropospheric assessment of the ERA-40, NCEP, and JRA-25 global reanalyses in the polar regions, *J. Geophys. Res.*, *112*, D10111, doi:10.1029/2006JD007859.

Bromwich, D. H., J. P. Nicolas, and A. J. Monaghan (2011), An assessment of precipitation changes over Antarctica and the Southern Ocean since 1989 in contemporary global reanalyses, *J. Clim.*, *24*, 4189–4209, doi:10.1175/2011JCLI4074.1.

Bromwich, D. H., J. P. Nicolas, A. J. Monaghan, M. A. Lazzara, L. M. Keller, G. A. Weidner, and A. B. Wilson (2013a), Central West Antarctica among the most rapidly warming regions on Earth, *Nat. Geosci.*, *6*, 139–145.

Bromwich, D. H., F. O. Otieno, K. M. Hines, K. W. Manning, and E. Shilo (2013b), Comprehensive evaluation of polar weather research and forecasting performance in the Antarctic, *J. Geophys. Res. Atmos.*, *118*, 274–292, doi:10.1029/2012JD018139.

Byrd, R. E. (1947), Our navy explores Antarctica, *Geogr. Mag.*, *92*(4), 429–522.

Clem, K. R., and J. A. Renwick (2015), Austral spring southern hemisphere circulation and temperature changes and links to the SPCZ, *J. Clim.*, *28*, 7371–7384.

Committee on the Development of a Strategic Vision for the U.S. Antarctic Program (2015), *A Strategic Vision for NSF Investments in Antarctic and Southern Ocean Research*, Natl. Acad. Press, Washington, D. C.

Connolley, W. M. (1997), Variability in annual mean circulation in southern high latitudes, *Clim. Dyn.*, *13*, 745–756.

Cornford, S. L., D. F. Martin, D. T. Graves, D. F. Ranken, A. M. Le Brocq, R. M. Gladstone, A. J. Payne, E. G. Ng, and W. H. Lipscomb (2013), Adaptive mesh, finite volume modeling of marine ice sheets, *J. Comput. Phys.*, *232*(1), 529–549, doi:10.1016/j.jcp.2012.08.037.

Cornford, S. L., et al. (2015), Century-scale simulations of the response of the West Antarctic Ice Sheet to a warming climate, *Cryosphere*, *9*(4), 1579–1600.

Corr, H. F. J., and D. G. Vaughan (2008), A recent volcanic eruption beneath the West Antarctic ice sheet, *Nat. Geosci.*, *1*, 122–125.

Cuffey, K. M., and W. S. B. Paterson (2010), *The Physics of Glaciers*, 4th edn., Academic Press.

Deb, P., A. Orr, J. S. Hosking, T. Phillips, J. Turner, D. Bannister, J. O. Pope, and S. Colwell (2016), An assessment of the Polar Weather Research and Forecast (WRF) model representation of near-surface meteorological variables over West Antarctica, *J. Geophys. Res. Atmos.*, *121*, 1532–1548, doi:10.1002/2015JD024037.

DeConto, R. M., and D. Pollard (2016), Contribution of Antarctica to past and future sea-level rise, *Nature*, *531*, 591–597.

Dee, D. P., et al. (2011), The ERA-Interim reanalysis: Configuration and performance of the data assimilation system, *Q. J. R. Meteorol. Soc.*, *137*(656), 553–597.

Depoorter, M. A., J. L. Bamber, J. A. Griggs, J. Lenaerts, S. R. M. Ligtenberg, M. R. Van den Broeke, and G. Moholdt (2013), Calving fluxes and basal melt rates of Antarctic ice shelves, *Nature*, *502*, 89–92.

De Rydt, J., P. R. Holland, P. Dutrieux, and A. Jenkins (2014), Geometric and oceanographic controls on melting beneath Pine Island Glacier, *J. Geophys. Res. Oceans*, *119*, 2420–2438, doi:10.1002/2013JC009513.
Ding, Q., E. J. Steig, D. S. Battisti, and M. Kuttel (2011), Winter warming in West Antarctica caused by central tropical Pacific warming, *Nat. Geosci.*, doi:10.1038/NGEO1129.
Doake, C. S. M., H. F. J. Corr, H. Rott, P. Skvarca, and N. W. Young (1998), Breakup and conditions for stability of the northern Larsen Ice Shelf, Antarctica, *Nature*, *391*(6669), 778–780.
Dowdeswell, J. A., J. Evans, C. Ó. Cofaigh, and J. B. Anderson (2006), Morphology and sedimentary processes on the continental slope off Pine Island Bay, Amundsen Sea, West Antarctica, *Geol. Soc. Am. Bull.*, *118*, 606–619.
Dunai, T. J. (2010), *Cosmogenic Nuclides: Principles, Concepts and Applications in the Earth Surface Sciences*, Cambridge Univ. Press, Cambridge.
Durand, G., O. Gagliardini, B. de Fleurian, T. Zwinger, and E. Le Meur (2009), Marine ice sheet dynamics: Hysteresis and neutral equilibrium, *J. Geophys. Res.*, *114*, F03009, doi:10.1029/2008JF001170.
Dutrieux, P., D. G. Vaughan, H. F. Corr, A. Jenkins, P. R. Holland, I. Joughin, and H. Fleming (2013), Pine Island Glacier ice shelf melt distributed at kilometre scales, *Cryosphere*, *7*, 1543–1555.
Dutrieux, P., J. De Rydt, A. Jenkins, P. R. Holland, H. K. Ha, S. H. Lee, E. J. Steig, Q. H. Ding, E. P. Abrahamsen, and M. Schroder (2014), Strong sensitivity of Pine Island Ice-Shelf melting to climatic variability, *Science*, *343*(6167), 174–178.
Evans, J., J. A. Dowdeswell, C. Ó. Cofaigh, T. J. Benham, and J. B. Anderson (2006), Extent and dynamics of the West Antarctic Ice Sheet on the outer continental shelf of Pine Island Bay during the last glaciation, *Mar. Geol.*, *230*, 53–72.
Favier, L., O. Gagliardini, G. Durand, and T. Zwinger (2012), A three-dimensional full Stokes model of the grounding line dynamics: Effect of a pinning point beneath the ice shelf, *Cryosphere*, *6*, 101–112.
Favier, L., G. Durand, S. L. Cornford, G. H. Gudmundsson, O. Gagliardini, F. Gillet-Chaulet, T. Zwinger, A. J. Payne, and A. M. Le Brocq (2014), Retreat of Pine Island Glacier controlled by marine ice-sheet instability, *Nat. Clim. Change*, *4*(2), 117–121.
Favier, V., C. Agosta, S. Parouty, G. Durand, G. Delaygue, H. Gallee, A. S. Drouet, A. Trouvilliez, and G. Krinner (2013), An updated and quality controlled surface mass balance dataset for Antarctica, *Cryosphere*, *7*(2), 583–597.
Ferrigno, J. G., R. S. Williams, C. E. Rosanova, B. K. Lucchitta, and C. Swithinbank (1998), Analysis of coastal change in Marie Byrd Land and Ellsworth Land, West Antarctica, using Landsat imagery, *Ann. Glaciol.*, *27*, 33–40.
Fogt, R. L., and D. H. Bromwich (2006), Decadal variability of the ENSO teleconnection to the high latitude South Pacific governed by coupling with the Southern Annular Mode, *J. Clim.*, *19*, 979–997.
Fogt, R. L., J. Perlwitz, A. J. Monaghan, D. H. Bromwich, J. M. Jones, and G. J. Marshall (2009), Historical SAM variability. Part II: Twentieth-century variability and trends from reconstructions, observations, and the IPCC AR4 models, *J. Clim.*, *22*(20), 5346–5365.
Fogt, R. L., D. H. Bromwich, and K. M. Hines (2011), Understanding the SAM influence on the South Pacific ENSO teleconnection, *Clim. Dyn.*, *36*(7–8), 1555–1576.
Fogt, R. L., A. J. Wovrosh, R. A. Langen, and I. Simmonds (2012), The characteristic variability and connection to the underlying synoptic activity of the Amundsen-Bellingshausen Seas Low, *J. Geophys. Res.*, *117*, D07111, doi:10.1029/2011JD017337.
Fretwell, P. T., et al. (2013), Bedmap2: Improved ice bed, surface and thickness datasets for Antarctica, *Cryosphere*, *7*, 375–393.
Gille, S. T. (2002), Warming of the Southern Ocean since the 1950s, *Science*, *295*, 1275–1277.
Gille, S. T. (2008), Decadal-scale temperature trends in the Southern Hemisphere ocean, *J. Clim.*, *21*, 4749–4765, doi:10.1175/2008JCLI2131.1.
Gillett, N. P., and J. C. Fyfe (2013), Annular mode changes in the CMIP5 simulations, *Geophys. Res. Let.*, *40*, 1189–1193, doi:10.1002/grl.50249.
Gladstone, R. M., V. Lee, J. Rougier, A. J. Payne, H. Hellmer, A. Le Brocq, A. Shepherd, T. L. Edwards, J. Gregory, and S. L. Cornford (2012), Calibrated prediction of Pine Island Glacier retreat during the 21st and 22nd centuries with a coupled flowline model, *Earth Planet. Sci. Lett.*, *333*, 191–199.
Gohl, K., et al. (2007), Geophysical survey reveals tectonic structures in the Amundsen Sea embayment, West Antarctica, U.S. Geological Survey and The National Academies; USGS OF-2007-1047, Short Res. Pap. 047, doi:10.3133/of2007-1047.srp047.
Gohl, K., G. Uenzelmann-Neben, R. D. Larter, C.-D. Hillenbrand, K. Hochmuth, T. Kalberg, E. Weigelt, B. Davy, G. Kuhn, and F. O. Nitsche (2013), Seismic stratigraphic record of the Amundsen Sea Embayment shelf from pre-glacial to recent times: Evidence for a dynamic West Antarctic ice sheet, *Mar. Geol.*, *344*, 115–131.
Graham, A. G. C., R. D. Larter, K. Gohl, C.-D. Hillenbrand, J. A. Smith, and G. Kuhn (2009), Bedform signature of a West Antarctic palaeo-ice stream reveals a multi-temporal record of flow and substrate control, *Quat. Sci. Rev.*, *28*, 2774–2793.
Graham, A. G. C., R. D. Larter, K. Gohl, J. A. Dowdeswell, C.-D. Hillenbrand, J. A. Smith, J. Evans, G. Kuhn, and T. Deen (2010), Flow and retreat of the Late Quaternary Pine Island-Thwaites palaeo-ice stream, West Antarctica, *J. Geophys. Res.*, *115*, F03025, doi:10.1029/2009JF001482.
Graham, A. G. C., P. Dutrieuz, D. G. Vaughan, F. O. Nitsche, R. Gyllencreutz, S. L. Greenwood, R. D. Larter, and A. Jenkins (2013), Sea-bed corrugations beneath an Antarctic ice shelf revealed by autonomous underwater vehicle survey: Origin and implications for the history of Pine Island Glacier, *J. Geophys. Res. Earth Surf.*, *118*, 1356–1366, doi:10.1002/jgrf.20087.
Gudmundsson, G. H. (2007), Tides and the flow of Rutford Ice Stream, West Antarctica, *J. Geophys. Res.*, *112*, F04007, doi:10.1029/2006JF000731.
Gudmundsson, G. H. (2013), Ice-shelf buttressing and the stability of marine ice sheets, *Cryosphere*, *7*, 647–655.
Gudmundsson, G. H., J. Krug, G. Durand, L. Favier, and O. Gagliardini (2012), The stability of grounding lines on retrograde slopes, *Cryosphere*, *6*, 1497–1505.
Heimbach, P., and M. Losch (2012), Adjoint sensitivities of sub-ice shelf melt rates to ocean circulation under Pine Island Ice Shelf, West Antarctica, *Ann. Glaciol.*, *53*, 59–69.
Hellmer, H. H., and D. J. Olbers (1989), A two-dimensional model for the thermohaline circulation under an ice shelf, *Antarct. Sci.*, *1*, 325–336.
Hellmer, H. H., S. S. Jacobs, and A. Jenkins (1998), Oceanic erosion of a floating Antarctic glacier in the Amundsen Sea, in *Ocean, Ice, and Atmosphere: Interactions at the Antarctic Continental Margin*, vol. 75, edited by S. S. Jacobs and R. F. Weiss, pp. 83–99, AGU, Washington, D. C.
Hellmer, H. H., F. Kauker, R. Timmermann, J. Determann, and J. Rae (2012), Twenty-first-century warming of a large Antarctic ice-shelf cavity by a redirected coastal current, *Nature*, *485*(7397), 225–228.
Hillenbrand, C.-D., J. A. Smith, G. Kuhn, O. Esper, R. Gersonde, R. D. Larter, B. Maher, S. G. Moreton, T. M. Shimmield, and M. Korte (2010), Age assignment of a diatomaceous ooze deposited in the western Amundsen Sea Embayment after the Last Glacial Maximum, *J. Quat. Sci.*, *25*, 280–295.
Hillenbrand, C.-D., et al. (2013), Grounding-line retreat of the West Antarctic Ice Sheet from inner Pine Island Bay, *Geology*, *41*, 35–38.
Hines, K. M., D. H. Bromwich, and G. J. Marshall (2000), Artificial surface pressure trends in the NCEP-NCAR reanalysis over the Southern Ocean and Antarctica, *J. Clim.*, *13*, 3940–3952.
Hochmuth, K., and Gohl, K. (2013), Glacio-marine sedimentation dynamics of the Abbot glacial trough of the Amundsen Sea Embayment shelf, West Antarctica, in *Antarct. Palaeoenvironments and Earth-Surface Processes, Geological Soc. Spec. Publ.*, vol. 381, edited by M. H. Barker et al., Geol. Soc., London, U. K., doi:10.1144/SP381.21.

Hogg, A. M., M. P. Meredith, J. R. Blundell, and C. Wilson (2008), Eddy heat flux in the Southern Ocean: Response to variable wind forcing, *J. Clim.*, *21*, 608–620.
Holland, D. M. (2001), Transient sea-ice polynya forced by environmental flow variability, *Prog. Oceanogr.*, *48*(475–532), 2001.
Holland, D. M., and A. Jenkins (2001), Adaptation of an isopycnic coordinate ocean model for the study of circulation beneath ice shelves, *Mon. Weather Rev.*, *129*, 1905–1927.
Holt, J. W., D. D. Blankenship, D. L. Morse, D. A. Young, M. E. Peters, S. D. Kempf, T. G. Richter, D. G. Vaughan, and H. F. Corr (2006), New boundary conditions for the West Antarctic Ice Sheet; subglacial topography of the Thwaites and Smith Glacier catchments, *Geophys. Res. Lett.*, *33*, L09502, doi:10.1029/2005GL025561.
Hosking, J. S., A. Orr, G. J. Marshall, J. Turner, and T. Phillips (2013), The influence of the Amundsen-Bellingshausen Seas Low on the climate of West Antarctica and its representation in coupled climate model simulations, *J. Clim.*, *26*, 6633–6648.
Hoskins, B. J., and D. J. Karoly (1981), The steady linear response of a spherical atmosphere to thermal and orographic forcing, *J. Atmos. Sci.*, *38*, 1179–1196.
Howat, I. M., K. Jezek, M. Studinger, J. A. MacGregor, J. Paden, D. Floriciouiu, R. Russel, M. Linkswiler, and R. T. Dominguez (2012), Rift in Antarctic Glacier: A unique chance to study ice shelf retreat, *Eos Trans. AGU*, *93*, 77–88.
Hughes, T. (1973), Is the West Antarctic Ice Sheet disintegrating?, *J. Geophys. Res.*, *78*(33), 7884–7910, doi:10.1029/JC078i033p07884.
Hughes, T. J. (1981), The weak underbelly of the West Antarctic ice-sheet, *J. Glaciol.*, *27*, 493–495.
Jacobs, S. (2006), Observations of change in the Southern Ocean, *Philos. Trans. R. Soc., A*, *364*, 1657–1681.
Jacobs, S., C. Giulivi, P. Dutrieux, E. Rignot, F. Nitsche, and J. Mouginot (2013), Getz Ice Shelf melting response to changes in ocean forcing, *J. Geophys. Res. Oceans*, *118*, 1–17, doi:10.1002/jgrc.20298.
Jacobs, S. S., H. H. Hellmer, and A. Jenkins (1996), Antarctic ice sheet melting in the southeast Pacific, *Geophys. Res. Lett.*, *23*(9), 957–960, doi:10.1029/96GL00723.
Jacobs, S. S., A. Jenkins, C. F. Giulivi, and P. Dutrieux (2011), Stronger ocean circulation and increased melting under Pine Island Glacier ice shelf, *Nat. Geosci.*, *4*(8), 519–523.
Jacobs, S. S., A. Jenkins, H. H. Hellmer, C. F. Giulivi, F. O. Nitsche, B. Huber, and R. Guerrero (2012), The Amundsen Sea and the Antarctic ice sheet, *Oceanography*, *25*, 154–163.
Jakobsson, M., et al. (2011), Geological record of ice shelf break-up and grounding line retreat, Pine Island Bay, West Antarctica, *Geology*, *39*, 691–694.
Jakobsson, M., J. B. Anderson, F. Nitsche, R. Gyllencreutz, A. Kirshner, N. Kirchner, M. O'Regan, R. Mohammad, and B. Eriksson (2012), Ice sheet retreat dynamics inferred from glacial morphology of the central Pine Island Bay Trough, West Antarctica, *Quat. Sci. Rev.*, *38*, 1–10.
Jenkins, A. (1999), The impact of melting ice on ocean waters, *J. Phys. Oceanogr.*, *29*, 2370–2381.
Jenkins, A., and S. S. Jacobs (2008), Circulation and melting beneath George VI Ice Shelf, Antarctica, *J. Geophys. Res.*, *113*, C04013, doi:10.1029/2007JC004449.
Jenkins, A., D. G. Vaughan, S. S. Jacobs, H. H. Hellmer, and J. R. Keys (1997), Glaciological and oceanographic evidence of high melt rates beneath Pine island glacier, West Antarctica, *J. Glaciol.*, *43*(143), 114–121.
Jenkins, A., P. Dutrieux, S. S. Jacobs, S. D. McPhail, J. R. Perrett, A. T. Webb, and D. White (2010), Observations beneath Pine Island Glacier in West Antarctica and implications for its retreat, *Nat. Geosci.*, *3*(7), 468–472.
Johnson, J. S., M. J. Bentley, and K. Gohl (2008), First exposure ages from the Amundsen Sea embayment, West Antarctica: The late Quaternary context for recent thinning of Pine Island, Smith, and Pope Glaciers, *Geology*, *36*, 223–226.
Johnson, J. S., M. J. Bentley, J. A. Smith, R. C. Finkel, D. H. Rood, K. Gohl, G. Balco, R. D. Larter, and J. M. Schaefer (2014), Rapid thinning of Pine Island Glacier in the early Holocene, *Science*, *343*, 999–1001.
Jordan, T. A., F. Ferraccioli, D. G. Vaughan, J. W. Holt, H. Corr, D. D. Blankenship, and T. M. Diehl (2010), Aerogravity evidence for major crustal thinning under the Pine Island Glacier region (West Antarctica), *Geol. Soc. Am. Bull.*, *122*, 714–726, doi:10.1130/B26417.1.
Joughin, I., E. Rignot, C. E. Rosanova, B. K. Lucchitta, and J. Bohlander (2003), Timing of recent accelerations of Pine Island Glacier, Antarctica, *Geophys. Res. Lett.*, *30*(13), 1706, doi:10.1029/2003GL017609.
Joughin, I., S. Tulaczyk, J. Bamber, D. Blankenship, J. Holt, T. Scambos, and D. G. Vaughan (2009), Basal conditions for Pine Island and Thwaites glaciers, West Antarctica, determined using satellite and airborne data, *J. Glaciol.*, *55*, 245–257, doi:10.3189/002214309788608705.
Joughin, I., B. E. Smith, and D. M. Holland (2010), Sensitivity of 21st century sea level to ocean-induced thinning of Pine Island Glacier, Antarctica, *Geophy. Res. Lett*, *37*, L20502, doi:10.1029/2010GL044819.
Joughin, I., B. E. Smith, and B. Medley (2014), Marine ice sheet collapse potentially under way for the Thwaites Glacier Basin, West Antarctica, *Science*, *344*, 735–738.
Kalberg, T., K. Gohl, G. Eagles, and C. Spiegel (2015), Rift processes and crustal structure of the Amundsen Sea Embayment, West Antarctica, from 3D potential field modelling, *Mar. Geophys. Res.*, *36*, 263–279, doi:10.1007/s11001-015-9261-0.
Kalén, O., K. M. Assman, A. K. Wåhlin, H. K. Ha, T. W. Kim, and S. H. Lee (2016), Is the oceanic heat flux on the central Amundsen sea shelf caused by barotropic or baroclinic currents?, *Deep Sea Res., Part II*, *123*, 7–15.
Kanamitsu, M., W. Ebisuzaki, J. Woolen, S. K. Yang, J. J. Hnilo, M. Fiorino, and G. L. Potter (2002), NCEP-DOE AMIP-II Reanalysis (R-2), *Bull. Am. Meteorol. Soc.*, *83*, 1631–1643.
Kellogg, T. B., and D. E. Kellogg (1987), Recent glacial history and rapid ice stream retreat in the Amundsen Sea, *J. Geophys. Res.*, *92*, 8859–8864.
Kellogg, T. B., D. E. Kellogg, and T. J. Hughes (1985), Amundsen Sea sediment coring, *Ant. J. U.S.*, *20*, 79–81.
Kennicutt, M. C., et al. (2014), Polar research: Six priorities for Antarctic science, *Nature*, *512*, 23–25.
King, M. A., R. J. Bingham, P. Moore, P. L. Whitehouse, M. J. Bentley, and G. A. Milne (2012), Lower satellite-gravimetry estimates of Antarctic sea-level contribution, *Nature*, *491*, 586–590.
Kirshner, A., J. B. Anderson, M. Jakobsson, M. O'Regan, W. Majewski, and F. Nitsche (2012), Post-LGM deglaciation in Pine island Bay, West Antarctica, *Quat. Sci. Rev.*, *38*, 11–26.
Klages, J. P., G. Kuhn, C.-D. Hillenbrand, A. G. C. Graham, J. A. Smith, R. D. Larter, and K. Gohl (2013), First geomorphological record and glacial history of an interice stream ridge on the West Antarctic continental shelf, *Quat. Sci. Rev.*, *61*, 47–61.
Klages, J. P., G. Kuhn, C.-D. Hillenbrand, A. G. C. Graham, J. A. Smith, R. D. Larter, K. Gohl, and L. Wacker (2014), Retreat of the West Antarctic Ice Sheet from the western Amundsen Sea shelf at a pre- or early LGM stage, *Quat. Sci. Rev.*, *91*, 1–15.
Klages, J. P., G. Kuhn, A. G. C. Graham, C.-D. Hillenbrand, J. A. Smith, F. O. Nitsche, R. D. Larter, and K. Gohl (2015), Palaeo-ice stream pathways and retreat style in the easternmost Amundsen Sea Embayment, West Antarctica, revealed by combined multibeam bathymetric and seismic data, *Geomorphology*, *245*, 207–222, doi:10.1016/j.geomorph.2015.05.020.
Klinck, J. M., and M. S. Dinniman (2010), Exchange across the shelf break at high southern latitudes, *Ocean Sci.*, *6*(2), 513–524.

Lachlan-Cope, T. A., W. M. Connolley, and J. Turner (2001), The role of the non-axisymmetric Antarctic orography in forcing the observed pattern of variability of the Antarctic climate, *Geophys. Res. Lett.*, *28*(21), 4111–4114, doi:10.1029/2001GL013465.
Larour, E., M. Morlighem, H. Seroussi, J. Schiermeier, and E. Rignot (2012), Ice flow sensitivity to geothermal heat flux of Pine Island Glacier, Antarctica, *J. Geophys. Res.*, *117*, F04023, doi:10.1029/2012JF002371.
Larter, R. D., A. G. C. Graham, K. Gohl, G. Kuhn, C.-D. Hillenbrand, J. A. Smith, T. J. Deen, R. A. Livermore, and H.-W. Schenke (2009), Subglacial bedforms reveal complex basal regime in a zone of paleo-ice stream convergence, Amundsen Sea embayment, West Antarctica, *Geology*, *37*, 411–414.
Larter, R. D., et al. (2014), Reconstruction of changes in the Amundsen Sea and Bellingshausen Sea sector of the West Antarctic Ice Sheet since the Last Glacial Maximum, *Quat. Sci. Rev.*, *100*, 55–86.
Lenaerts, J. T. M., M. R. Van den Broeke, S. J. Dery, E. van Meijgaard, W. J. van de Berg, S. P. Palm, and J. S. Rodrigo (2012a), Modeling drifting snow in Antarctica with a regional climate model: 1. Methods and model evaluation, *J. Geophys. Res.*, *117*, D05108, doi:10.1029/2011JD016145.
Lenaerts, J. T. M., M. R. Van den Broeke, W. J. van de Berg, E. van Meijgaard, and P. Kuipers Munneke (2012b), A new, high-resolution surface mass balance map of Antarctica(1979–2010) based on regional atmospheric climate modeling, *Geophys. Res. Lett.*, *39*, L04501, doi:10.1029/2011GL050713.
Li, X., D. M. Holland, E. P. Gerber, and C. Yoo (2015), Rossby waves mediate impacts of tropical oceans on West Antarctic atmospheric circulation in Austral Winter, *J. Clim.*, *28*, 8151–8164.
Li, X. C., D. M. Holland, E. P. Gerber, and C. Yoo (2014), Impacts of the north and tropical Atlantic Ocean on the Antarctic Peninsula and sea ice, *Nature*, *505*(7484), 538–542.
Lindow, J., M. Castex, H. Wittmann, J. S. Johnson, F. Lisker, K. Gohl, and C. Spiegel (2014), Glacial retreat in the Amundsen Sea sector, West Antarctica - first cosmogenic evidence from central Pine Island Bay and the Kohler Range, *Quat. Sci. Rev.*, *98*, 166–173.
Livingstone, S. J., C. Ó. Cofaigh, C. Stokes, C.-D. Hillenbrand, A. Vieli, and S. S. R. Jamieson (2012), Antarctic palaeo-ice streams, *Earth Sci. Rev.*, *111*, 90–128.
Losch, M. (2008), Modeling ice shelf cavities in a z coordinate ocean general circulation model, *J. Geophys. Res.*, *113*, C08043, doi:10.1029/2007JC004368.
Lowe, A. L., and J. B. Anderson (2002), Reconstruction of the West Antarctic Ice Sheet in Pine Island Bay during the last glacial maximum and its subsequent retreat history, *Quat. Sci. Rev.*, *21*(16–17), 1879–1897.
Lowe, A. L., and J. B. Anderson (2003), Evidence for abundant subglacial meltwater beneath the paleo-ice sheet in Pine Island Bay, Antarctica, *J. Glaciol.*, *49*, 125–138.
Lythe, M., D. G. Vaughan, and The BEDMAP Consortium (2001), BEDMAP: A new ice thickness and subglacial topographic model of Antarctica, *J. Geophys. Res.*, *106*, 11,335–11,352, doi:10.1029/2000JB900449.
MacAyeal, D. R. (1989), Large-scale ice flow over a viscous basal sediment—Theory and application to Ice Stream-B, Antarctica, *J. Geophys. Res.*, *94*(B4), 4071–4087.
MacAyeal, D. R., R. A. Bindschadler, and T. A. Scambos (1995), Basal friction of Ice-Stream-E, West Antarctica, *J. Glaciol.*, *41*(138), 247–262.
MacGregor, J. A., G. A. Catania, M. S. Markowski, and A. G. Andrews (2012), Widespread rifting and retreat of ice-shelf margins in the eastern Amundsen Sea Embayment between 1972 and 2011, *J. Glaciol.*, *58*, 458–466.
Mankoff, K. D., S. S. Jacobs, S. M. Tulaczyk, and S. E. Stammerjohn (2012), The role of Pine Island Glacier ice shelf basal channels in deep-water upwelling, polynyas and ocean circulation in Pine Island Bay, Antarctica, *Ann. Glaciol.*, *53*(60), 123–128, doi:10.3189/2012AoG60A062.
Marshall, G. J. (2003), Trends in the Southern Annular Mode from observations and reanalyses, *J. Clim.*, *16*, 4134–4143.
Marshall, G. J., and S. A. Harangozo (2000), An appraisal of NCEP/NCAR reanalysis MSLP viability for climate studies in the South Pacific, *Geophys. Res. Lett.*, *27*, 3057–3060, doi:10.1029/2000GL011363.
Marshall, J., C. Hill, L. Perelman, and A. Adcroft (1997), Hydrostatic, quasi-hydrostatic, and nonhydrostatic ocean modeling, *J. Geophys. Res.*, *102*(C3), 5733–5752, doi:10.1029/96JC02776.
Maule, C. F., M. E. Purucker, N. Olsen, and K. Mosegaard (2005), Heat flux anomalies in Antarctica revealed by satellite magnetic data, *Science*, *309*, 464–467.
Medley, B., et al. (2013), Airborne-radar and ice-core observations of annual snow accumulation over Thwaites Glacier, West Antarctica confirm the spatiotemporal variability of global and regional atmospheric models, *Geophys. Res. Lett.*, *40*, 3649–3654, doi:10.1002/grl.50706.
Medley, B., et al. (2014), Constraining the recent mass balance of Pine Island and Thwaites glaciers, West Antarctica, with airborne observations of snow accumulation, *Cryosphere*, *8*(4), 1375–1392.
Meijers, A. J. S. (2014), The Southern Ocean in the Coupled Model Intercomparison Project phase 5, *Philos. Trans. R. Soc., A*, *372*(2019).
Mengel, M., J. Feldmann, and A. Leverman (2015), Linear sea-level response to abrupt ocean warming of major West Antarctic ice basin, *Nat. Clim. Change*, doi:10.1038/nclimate2808.
Mercer, J. H. (1978), West Antarctic ice sheet and CO_2 greenhouse effect: A threat of disaster, *Nature*, *271*, 321–325, doi:10.1038/271321a0.
Meredith, M. P., et al. (2011), Sustained monitoring of the Southern Ocean at Drake Passage: Past achievements and future priorities, *Rev. Geophys.*, *49*, RG4005, doi:10.1029/2010RG000348.
Monaghan, A. J., et al. (2006a), Insignificant change in Antarctic snowfall since the International Geophysical Year, *Science*, *313*, 827–831.
Monaghan, A. J., D. H. Bromwich, and S.-H. Wang (2006b), Recent trends in Antarctic snow accumulation from Polar MM5 simulations, *Philos. Trans. R. Soc. London, Ser. A*, *364*, 1683–1708.
Mouginot, J., E. Rignot, and B. Scheuchl (2014), Sustained increase in ice discharge from the Amundsen Sea Embayment, West Antarctica, from1973 to 2013, *Geophys. Res. Lett.*, *41*, 1576–1584, doi:10.1002/2013GL059069.
Muto, A., S. Anandakrishnan, and R. B. Alley (2013), Subglacial bathymetry and sediment layer distribution beneath the Pine Island Glacier ice shelf, West Antarctica, modelled using aerogravity and autonomous underwater vehicle data, *Ann. Glaciol.*, *54*(64), 27–32, doi:10.3189/2013AoG64A110.
Muto, A., L. E. Peters, K. Gohl, I. Sasgen, R. B. Alley, S. Anandakrishnan, and K. L. Riverman (2016), Subglacial bathymetry and sediment distribution beneath Pine Island Glacier ice shelf modeled using aerogravity and in situ geophysical data: New results, *Earth Planet. Sci. Lett.*, *433*, 63–75.
Naish, T., et al. (2009), Obliquity-paced Pliocene West Antarctic ice sheet oscillations, *Nature*, *458*, 322–329.
Nakayama, Y., M. Schroder, and H. H. Hellmer (2013), From circumpolar deep water to the glacial meltwater plume on the eastern Amundsen Shelf, *Deep Sea Res., Part I*, *77*, 50–62.
Nakayama, Y., R. Timmermann, C. B. Rodehacke, M. Schroder, and H. H. Hellmer (2014), Modeling the spreading of glacial meltwater from the Amundsen and Bellingshausen Seas, *Geophys. Res. Lett.*, *41*, 7942–7949, doi:10.1002/2014GL061600.
Nicolas, J. P., and D. H. Bromwich (2011), Climate of West Antarctica and influence of marine air intrusions, *J. Clim.*, *24*(1), 49–67.

Nitsche, F. O., S. S. Jacobs, R. D. Larter, and K. Gohl (2007), Bathymetry of the Amundsen Sea continental shelf: Implications for geology, oceanography, and glaciology, *Geochem. Geophys. Geosyst.*, *8*, Q10009, doi:10.1029/2007GC001694.
Nitsche, F. O., K. Gohl, R. D. Larter, C.-D. Hillenbrand, G. Kuhn, J. A. Smith, S. Jacobs, J. B. Anderson, and M. Jakobsson (2013), Paleo ice flow and subglacial meltwater dynamics in Pine Island Bay, West Antarctica, *Cryosphere*, *7*, 249–262, doi:10.5194/tc-7-249-2013.
Onogi, K., et al. (2007), The JRA-25 Reanalysis, *J. Meteorol. Soc. Jpn.*, *85*, 369–432.
Orr, A., T. Phillips, S. Webster, A. Elvidge, M. Weeks, J. S. Hosking, and J. Turner (2013), Unified model high resolution simulations of a strong wind event in Antarctica, *Q. J. R. Meteorol. Soc.*, *140*(684), 2287–2297.
Park, J. W., N. Gourmelen, A. Shepherd, S. W. Kim, D. G. Vaughan, and D. J. Wingham (2013), Sustained retreat of the Pine Island Glacier, *Geophys. Res. Lett.*, *40*, 2137–2142, doi:10.1002/grl.50379.
Pattyn, F., et al. (2013), Grounding-line migration in plan-view marine ice-sheet models: Results of the ice2sea MISMIP3d intercomparison, *J. Glaciol.*, *59*, 410–422, doi:10.3189/2013JoG12J129.
Payne, A. J., A. Vieli, A. Shepherd, D. J. Wingham, and E. Rignot (2004), Recent dramatic thinning of largest West Antarctic ice stream triggered by oceans, *Geophys. Res. Lett.*, *31*, L23401, doi:10.1029/2004GL021284.
Payne, A. J., P. R. Holland, A. Shepherd, I. C. Rutt, A. Jenkins, and I. Joughin (2007), Numerical modeling of ocean-ice interactions under Pine Island Bay's ice shelf, *J. Geophys. Res.*, *112*, C10019, doi:10.1029/2006JC003733.
Pfeffer, W. T., J. T. Harper, and S. O'Neel (2008), Kinematic constraints on glacier contributions to 21st-century sea-level rise, *Science*, *321*(5894), 1340–1343.
Pritchard, H. D., R. J. Arthern, D. G. Vaughan, and L. A. Edwards (2009), Extensive dynamic thinning on the margins of the Greenland and Antarctic ice sheets, *Nature*, *461*(7266), 971–975.
Pritchard, H. D., S. R. M. Ligtenberg, H. A. Fricker, D. G. Vaughan, M. R. Van den Broeke, and L. Padman (2012), Antarctic ice-sheet loss driven by basal melting of ice shelves, *Nature*, *484*(7395), 502–505.
Rienecker, M. M., et al. (2011), MERRA: NASA's Modern-Era Retrospective Analysis for Research and Applications, *J. Clim.*, *24*, 3624–3648.
Rignot, E. (2002), Ice-shelf changes in Pine Island Bay, Antarctica, 1947-2000, *J. Glaciol.*, *48*, 247–256.
Rignot, E. (2006), Changes in ice dynamics and mass balance of the Antarctic ice sheet, *Philos. Trans. R. Soc., A*, *364*, 1637–1655.
Rignot, E. (2008), Changes in West Antarctic ice stream dynamics observed with ALOS PALSAR data, *Geophys. Res. Lett.*, *35*, L12505, doi:10.1029/2008GL033365.
Rignot, E., D. G. Vaughan, M. Schmeltz, T. Dupont, and D. R. MacAyeal (2002), Acceleration of Pine Island and Thwaites Glaciers, West Antarctica, *Ann. Glaciol.*, *34*, 189–194.
Rignot, E., J. L. Bamber, M. R. Van den Broeke, C. Davis, Y. H. Li, W. J. van de Berg, and E. van Meijgaard (2008), Recent Antarctic ice mass loss from radar interferometry and regional climate modelling, *Nat. Geosci.*, *1*(2), 106–110.
Rignot, E., J. Mouginot, and B. Scheuchl (2011), Antarctic grounding line mapping from differential satellite radar interferometry, *Geophys. Res. Lett.*, *38*, L10504, doi:10.1029/2011GL047109.
Rignot, E., S. Jacobs, J. Mouginot, and B. Scheuchl (2013), Ice shelf melting around Antarctica, *Science*, *341*, 266–270.
Rignot, E., J. Mouginot, M. Morlighem, H. Seroussi, and B. Scheuchl (2014), Widespread, rapid grounding line retreat of Pine Island, Thwaites, Smith, and Kohler glaciers, West Antarctica, from 1992 to 2011, *Geophys. Res. Lett.*, *41*, 3502–3509, doi:10.1002/2014GL060140.
Rignot, E. J. (1998), Fast recession of a West Antarctic glacier, *Science*, *281*(5376), 549–551.
Rignot, E. J., and S. S. Jacobs (2002), Rapid bottom melting widespread near Antarctic Ice Sheet grounding lines, *Science*, *296*(2020), 2023.
Rignot, E. J., et al. (2004), Improved estimation of the mass balance of glaciers draining into the Amundsen Sea sector of West Antarctica from the CECS/NASA 2002 campaign, *Ann. Glaciol.*, *39*, 231–237, doi:10.3189/172756404781813916.
Rippin, D. M., D. G. Vaughan, and H. F. J. Corr (2011), The basal roughness of Pine Island Glacier, West Antarctica, *J. Glaciol.*, *57*, 67–76.
Saha, S., et al. (2010), The NCEP Climate Forecast System Reanalysis, *Bull. Am. Meteorol. Soc.*, *91*, 1015–1057.
Scambos, T., C. Hulbe, and M. Fahnestock (2003), Climate-induced ice shelf disintegration in the Antarctic Peninsula, in *Antarctic Peninsula Climate Variability: Historical and Paleoenvironmental Perspectives*, *Ant. Res. Ser.*, vol. 79, edited by E. Domack et al., pp. 79–92, AGU, Washington D. C.
Scambos, T. A., T. Haran, M. A. Fahnestock, T. H. Painter, and J. Bohlander (2007), MODIS-based Mosaic of Antarctica (MOA) data sets: Continent-wide surface morphology and snow grain size, *Remote Sens. Environ.*, *111*, 242–257.
Scherer, R. P., A. Aldahan, S. Tulaczyk, G. Possnert, H. Engelhardt, and B. Kamb (1998), Pleistocene collapse of the West Antarctic ice sheet, *Science*, *281*(5373), 82–85.
Schmeltz, M., E. Rignot, T. D. Dupont, and D. R. Macayeal (2002), Sensitivity of Pine Island Glacier, West Antarctica, to changes in ice-shelf and basal conditions: A model study, *J. Glaciol.*, *48*, 552–558.
Schodlok, M. P., D. Menemenlis, E. Rignot, and M. Studinger (2012), Sensitivity of the ice shelf ocean system to the sub-ice shelf cavity shape measured by NASA IceBridge in Pine Island Glacier, West Antarctica, *Ann. Glaciol.*, *53*, 156–162.
Schoof, C. (2007), Ice sheet grounding line dynamics: Steady states, stability and hysteresis, *J. Geophys. Res.*, *112*, F03S28, doi:10.1029/2006JF000664.
Schroeder, D. M., D. D. Blankenship, D. A. Young, and E. Quartini (2014), Evidence for elevated and spatially variable geothermal flux beneath the West Antarctic Ice Sheet, *Proc. Natl. Acad. Sci. U. S. A.*, *111*(25), 9070–9072.
Scott, J. B. T., G. H. Gudmundsson, A. M. Smith, R. G. Bingham, H. D. Pritchard, D. Vaughan, and D. G. Vaughan (2009), Increased rate of acceleration on Pine Island Glacier strongly coupled to changes in gravitational driving stress, *Cryosphere*, *3*, 125–131.
Seroussi, H., M. Morlighem, E. Rignot, J. Mouginot, E. Larour, M. Schodlok, and A. Khazendar (2014), Sensitivity of the dynamics of Pine Island Glacier, West Antarctica, to climate forcing for the next 50 years, *Cryosphere*, *8*, 1699–1710.
Shepherd, A., D. J. Wingham, J. A. D. Mansley, and H. F. J. Corr (2001), Inland thinning of Pine Island Glacier, West Antarctica, *Science*, *291*(5505), 862–864, 2.
Shepherd, A., D. J. Wingham, and J. A. D. Mansley (2002), Inland thinning of the Amundsen Sea sector, West Antarctica, *Geophys. Res. Lett.*, *29*(10), 1364, doi:10.1029/2001GL014183.
Shepherd, A., D. Wingham, and E. Rignot (2004), Warm ocean is eroding West Antarctic ice sheet, *Geophys. Res. Lett.*, *31*, L23402, doi:10.1029/2004GL021106.
Shepherd, A., et al. (2012), A reconciled estimate of ice-sheet mass balance, *Science*, *338*(6111), 1183–1189.
Skamarock, W. C., J. B. Klemp, J. Dudhia, D. O. Gill, D. M. Barker, M. Duda, W.-Y. Huang, W. Wang, and J. G. Powers (2008), A description of the advanced research WRF version 3, *NCAR Tech. Note, NCAR/TN-475+STR*, pp. 1–125, NCAR, Boulder, Colo.
Smith, J. A., C.-D. Hillenbrand, G. Kuhn, R. D. Larter, A. G. C. Graham, W. Ehrmann, S. G. Moreton, and M. Forwick (2011), Deglacial history of the west Antarctic ice sheet in the western Amundsen sea embayment, *Quat. Sci. Rev.*, *30*, 488–505.

Smith, J. A., C.-D. Hillenbrand, G. Kuhn, J. P. Klages, A. G. C. Graham, R. D. Larter, W. Ehrmann, S. G. Moreton, S. Wiers, and T. Frederichs (2014), New constraints on the timing of West Antarctic Ice Sheet retreat in the eastern Amundsen Sea since the Last Glacial Maximum, *Global Planet. Change*, *122*, 224–237.

Smith, J., M. Short, R. Bindschadler, M. Truffer, T. Stanton, C.-D. Hillenbrand, D. G. Vaughan, and H. Corr (2013), A PIG unknown: The first sediment cores recovered from beneath Pine Island Glacier, Abstracts of the 20th Annual WAIS Workshop, September 29 to October 2, 2013, Algonkian Meeting Center, Sterling, Va. [Available at https://www.waisworkshop.org/sites/waisworkshop.org/files/files/agendas/2013/abstracts/Smith_J.pdf.]

Smith, J. A., et al. (2016), Sub-ice-shelf sediments record history of twentieth-century retreat of Pine Island Glacier, *Nature*, doi:10.1038/nature20136.

Stanton, T. P., W. J. Shaw, M. Truffer, H. F. J. Corr, L. E. Peters, K. L. Riverman, R. Bindschadler, D. M. Holland, and S. Anandakrishnan (2013), Channelized ice melting in the ocean boundary layer beneath Pine Island Glacier, Antarctica, *Science*, *341*, 1236–1239.

Steig, E. J., Q. Ding, D. S. Battisti, and A. Jenkins (2012), Tropical forcing of Circumpolar Deep Water Inflow and outlet glacier thinning in the Amundsen Sea Embayment, West Antarctica, *Ann. Glaciol.*, *53*, doi:10.3189/2012AoG60A110.

Taylor, K. E., R. J. Stouffer, and G. A. Meehl (2012), An overview of CMIP5 and the experiment design, *Bull. Am. Meteorol. Soc.*, *93*(4), 485–498.

Teitler, L., F. Florindo, D. A. Warnke, G. M. Filippelli, G. Kupp, and B. Taylor (2015), Antarctic Ice Sheet response to a long warm interval across Marine Isotope Stage31: Across-latitudinal study of iceberg-rafted debris, *Earth Planet. Sci. Lett.*, *409*, 109–119.

Thoma, M., A. Jenkins, D. Holland, and S. Jacobs (2008), Modelling Circumpolar Deep Water intrusions on the Amundsen Sea continental shelf, Antarctica, *Geophys. Res. Lett.*, *35*, L18602, doi:10.1029/2008GL034939.

Thomas, E. R., T. J. Bracegirdle, J. Turner, and E. W. Wolff (2013), A 308 year record of climate variability in West Antarctica, *Geophys. Res. Lett.*, *40*, 5492–5496, doi:10.1002/2013GL057782.

Thomas, E. R., J. S. Hosking, R. R. Tuckwell, R. A. Warren, and E. C. Ludlow (2015), Twentieth century increase in snowfall in coastal West Antarctica, *Geophys. Res. Lett.*, *42*, 9387–9393, doi:10.1002/2015GL065750.

Thomas, R., et al. (2004), Accelerated sea-level rise from West Antarctica, *Science*, *306*(5694), 255–258.

Thomas, R. H., T. J. O. Sanderson, and K. E. Rose (1979), Effect of climatic warming on the West Antarctic ice sheet, *Nature*, *277*, 355–358.

Thompson, D. W. J., and S. Solomon (2002), Interpretation of recent Southern Hemisphere climate change, *Science*, *296*, 895–899.

Thompson, D. W. J., and J. M. Wallace (2000), Annular modes in the extratropical circulation. Part I: Month-to-month variability, *J. Clim.*, *13*, 1000–1016.

Thurnherr, A. M., S. S. Jacobs, P. Dutrieux, and C. F. Giulivi (2014), Export and circulation of ice cavity water in Pine Island Bay, West Antarctica, *J. Geophys. Res. Oceans*, *119*, 1754–1764, doi:10.1002/2013JC009307.

Tinto, K. J., and R. E. Bell (2011), Progressive unpinning of Thwaites Glacier from newly identified offshore ridge: Constraints from aerogravity, *Geophys. Res. Lett.*, *38*, L20503, doi:10.1029/2011GL049026.

Truffer, M., and R. J. Motyka (2016), Where glaciers meet water: Subaqueous melt and its relevance to glaciers in various settings, *Rev. Geophys.*, *54*, 220–239, doi:10.1002/2015RG000494.

Turner, J. (2004), The El Niño-Southern Oscillation and Antarctica, *Int. J. Climatol.*, *24*, 1–31.

Turner, J., S. R. Colwell, G. J. Marshall, T. A. Lachlan-Cope, A. M. Carleton, P. D. Jones, V. Lagun, P. A. Reid, and S. Iagovkina (2005), Antarctic climate change during the last 50 years, *Int. J. Climatol.*, *25*, 279–294.

Turner, J., T. Phillips, S. Hosking, G. J. Marshall, and A. Orr (2012a), The Amundsen Sea Low, *Int. J. Climatol.*, doi:10.1002/joc.3558.

Turner, J., T. Maksym, T. Phillips, G. J. Marshall, and M. P. Meredith (2012b), Impact of changes in sea ice advance on the large winter warming on the western Antarctic Peninsula, *Int. J. Climatol.*, doi:10.1002/joc.3474.

Turner, J., T. J. Bracegirdle, T. Phillips, G. J. Marshall, and J. S. Hosking (2013), An initial assessment of Antarctic sea ice extent in the CMIP5 models, *J. Clim.*, *26*, 1473–1484.

Turner, J., J. S. Hosking, T. J. Bracegirdle, G. J. Marshall, and T. Phillips (2015), Recent changes in Antarctic sea ice, *Philos. Trans. R. Soc. London, Ser. A*, *373*, doi:10.1098/rsta.2014.0163.

Turner, J., H. Lu, I. White, J. C. King, T. Phillips, J. S. Hosking, T. J. Bracegirdle, G. J. Marshall, R. Mulvaney, and P. Deb (2016), Absence of 21st century warming on Antarctic Peninsula consistent with natural variability, *Nature*, *535*, 411–415.

van de Berg, W. J., M. R. Van den Broeke, C. H. Reijmer, and E. van Meijgaard (2006), Reassessment of the Antarctic surface mass balance using calibrated output of a regional atmospheric climate model, *J. Geophys. Res.*, *111*, D11104, doi:10.1029/2005JD006495.

van Lipzig, N. P. M., J. Turner, S. R. Colwell, and M. R. Van den Broeke (2004), The near-surface wind field over the Antarctic continent, *Int. J. Climatol.*, *24*, 1973–1982.

van Meijgaard, E., L. H. van Ulft, W. J. van de Berg, F. C. Bosvelt, B. J. J. M. van den Hurk, G. Lenderink, and A. P. Siebesma (2008), The KNMI regional atmospheric model RACMO version 2.1, *Tech. Rep. 302*, R. Netherlands Meteorol. Inst., De Bilt, Netherlands.

Vanderveen, C. J., and I. M. Whillans (1989), Force budget 1. Theory and numerical-methods, *J. Glaciol.*, *35*(119), 53–60.

Vaughan, D. G. (2008), West Antarctic Ice Sheet collapse—The fall and rise of a paradigm, *Clim. Change*, *91*, 65–79.

Vaughan, D. G., H. F. J. Corr, F. Ferraccioli, N. Frearson, A. O'Hare, D. Mach, J. W. Holt, D. D. Blankenship, D. L. Morse, and D. A. Young (2006), New boundary conditions for the West Antarctic ice sheet: Subglacial topography beneath Pine Island Glacier, *Geophys. Res. Lett.*, *33*, L09501, doi:10.1029/2005GL025588.

Vaughan, D. G., H. F. J. Corr, R. A. Bindschadler, P. Dutrieux, G. H. Gudmundsson, A. Jenkins, T. Newman, P. Vornberger, and D. J. Wingham (2012), Subglacial melt channels and fracture in the floating part of Pine Island Glacier, Antarctica, *J. Geophys. Res.*, *117*, F03012, doi:10.1029/2012JF002360.

Vieli, A., and A. J. Payne (2003), Application of control methods for modelling the flow of Pine Island Glacier, West Antarctica, *Ann. Glaciol.*, *36*, 197–204.

Wåhlin, A. K., X. Yuan, G. Bjork, and C. Nohr (2010), Inflow of warm Circumpolar Deep Water in the Central Amundsen Shelf, *J. Phys. Oceanogr.*, *40*(6), 1427–1434.

Wåhlin, A. K., O. Kalen, L. Arneborg, G. Bjork, G. K. Carvajal, H. K. Ha, T. W. Kim, S. H. Lee, and C. Stranne (2013), Variability of warm deep water inflow in a submarine trough on the Amundsen Sea shelf, *J. Phys. Oceanogr.*, *43*, 2054–2070.

WAIS Divide Project Members (2013), Onset of deglacial warming in West Antarctica driven by local orbital forcing, *Nature*, *500*, 440–444, doi:10.1038/nature12376.

Walker, D. P., M. A. Brandon, A. Jenkins, J. T. Allen, J. A. Dowdeswell, and J. Evans (2007), Oceanic heat transport onto the Amundsen Sea shelf through a submarine glacial trough, *Geophys. Res. Lett.*, *34*, L18602, doi:10.1029/2006GL028154.

Walker, D. P., A. Jenkins, K. M. Assman, D. R. Shoosmith, and M. A. Brandon (2013), Oceanographic observations at the shelf break of the Amundsen Sea, Antarctica, *J. Geophys. Res. Oceans*, *118*, 2906–2918, doi:10.1002/jgrc.20212.

Wilch, T. I., W. C. McIntosh, and N. W. Dunbar (1999), Late Quaternary volcanic activity in Marie Byrd Land: Potential 40Ar/39Ar-dated time horizons in West Antarctic ice and marine cores, *Geol. Soc. Am. Bull.*, *111*, 1563–1580.

Wingham, D. J., D. W. Wallis, and A. Shepherd (2009), Spatial and temporal evolution of Pine Island Glacier thinning, 1995–2006, *Geophys. Res. Lett.*, *36*, L17501, doi:10.1029/2009GL039126.

Witus, A. E., C. M. Branecky, J. B. Anderson, W. Szczuciński, D. M. Schroeder, D. D. Blankenship, and M. Jakobsson (2014), Meltwater intensive glacial retreat in polar environments and investigation of associated sediments: Example from Pine Island Bay, West Antarctica, *Quat. Sci. Rev.*, *85*, 99–118.